FERROUS OXIDE ACTIVITY MEASUREMENTS IN $FeO-TiO_2-SiO_2$, $FeO-TiO_2-CaO$ TERNARY SYSTEMS AND $FeO-TiO_2-SiO_2-MnO$, $FeO-TiO_2-SiO_2-CaO$ QUATERNARY SYSTEMS

by

OMAR IBRAHIM HUSSEIN ABDELKARIM
B.Sc., M.Sc., Metallurgy
(Cairo University)

Thesis submitted to the Department of Metallurgy,

University of Strathclyde in fulfilment of the

requirements for the award of the

Degree of Doctor of Philosophy

Jan.1977

SUMMARY

Ferrous oxide activity has been determined in titania rich slags. Molten synthetic slag mixtures of the ternary systems $FeO-TiO_2-SiO_2$ and $FeO-TiO_2-CaO$ and of the system $FeO-TiO_2-SiO_2$ containing MnO and CaO at constant levels of each have been investigated.

The slags were contained in iron crucibles and were equilibrated for four hours at 1475°C or 1470°C with gas mixtures containing CO_2, H_2, and argon of varying oxygen potentials. The equilibration technique made use of the equilibrium reaction:-

$$\underset{\text{(solid)}}{Fe} + \tfrac{1}{2}\underset{\text{(gas)}}{O_2} \rightleftharpoons \underset{\text{(slag)}}{FeO}\ .$$

Each gas mixture used had an oxygen potential corresponding to a certain ferrous oxide activity in the slag and after equilibration the final chemical analysis of the slags gave the compositions having this particular ferrous oxide activity.

In the course of determining the activity in the ternary systems, the binary systems $FeO-SiO_2$ and FeO-CaO were investigated at 1475°C and 1470°C respectively. The ferrous oxide activities determined had a satisfactory agreement with other investigators of these systems. Silica activity was calculated by Gibbs-Duhem equation and calcium oxide activity was calculated by both Gibbs-Duhem equation and regular solution model.

In the ternary system $FeO-TiO_2-SiO_2$ at 1475°C, FeO iso-activity curves are bowed towards FeO corner and this was related to the miscibility gap in the binary system TiO_2-SiO_2 which show that the two liquid oxides are incompatible and must have a positive deviation from

ideality. Ferrous oxide activity in this system was compared to MnO activity in the system $MnO-TiO_2-SiO_2$ and the comparison showed that MnO have lower activity than FeO. Silica activity was calculated by Gibbs-Duhem equation.

FeO iso-activity curves in the system $FeO-TiO_2-CaO$ at 1470°C are bowed away from FeO corner. The formation of a series of interoxide compounds in the phase diagram of $CaO-TiO_2$ explain the increase in FeO activity with the addition of CaO to $FeO-TiO_2$ binary or vice versa. TiO_2 and CaO activities were calculated by Gibbs-Duhem equation and regular solution model.

Basic oxide additions to the ternary $FeO-TiO_2-SiO_2$ increased FeO activity. Increasing MnO additions from about 8 mole % to about 24 mole % increased FeO activity but had no effect on the direction of bowing of the curves. Increasing CaO additions reversed the direction of bowing of the iso-activity curves. For all TiO_2 : SiO_2 ratios the addition of 16.1 mole % CaO increased FeO activity more than the same addition of MnO.

CONTENTS

INTRODUCTION

A major portion of the research on the physical chemistry of iron and steel making as well as the extraction of non-ferrous metals has been directed to obtaining the relationships between the activities of components and their concentration in the slag phase. The knowledge of the relationship between activity and chemical analysis of a complex slag helps in understanding and prediction of slag-metal distribution equilibria.

The activity of a metallic oxide is a thermodynamic property which is used to assess the degree to which this metallic oxide is bonded or associated with other oxides either in the solid or in the liquid state.

In molten slag mixtures, the knowledge of the activity of each of the oxides forming the slag gives an indication of the interaction between these oxides and the structure of the slag.

Measurements of the activities of the oxides of the slags containing mainly silica and iron oxides have a particular practical importance in acid steel making, copper smelting, and in the understanding of the behaviour of the refractories in contact with molten slags.

The importance of the role that slag composition plays in the refining of steel has been known for many years. From the activity-composition relationship of a refining slag, the removal of the undesired elements dissolved in the steel can be speeded up and completed.

The activity-composition diagrams are also used to prevent the loss of the valuable alloying elements by adjusting the composition of the molten slag in contact with the molten steel.

The determination of the solution thermodynamics of liquid slags containing basically iron oxide, silica and titania became important because of the large deposits of titaniferrous magnetites in Malysia, Japan, South Africa and Canada. The use of ores containing TiO_2 in steel making will probably be made necessary by economic considerations within the next 10-15 years. Some of these ores are being smelted to extract their iron content and in some cases the resulting slag is treated to recover titania.

In addition to thermodynamic studies of the molten titanate slags other investigations are being carried out to study the phase equilibria, sulphide capacity, and physical properties of such slags to establish a comprehensive method for their exploitation.

CHAPTER 1.

LITERATURE REVIEW

1. LITERATURE REVIEW

1.1 EXPERIMENTAL METHODS USED TO DETERMINE FERROUS OXIDE ACTIVITY AND RESULTS:

1.1.1 Liquid Steel-Liquid Slag Reaction Under Neutral Atmosphere.

In this type of experimental work the oxygen content of the steel in equilibrium with the slag under investigation relative to the oxygen content of the steel in contact with pure ferrous oxide slag at the temperature concerned as determined by Darken and Gurry[1][2] or by Taylor and Chipman[3] was taken as a measure of ferrous oxide activity in the slag or the oxidizing activity of the slag.

This group of experiments was carried out in a magnesia crucible as a container of the molten iron and the slag, and the melt was heated by an induction furnace. Vacuum or neutral atmospheres were maintained using nitrogen or helium gas with equilibration times around 30–45 minutes.

Fetters and Chipman[4] investigated FeO activity in the system $FeO-CaO-SiO_2+MgO$ at $1600^{o}C$. The main disadvantage was the contamination of the slag with MgO from the crucible.

Taylor and Chipman[3] modified the technique to a rotating crucible to reduce the surface of contact between the slag and the MgO crucible in order to minimize slag attack on the crucible wall. They concluded that FeO combines with CaO to form $CaFe_2O_4$ in amounts depending on the CaO available after the formation of $(2CaO.SiO_2)_2$.

The theoretical treatment of Elliot[5] in the system FeO-CaO-SiO_2 pointed to the stability of the compound ($2CaO.SiO_2$) and showed that the experimentally determined activities in this system by other investigators[3][6] have maximum values along the quasi-binary line between $2CaO.SiO_2$ and Fe_TO.

Winkler and Chipman[6] in the course of studying the factors controlling the distribution of phosphorus between molten iron and complex slags determined FeO activity in the system FeO-(SiO_2+P_2O_5+Fe_2O_3+Al_2O_3) - (CaO+MgO+MnO) at 1600°C. They found a minimum FeO content for every FeO iso-activity curve along the joins FeO-$4CaO.2SiO_2$ and FeO-$2CaO.2SiO_2$.

Bell, Murad and Carter[7] determined FeO and MnO activities in the system FeO-SiO_2-MnO at 1550°C, they reported that MnO shows a tendency to silicate formation less than that of CaO but more marked than that of FeO.

Bishop, Grant and Chipman[8] undertook an investigation to establish the equilibrium conditions for simple FeO-CaO, and FeO-CaO-SiO_2 slags at 1530°C - 1700°C. They lined the magnesia crucible used with lime and di-calcium silicate to reduce MgO passing to the slag. They reported a negative deviation for FeO activity in the system FeO-CaO as well as a decrease in FeO activity with temperature increase. This high negative deviation was explained by the tendency of ferric ions in the non-stoichiometric wustite to form oxy-acid complexes and associate with calcium ions. Their data on the variation of the FeO activity with (CaO+MgO) /(SiO_2+

P_2O_5+Al_2O_3)agreed in general with the earlier data of Bishop, Lander, Grand and Chipman[9] on the variation of FeO activity with the basicity defined as the ratio (CaO+MgO) / SiO_2.

With the same technique Chipman et al[10] investigated FeO activity in slags containing MnO, P_2O_5, and Al_2O_3 in percentages commonly found in open hearth refining slags. They found higher FeO activity values for complex slags than for simple slags[8]. They also reported stronger interaction between MnO and SiO_2 than between FeO and SiO_2 as well as more interaction between CaO and FeO than that between CaO and MnO.

Bell[11] using silica and magnesia crucibles and a platinum resistance furnace studied FeO activity in the system FeO-MnO-SiO_2 at 1550°C. He showed that FeO shows a positive deviation from ideality in the system FeO-(MnO+MgO)-SiO_2 similar in type but less in magnitude than its positive deviation in the system FeO-(CaO+MgO) - SiO_2. The maximum positive deviation was along the FeO-2(CaO+MgO).SiO_2 join.

1.1.2 Gas-Slag-Metal Reaction Under Controlled Oxygen Atmosphere:

The majority of investigators used mixtures of different gases in order to obtain certain oxygen partial pressures in the furnace atmosphere. Slags under investigation were equilibrated with these gas mixtures and ferrous oxide activity in the slags was computed from the oxygen potential of the gas mixture concerned by using suitable thermodynamic calculations. Slags were contained in iron crucibles, platinum crucibles, or suspended in the form of pellets in the furnace atmosphere depending on the method of attainment of equilibrium. The different investigators are

classified according to the gas mixture used for the equilibration of the slag.

(a) Equilibration with CO_2-CO gas mixture :

Darken and Gurry[1] in studying the iron-oxygen system, suspended a specimen of lightly oxidized iron in the temperature gradient of a vertical furnace where a mixture of constant CO_2/CO ratio was passing in the furnace. They were able to calculate FeO activity in the wustite using their experimental results.

Schuhmann and Ensio[12] and Michal and Schuhmann[13] studied FeO activity in iron saturated and SiO_2 saturated slags of the system $FeO-Fe_2O_3-SiO_2$ in the temperature range of 1250-1400°C. The slag was contained in armco iron and silica crucibles and CO/CO_2 ratio adjusted by differential flowmeters. The gas mixture was bubbled through the molten slag, the equilibrium CO_2/CO ratio being that established when no difference in the analyses of the ingoing and outgoing gases was detected.

(b) Equilibration with H_2O-H_2 gas mixture :

Bodsworth[14] and Davidson and Bodsworth[15] determined FeO activity in the systems $FeO-SiO_2$, $FeO-CaO-SiO_2$, $FeO-CaO-SiO_2-MnO$ between 1265°C and 1365°C. The gas mixture from cylinders containing premixed hydrogen and argon was passed through a saturator acting as a source of H_2O vapour in the gas mixture. The gases containing up to 60% argon were bubbled under the surface of the molten slag which was contained in armco iron crucibles. Bodsworth[14] found positive deviation of FeO activity from ideality for constant N_{FeO} which changed to negative deviation with increasing SiO_2 or CaO.

(c) Equilibration with H_2-CO_2 gas mixture :

Smith and Bell[16][17] used armco iron crucibles to contain the slags of the systems FeO-TiO_2, and FeO-MnO-TiO_2 at 1475°C. The gases contained 50% argon and the gas mixture was supplied from premixed cylinders. Equilibrium runs aimed at increasing FeO content of the slags whose final compositions were determined by chemical analysis.

(d) Equilibration with other gas mixtures :

Other investigators used higher oxygen potential to investigate ferrous oxide activity in the slags.

Darken and Gurry[2] used gas mixtures consisting of all the previous mixtures mentioned in sections(a), (b) and (c) as well as the gas mixture of CO_2-CO-H_2O to study the iron-oxygen system at temperatures of 1400°C, 1500°C and 1600°C. A platinum crucible contained the molten oxides and FeO activity was calculated in these molten oxides using Gibbs-Duhem equations.

Larson and Chipman[18][19] and Turkdogan and Bills[20][21] used gas mixture of air, CO_2 and CO_2-CO to study ferrous oxide activity and the ratio (j) defined as $Fe^{3+}/Fe^{2+} + Fe^{3+}$ in different slag mixtures containing basic and acidic oxides. All the slags were contained in platinum crucibles at a fixed temperature of 1550°C and constant oxygen potential. They found that this ratio j is strongly increased by basic additions in the order BaO, CaO and MgO and that it decreases with acidic additions in the order P_2O_5, SiO_2 and TiO_2. This was explained by Bodsworth[22] who showed that acidic additions increase the ratio $a\ Fe^{3+}/a\ Fe^{2+}$ and basic additions decrease

it and concluded that (j) is inversely proportional to the activity ratio.

Timucin and Morris[23] used gas mixtures of O_2, N_2, CO or CO_2 to obtain partial pressures of O_2 between 1 atmosphere and 10^{-11} atmosphere. They determined FeO activity in the systems $FeO-Fe_2O_3-CaO$ and $FeO-Fe_2O_3-CaO-SiO_2$ at 1450°C and 1550°C. Using Schuhmann's solution of Gibbs-Duhem équation they found that a FeO decreases with increasing the temperature, a result which agrees with Chipman et al[8]. They also found a decrease in FeO activity with SiO_2 additions for a constant CaO and FeO contents.

1.1.3 Electrochemical Measurements Of Activity :

A galvan ic cell can be used to determine ferrous oxide activity in the slag in equilibrium with iron. The cell is comprised of a standard pellet containing ferrous oxide and iron powders in contact with solid electrolyte which is in term in contact with another pellet containing ferrous oxide in the slag mixture under investigation.

The solid electrolyte (zirconia ZrO_2) acts as a carrier of ions and the ratio of the square roots of the partial pressures of oxygen on the two sides of the cell is equal to the ratio of ferrous oxide activity on the two sides and since the activity of ferrous oxide is one in the standard pellet then :

$$\frac{P_{O_2}^{\frac{1}{2}}\text{(slag pellet)}}{P_{O_2}^{\frac{1}{2}}\text{(standard pellet)}} = \frac{a_{FeO}\text{(slag pellet)}}{1}$$

The electromotive force E produced by the difference in oxygen potentials on the two sides of the cell serve as a direct measure of the activity of FeO

in the slag according to the equations :-

$$\Delta G = -RT \ln a_{FeO} = -nFE$$

$$E = \frac{RT}{2F} \ln a_{FeO}$$

where E = the emf of the cell in volts

F = the Faraday

n = the valency of the ion

(in case of oxygen n = 2)

ΔG = the free energy change

T = temperature in ^{o}K

Wanibe, Yamachi, Kawai and Sakoa[24] used this principle to measure FeO activity in the system FeO-SiO_2 at 1250-1340^{o}C. They modified the technique by using liquid silver below the slag layer in an iron crucible to eliminate the slag attack on the zirconia pipe which was inserted into silver. The oxygen potential of the slag was calculated by measuring the potential in silver. The zirconia pipe was in contact with the air which acted as a reference electrode because of the stability of its O_2 potential. Their results showed a reasonable agreement with those of Schuhmann and Ensio[12].

1.2 SHORT REVIEW OF SOME OF FeO ACTIVITY RESULTS IN THE SYSTEMS RELEVANT TO THE PRESENT WORK:

1.2.1 The Systems FeO-TiO_2 And FeO-TiO_2-MnO :

Smith and Bell[16][17] found that FeO activity deviates negatively from ideal behaviour in the binary system FeO-TiO_2. In the ternary system FeO activity shows a maximum value for any FeO content along the FeO-

orthotitanate join ($2MnO.TiO_2$) then it decreases towards the FeO-meta-titanate join ($MnO.TiO_2$), mainly due to the tendency of formation of ferrous titanate at high TiO_2 contents. They suggested that $2MnO.TiO_2$ and $MnO.TiO_2$ are more stable compounds than their counterparts $2FeO.TiO_2$ and $FeO.TiO_2$.

1.2.2 The System FeO-SiO_2.

Schuhmann and Ensio[12] reported no temperature dependence in iron saturated slags of this system, and Michal and Schuhmann[13] used Gibbs-Duhem equation to calculate FeO activity.

Elliot[5] treated the data of Schuhmann and Ensio[12] and found a linear relation between log $\frac{FeO}{T}$ and the reciprocal of the temperature. He used this relation to calculate FeO activity at 1600°C.

The work of Bodsworth[14] in this system confirmed the temperature dependence.

Finally Turkdogan and Pearson[25] made a theoretical coverage of the results of the above investigators and also found that FeO activity is temperature dependent. They also concluded that their calculated FeO activity in the system FeO-(SiO_2+P_2O_5)-(CaO+MgO+MnO) holds at any temperature at which the slags are molten.

1.2.3 The Systems FeO-CaO And FeO-Fe_2O_3-CaO :

In addition to the work of Chipman et al[8] mentioned in section 1.1.1, Larson and Chipman[19] computed FeO activity in the system FeO-Fe_2O_3-CaO and reported that the addition of CaO to FeO-Fe_2O_3 increases FeO activity, for a given N_{FeO}, to a maximum then it decreases again. Turkdogan[26] recalculated their FeO activities and reported a positive

deviation in FeO-Fe_2O_3-CaO system. He also found that FeO activity curves in the system FeO-Fe_2O_3-CaO are identical with those of the system FeO-SiO_2-CaO, indicating a similarity of behaviour between Fe_2O_3 and SiO_2 in melts.

1.2.4 The Effect Of MnO Additions To The System FeO-SiO_2-CaO :

The investigation by Davidson and Bodsworth[15] included the FeO iso-activity curves in the quaternary system FeO-SiO_2-CaO-MnO. They also extrapolated these curves to 1600°C.

They reported that the replacement of CaO by MnO lowers the FeO activity coefficient to values intermediate between these found in FeO-SiO_2 and the system FeO-CaO-SiO_2. A similar observation applies to the extrapolated iso-activity curves at 1600°C.

1.3 MODELS PROPOSED TO CALCULATE THE ACTIVITY OF THE DIFFERENT COMPONENTS OF THE SLAG FROM ITS COMPOSITION :

Several investigators tried to propose theories to elucidate the structure of the liquid slags, and from the theories they postulated, the activity of the different components of the liquid slag could be computed. By comparing calculated and experimentally determined activities the extent to which a certain theory was applicable could be inferred.

1.3.1 The Structure Of Liquid Slags :

The molten mixtures of oxides such as CaO, MgO, MnO and FeO can be regarded as completely dissociated into basic cations and oxygen anions[22].

From the studies of Bockris and co-workers[27][28][29], the

liquid silica structure is mainly linked tetrahedra. A silicon cation occupies the centre of each tetrahedron and is surrounded by four oxygen anions forming one tetrahedron of formula SiO_4^{4-} . The tetrahedra share the corners which are occupied by oxygen anions to preserve the electroneutrality of the SiO_2 liquid, forming anions varying in size and bigger than the SiO_4^{4-} anion itself and formed by the condensation of this anion. The liquid silica structure is distorted and the long range order it passes in the solid state is absent and the liquid is characterized by high viscosity.

When a basic oxide such as CaO, MgO or MnO is added to molten silica, an oxygen anion from the added oxide join into the silica tetrahedra so that a shared corner is freed. Each oxygen atom at such breaks carries a negative charge and the positive cation is localized near the breaks. This continues with the addition of MxOy until all the silica is present as SiO_4^{4-} groups.

It is now accepted that liquid silicates are polyionic melts which contain, in addition to cations and free oxygen ions, an array of silicate ions of varying size and complexity in a state of dynamic chemical equilibrium[30].

Liquid phosphates and aluminates form the same structure as silica and liquid silicates.

1.3.2 Activity In The Binary Silicates :

Masson[31][32] derived an equation to calculate the activity of the metal oxide MO in MO-SiO_2 binary melts in which the metallic oxide MO to the SiO_2 ratio is sufficiently high. In other words his treatment was confined to linear and branched chains formations whereas crosslinking was considered unimportant.

Using Temkins equation[33][34] :-

$$a_{MO} = N_{M^{2+}} \cdot N_{O^{2-}}$$

He calculated the mole fraction of silica and used the following equation :-

$$N_{SiO_2} = 1 - N_{MO} = 1 \Big/ \left[3 - K + \frac{a_{MO}}{1 - a_{MO}} + \frac{K(K-1)}{\frac{a_{MO}}{1 - a_{MO}} + K} \right]$$

which gives the activity of MO as a function of composition if K is known. He applied his model to $FeO-Fe_2O_3$ and $FeO-SiO_2$ binary systems.

Later, Masson et al[35] revised the model he previously proposed to allow for all chain configurations. The equation he proposed was in the form :-

$$\frac{1}{N_{SiO_2}} = \frac{1 - \frac{1}{3} + \frac{a_{MO}}{K_{11}(1 - a_{MO})}}{1 - a_{MO}} + 2$$

where N_{SiO_2} = mole fraction of silica

a_{MO} = activity of metal oxide

K_{11} = the equilibrium constant of the reaction involving two SiO_4^{4-} tetrahedra.

The equation allow the calculation of the activity of the metal oxide if K is known. The standard state for both models is the pure liquid stoichiometric oxide. Compositions for his second model are only those where ring and network formations are absent. He[36] found that the system $CoO-SiO_2$ corresponds well with the theoretical curves calculated on the assumption of linear chains of his first model. He tried[30] to correlate

the constant k with the standard free energy of formation from liquid MO and SiO_2 of pure liquid ortho and pyro silicates of the melt.

1.3.3 Regular Solution Model :

The regular solution is defined as one in which the entropy of mixing is the same as that for an ideal solution but in which the heat of mixing may have any value, positive or negative up to about one k cal per mole[22].

For a regular solution the ratio

$$\frac{\log \gamma_i}{(1 - N_i)^2} = \text{constant}$$

The constant is given the symbol b in the present work.

In particular such behaviour enables activities to be calculated from much more limited experimental data than is possible for a non-regular solution.

The sign of b is the sign of the $\log \gamma_A$ of the component A in the solution of A and B. It follows then that for negative b function there would be negative deviation from ideality for the component A and vice versa.

Lumsden[37] applied the regular solution model to the system $FeO-Fe_2O_3$ because his data suggested a linear relation between $\log \gamma_{FeO}$ and N_{Fe}^{3+} at low FeO concentrations.

Extending this approach to ternary systems the following expression was used for a system containing the components A, B and C.

$$\log \gamma_A = b_{AB} N_B^2 + b_{AC} N_C^2 + (b_{AB} + b_{AC} - b_{BC}) \cdot N_B N_C$$

where b = the constant obtained by application of the regular solution model to every binary in the system.

Smith and Bell[16][17] applied this model to the binary system $FeO-TiO_2$ and the ternary system $FeO-TiO_2-MnO$.

Martin[38] applied it to the systems $MnO-TiO_2-SiO_2$, $MnO-TiO_2-CaO$ and $MnO-TiO_2-SiO_2-CaO$.

1.3.4 Physical Properties And Structure Of Liquid High Titania Slags :

None of the well known "ionic" or "molecular" theories of slags can be satisfactorily applied to establish the structure of the TiO_2-rich melts. This is mainly because these theories were developed to explain physico-chemical properties of silicate type melts.

The measurements of the physical properties of high TiO_2 melts such as viscosity and electrical conductivity showed that they were different from the polymerizing melts. This clearly indicates that these melts are structurally different.

Taking viscosity, the work of Fronberg and Weber[39] showed that TiO_2 additions lower the viscosity of slags showing that TiO_2 acts as a network breaker. However, the most important and relevant results are those of Handfield and Charette[40] who studied Sorel slags originating in electric arc furnace. These are composed mainly of FeO and TiO_2 with TiO_2 contents of 67 to 80%. the corresponding FeO contents being from 15 to 3%. They found very low viscosity values of $\sim$ 30 cp, typical of melts with cations in octahedral coordination, and very much lower than for silicates, which is an indicative of the absence of large directionally bonded polymeric anions in these titanate melts.

On the other hand, there is qualitative agreement among the

results of Mori[41], Reznichenko[42] and Deatyarov an Denisov[43] that the values of specific electrical conductivity from 10 to 300 $^{-1}$ cm^{-1} in slags containing TiO_2 but no SiO_2, are higher than those of molten silicates. Such slags must be completely different in structure from silicate melts.

The only results for a system containing appreciable amounts of both SiO_2 and TiO_2 are those of Mori[44] for the $CaO-SiO_2-TiO_2$ system, where the values of specific electrical conductivity were in the range of typical silicates, but increased with TiO_2 content at constant CaO/SiO_2 ratio, and with CaO/SiO_2 ratio and constant TiO_2 concentration, again implying that TiO_2 acts like CaO as a network breaker, with a coordination number of six rather than four.

The high values for electrical conductivity these slags have, imply that these slags cannot correspond to purely ionic melts where the specific conductivity never exceeds 5 $^{-1}$ cm^{-1}. A mixed ionic-electronic conductivity of a prevailing electronic nature is the most probable type of conductivity characterizing molten industrial TiO_2 rich slags.

Reznichenko[42] suggested that molten high TiO_2 slags are constructed mainly from simple anions of the type TiO_6^{8-} based on the fact that TiO_6 octahedron is the basic structural unit in solid anosovite. Anosovite group of minerals is a principle constitutent of high TiO_2 slags in the solid state based on Ti_3O_5 type of structure (orthorhombic). His hypothesis that the basic structural unit is found in both solid and molten slags accounts for the metls ease of crystallization. His suggestion is also compatible with the fact that, as a rule, non-polymerized ionic melts are very

fluid. However it is not compatible wi th the high electrical conductivity of these slags and its strong dependence on their composition. For this reason, it is unlikely that TiO_6^{8-} anions are the basic structural units of molten TiO_2 based slags.

1.3.5 Phase Diagrams :

The important features of the phase diagrams relevant to this work are discussed below :-

(a) $FeO-SiO_2$:

The phase diagram is shown in Figure (1.1). It is characterized by an immiscibility gap at a temperature of 1800°C and near the silica side. The high FeO content part of the diagram is liquid at 1475°C.

(b) FeO-CaO :

The phase diagram is shown in Figure (1.2). It is characterized by the formation of the compound $2CaO.Fe_2O_3$ which has a relatively low melting point of about 1100°C, indicating a strong association between CaO and Fe_2O_3 in the molten state as shown by other investigators.

(c) $FeO-TiO_2$:

The phase diagram is shown in Figure (1.3). There is a series of inter-oxide compounds. These compounds have melting points below 1475°C for high FeO contents.

(d) $FeO-TiO_2-SiO_2$ and $CaO-TiO_2-SiO_2$:

The immiscibility gap of the $FeO-TiO_2-SiO_2$ system was recently investigated by Bell[45] as shown in Figure (1.4). By comparing it to the

corresponding one in the system $CaO-TiO_2-SiO_2$ in Figure (1.5) it is clear that in the second system CaO which is a strong basic oxide has narrowed the immiscibility gap i.e. the two liquid region occurs at lower CaO contents compared to FeO contents in the first phase diagram.

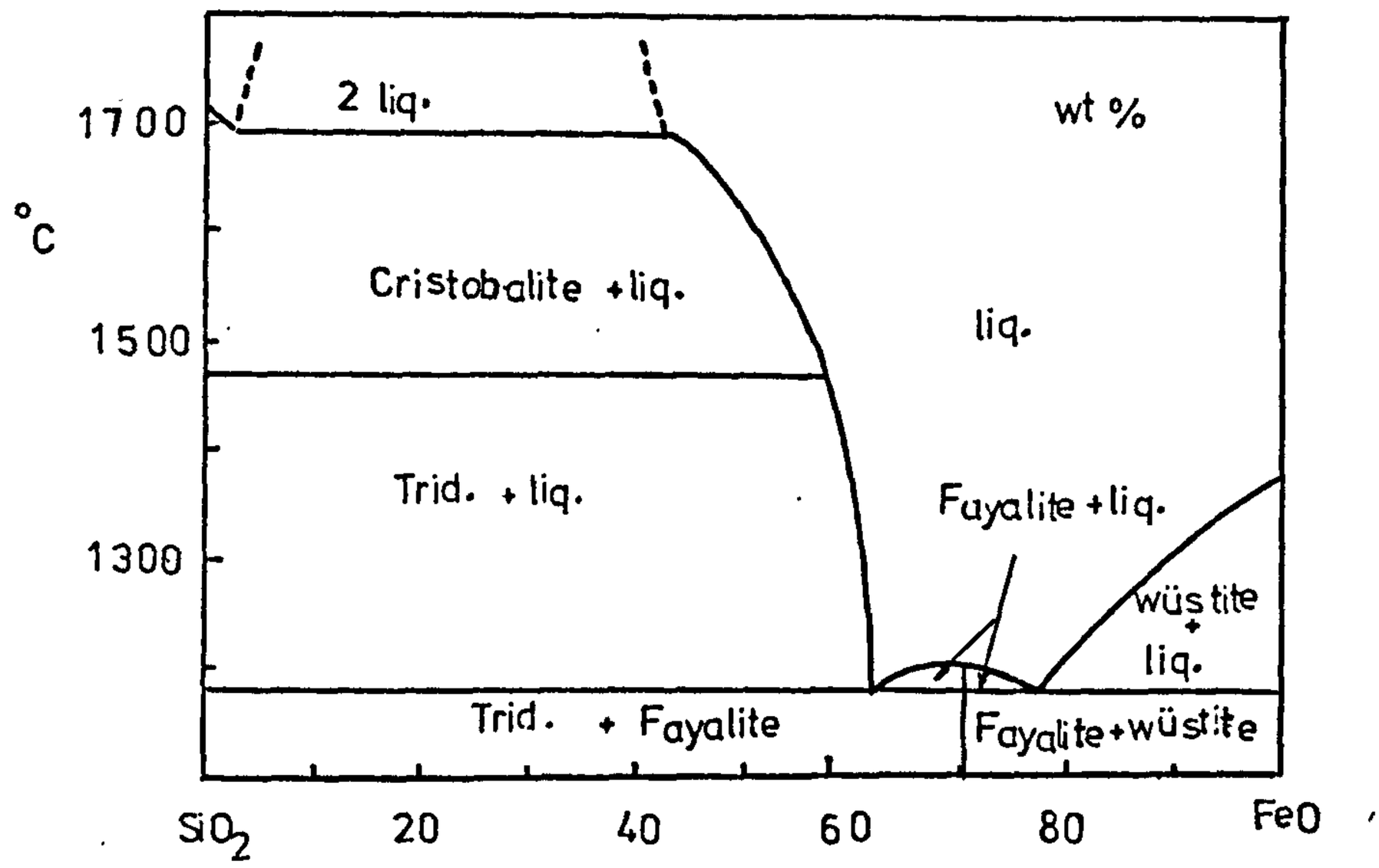

Fig.(1.1) The $FeO-SiO_2$ Phase Diagram

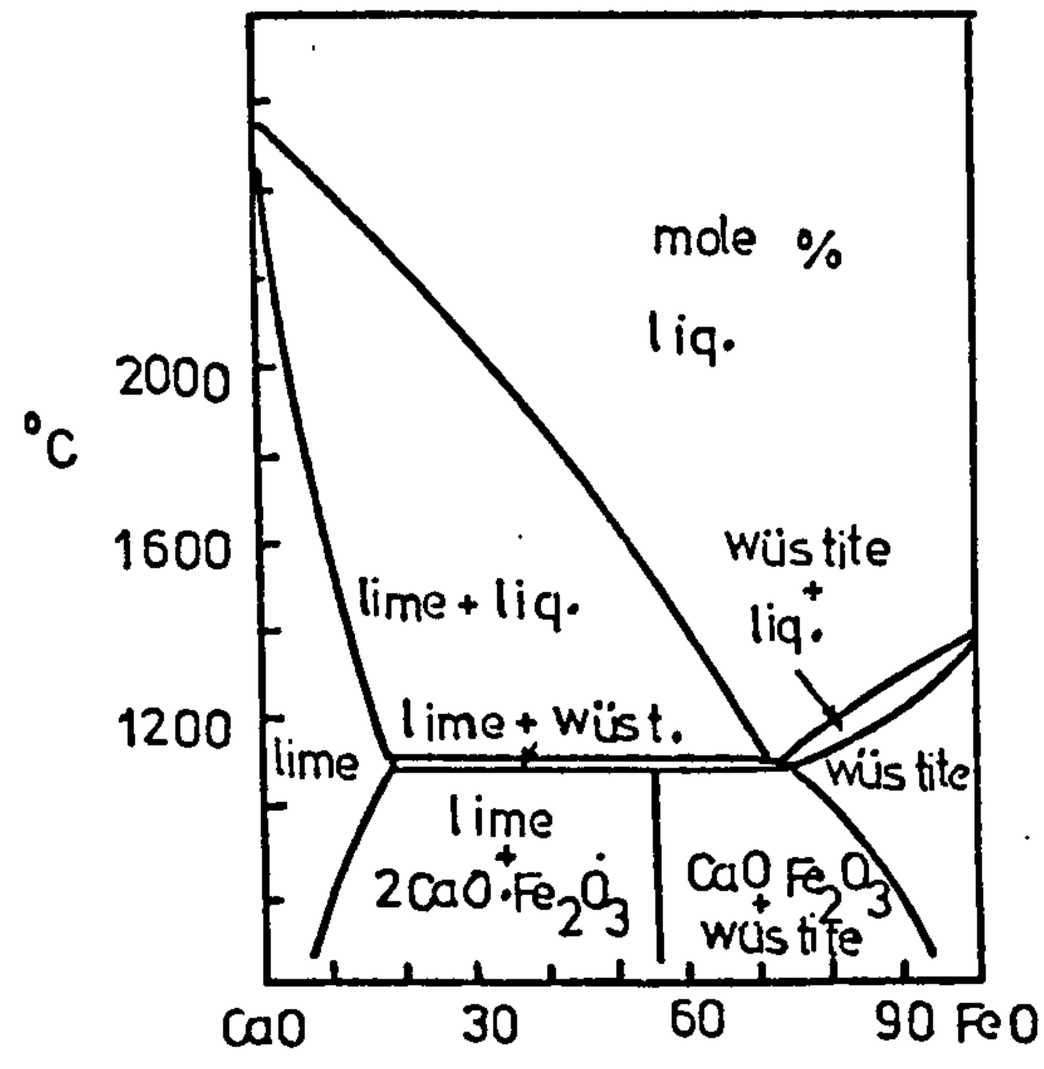

Fig. (1.2) The FeO-CaO Phase Diagram

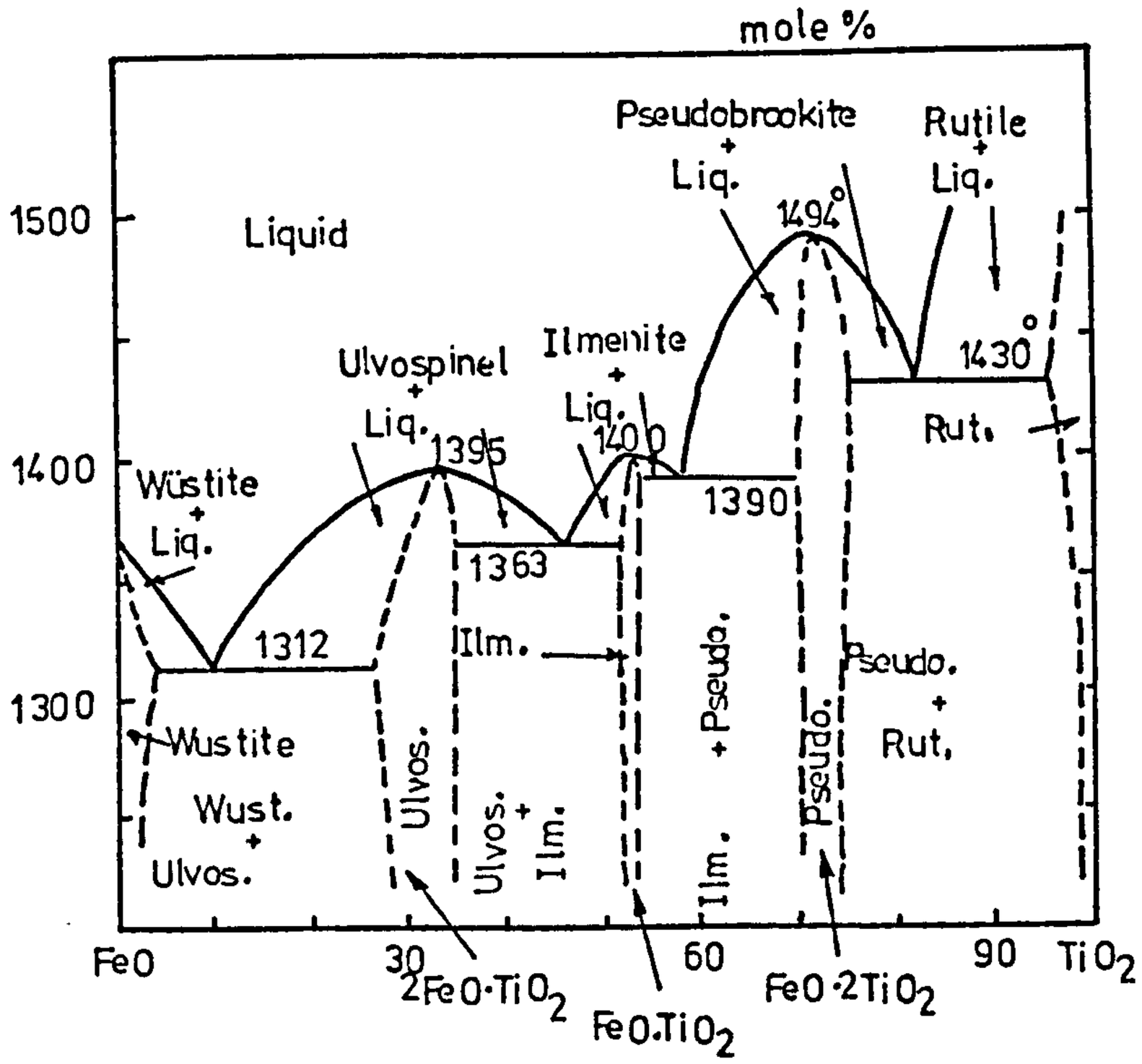

Fig. (1.3) The $FeO-TiO_2$ Phase Diagram

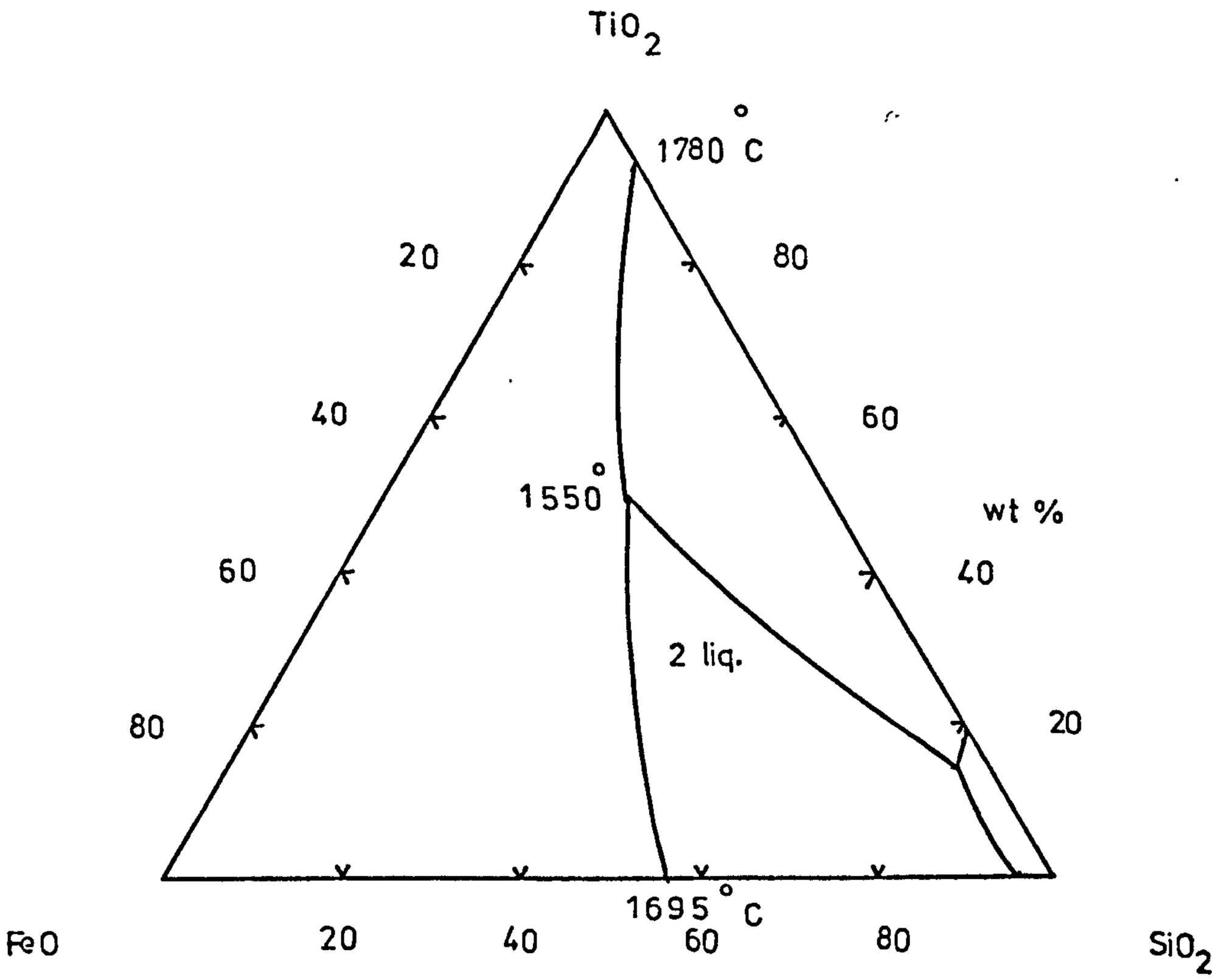

Fig. (1.4) The miscibility Gap In The System $FeO-TiO_2-SiO_2$.

$CaO–SiO_2–TiO_2$

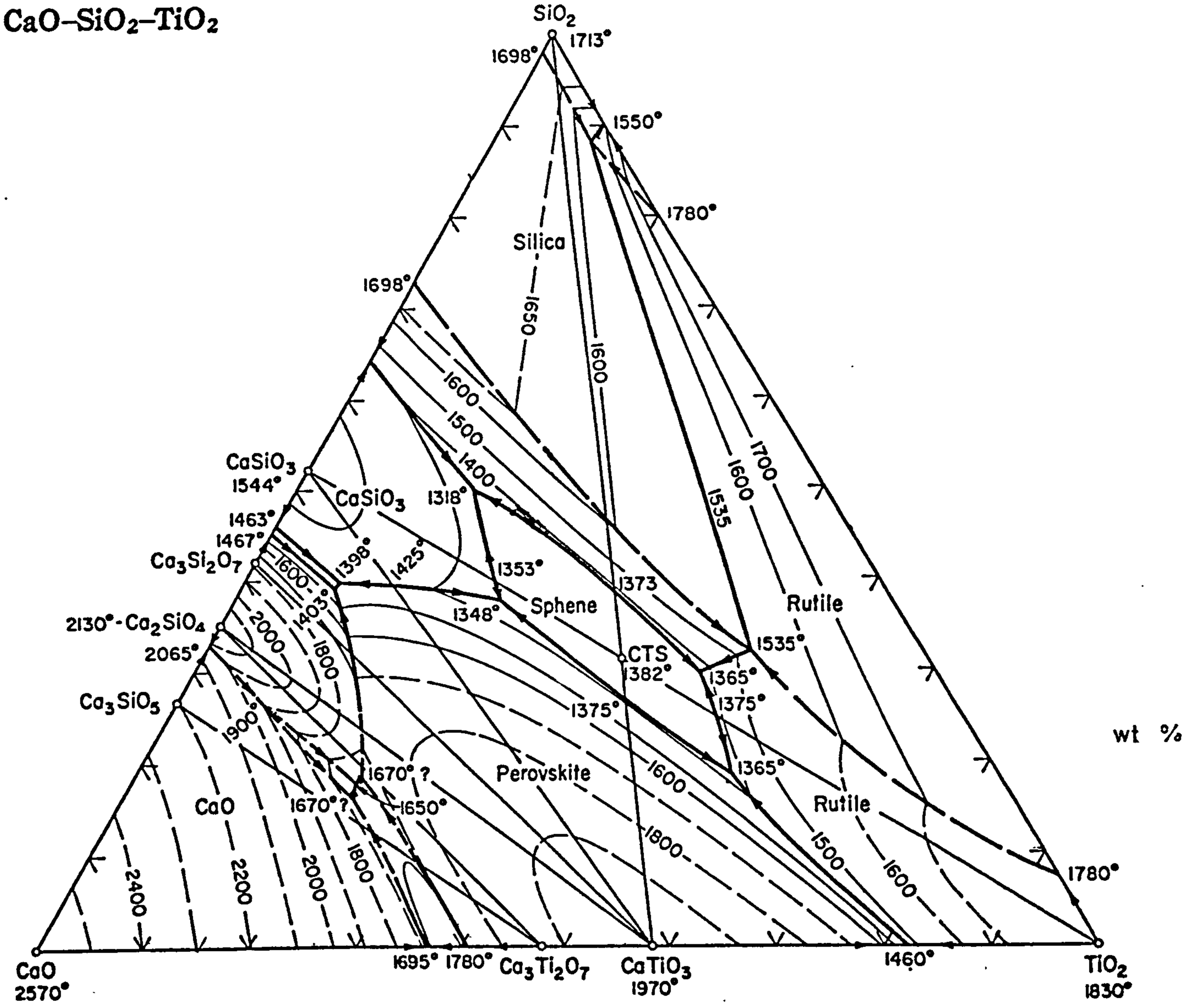

Fig. (1.5) The $CaO–TiO_2–SiO_2$ Phase Diagram.

CHAPTER 2

EXPERIMENTAL

2. EXPERIMENTAL

2.1 INTRODUCTION :

Ferrous oxide activity was measured in each slag system investigated by equilibrating the gas mixtures of hydrogen, carbon dioxide and argon with various molten slag compositions of the systems studied at temperatures of 1470°C or 1475°C.

Each gas mixture used for the equilibration of the slags had a particular oxygen potential at the above temperatures depending on its CO_2/H_2 ratio. This oxygen potential in turn corresponds to a certain ferrous oxide activity in the slag.

The molten slags were held in armco iron crucibles to react with the oxygen of the gas mixture and oxidize the iron from the crucibles according to the reaction.

$$Fe_{(s)} + \tfrac{1}{2} O_{2(g)} \rightleftharpoons FeO_{(slag)} \qquad (2.1)$$

This also fixes the standard state of the ion oxide i.e. FeO_x saturated with δ iron at the temperature studied.

Consequently the ferrous oxide content of the slags increased with time and their starting compositions changed until chemical equilibrium was attained. The final compositions of the slags were then determined by chemical analysis.

The results are presented as a series of iso-activity curves on ternary diagrams for the systems $FeO-TiO_2-SiO_2$ and $FeO-TiO_2-CaO$.

In order to investigate the iso-activity curves in the quaternary systems at constant levels of MnO and CaO, the slags of the basic ternary

$FeO-TiO_2-SiO_2$ containing the same initial MnO or CaO, were equilibrated with the different gas mixtures. After equilibration the MnO or CaO contents of these slags decreased, and the average of the final MnO or CaO contents of all the slags was calculated and was considered the MnO or CaO content of these slags.

For the quaternary systems $FeO-TiO_2-SiO_2-MnO$ and $FeO-TiO_2-SiO_2-CaO$ the results are presented as a series of iso-activity curves on pseudo-ternary diagrams each corresponding to a constant mole % of MnO or CaO.

2.2 MATERIALS FOR THE PREPARATION OF THE STARTING SLAGS:

2.2.1 Ferrous Oxide :

Ferrous oxide was prepared by decomposition of ferrous oxalate at 1050°C for two hours. The decomposition was carried out in a sealed reaction tube provided with a means to release the CO_2 into the atmosphere. This was followed by rapid quenching. The ferrous oxide produced was ground to -150 mesh, demagnetized, and analysed to determine its iron content.

2.2.2 Manganous Oxide :

Manganous oxide was prepared by decomposing manganous oxalate in a tube furnace at 550°C. This was followed by passing H_2 and increasing the temperature to 1100°C then quenching the manganous oxide. The oxide was then crushed to -150 mesh, and analysed to determine its manganese content.

2.2.3 Titania.

The purest form of commercial titania (TiO_2) was used and its titanium content was chekced by chemical analysis.

2.2.4 Calcium Oxide :

Analytical grade calcium oxide was used. It was calcined at $1000^{o}C$ every time it was used to decompose any carbonate or hydroxide formed.

2.2.5 Silica.

Pure silica (99.9% SiO_2) was obtained by grinding sand to -170 mesh and washing with dilute hydrochloric acid until no trace of iron remained, then with deionized water, after which it was dried.

2.2.6 Armco Iron Crucibles :

Armco iron, containing only traces of other elements such as carbon, silicon, manganese and sulphur, was used to make all the crucibles to contain the liquid slags during the equilibration experiments. The dimensions of the crucibles used are shown in Figure (2.1)A.

2.3 FURNACE APPARATUS :

A horizontal platinum wound furnace was used to conduct the different equilibration experiments and it is shown in Figure (2.1)B. The furnace provided a hot zone 6 cm. in length over which the variation of temperature was not more than $\pm 2^{o}C$. A mullite reaction tube was used and a platinum-platinum-13% rhodium thermocouple was inserted inside the reaction tube and in the centre of the hot zone. The thermocouple was connected to a Eurotherm controller to keep the temperature in the hot zone

at the desired value. The EMF generated by the thermocouple was measured by a cambridge potentiometer to check the actual temperature inside the hot zone. The temperature variation was about $\pm$ 2°C during the equilibration time. The equilibration temperatures chosen were 1475°C for the system $FeO-TiO_2-SiO_2$ and the system $FeO-TiO_2-SiO_2-MnO$ but 1470°C for the other systems to inhibit creeping. These temperatures are considered to be the maximum temperatures at which it is advisable to hold armco iron crucibles over prolonged periods.

2.4 GAS MIXING APPARATUS :

To provide the different oxygen potentials necessary to generate the various iron oxide activities in the slags, gas mixtures containing CO_2, H_2 and argon were used. High purity hydrogen, argon and research grade carbon dioxide were used. The gas mixing apparatus is shown in Figure (2.2)A.

Each gas mixture contained 50% argon by volume. In order to remove oxygen traces from the argon, it was passed through a small furnace containing pure titanium at 300°C. Titanium reacted with oxygen forming titantium oxide and ensured that no traces of oxygen entered the furnace with the gas mixture.

The ratio of CO_2/H_2 was varied according to the ferrous oxide activity desired (see appendix (1)). This was done by changing the flow rate of each by means of calibrated flowmeters containing Di-N-Butyl-phthalate. The design of the capillary and the flowmeter is shown in Figure (2.2)B.

To prevent occurrence of thermal diffusion the total flow rate used was 400 $cm.^3$ $min.^{-1}$. The gases were intimately mixed in a tube

filled with small glass beads and dried just before entering the reaction tube by passing through a tower containing magnesium perchlorate. A bubbler sited after the reaction tube provided a visual record of the flowing gas, which was thereafter discharged into the atmosphere. It should be mentioned that the water head in the bubbler was kept to a minimum to prevent back-pressure.

2.5 EXPERIMENTAL PROCEDURE :

An alumina tray carrying four armco iron crucibles containing different slag mixtures was placed in the hot zone of the furnace, which was then closed and argon gas passed through the reaction tube. The furnace was then switched on and the temperature in the furnace was raised over a period of around four hours to the working temperature of 1470^{o}C or 1475^{o}C. During this time argon gas was passing continuously through the reaction tube at a flow rate of 200 cm.^{3} min.$^{-1}$. Once the correct temperature had been reached half an hour was allowed to ensure complete melting and homogeneity of the slag mixtures. The CO_2 and H_2 gases, in the requisite proportions, were then passed through the reaction zone to equilibriate with the slags. Preliminary investigations had shown that a period of four hours was sufficient to establish equilibrium and that was the equilibration time used throughout this work. Each slag mixture contained about 5-8% less ferrous oxide than the predicted equilibrium content, and it is important to note that the preliminary investigations had shown that the equilibrium attained by the use of slag mixtures containing free oxides was indeed the true equilibrium, being exactly the same as that attained by previously melted master slags. After the equilibration time was finished the CO_2 and

H_2 gases were turned off and the furnace was cooled to room temperature while the argon gas continued to pass through the reaction tube.

After each equilibration experiment, the alumina tray was removed from the furnace and each of the four crucibles was compressed to break away the slag, which was crushed to -170 mesh in an agate mortar and stored in sealed containers ready for chemical analysis. The crushing of the slag took usually only a few minutes to avoid any oxidation of the ferrous oxide by the atmosphere, which would require considerably larger times at such low temperatures.

2.6 CHEMICAL ANALYSIS :

2.6.1 Introduction :

The slags investigated in this study contained a fair proportion of titania and fusion was necessary to render all the slag constituents soluble in acid solutions. Ferrous oxide was determined in the slag solution by conventional titration against a standard solution of potassium dichromate. Other oxides in the slags were determined by atomic absorption spectrometry. Each slag was analysed in duplicate and the results were accepted if the difference between the two analyses was within $\pm$ 1% for each oxide determined.

2.6.2 Determination Of Elements By Atomic Absorption Spectrometry:

(a) Theory :

When a solution containing metal ions is aspirated into a flame, there is produced in the flame a population of ground state metal atoms proportional to the concentration of metal ions in the solu tion aspirated. If

the flame is irradiated by a light source which generates the atomic spectrum of the particular metal under investigation, the ground state atom population of this metal will absorb a portion of the light. By comparing the intensity of the light transmitted by the flame when no metal atoms are present and when metal atoms are present a value of the absorbed light can be obtained. The amount of light absorbed is proportional to the metal atom concentration in the flame.

These facts are utilized by the technique of atomic absorption spectrometry. Hollow cathode lamps are used to produce the atomic spectrum of different elements, the solution containing the metal ions is aspirated by a nebulizer and introduced into the flame, and a photoelectric cell is used to measure the value of the absorbed light.

By using solutions of known concentrations of the element to be determined a calibration curve is constructed and the concentration of the element in unknown solutions are obtained from the curve.

A Perkin-Elmer type 103 atomic absorption spectrometer was used for the determination of different elements. An air-acetylene flame was used for calcium, and manganese determinations whereas a nitrous oxide-acetylene flame was used for titanium and silicon determinations.

(b) Interferences in the atomic absorption spectrometry :

Atomic absorption spectrometry is subject to interferences which arise from several sources.

Spectral interferences arise due to overlap of absorption lines or bands of the elements other than the analyte.

Physical interference is caused by the differences in the physical properties of the solutions being nebulized e.g. surface tension, viscosity, density, etc. which all directly affect the aspiration rate.

Chemical interferences are due to reactions between the analyte and other elements in the liquid or vapour state in the flame affecting the formation of ground state atoms[46].

The above mentioned interferences were overcome by making the matrix of the standard solutions and the slag solutions the same and by using interference inhibitors where possible.

(c) Preparation of stock standard solutions :

Iron, manganese, and calcium stock standard solutions were prepared by dissolving known weights of pure iron, manganese and calcium carbonate in "analar" hydrochloric acid and making each solution up to a certain volume with deionized water. Sodium tetraborate and sodium carbonate were added to every one of these stock standard solutions to make its matrix the same as that of the slag solutions whose preparation will be mentioned later.

Silicon and titanium stock standard solutions were prepared by fusing pure silica and titania with sodium tetraborate and sodium carbonate in a platinum crucible. The fused silica and titania were then dissolved in "analar" hydrochloric acid and each solution was made up to a certain volume with deionized water.

Each stock standard solution contained a certain concentration of one of the above mentioned elements which was suitable for long storage.

Stock standard solutions were checked periodically for their titanium, calcium, manganese and silicon contents.

2.6.3 Chemical Analysis In The Systems $FeO-TiO_2-SiO_2$, $FeO-TiO_2-CaO$ and $FeO-TiO_2-SiO_2-CaO$:

The same fusion technique was applied to all the slags of the above systems and after fusion and dissolution in acid, the solutions obtained were used to determine the various metal oxide concentrations. This enabled all metal oxide concentrations to be determined on one solution of the slag.

(a) Technique of fusion of the slag :

About 0.03–0.05 gm. of slag was fused in a platinum crucible with about 1.5 gm. of a 2:1 mixture of sodium carbonate and sodium tetraborate. The fused mixture was dissolved in 10 cc. of deionized water and 10 cc. of concentrated HCl with the aid of a magnetic stirrer. The solution was then transferred quantitatively to a 100 cc. graduated flask and made up to volume with deionized water[47].

(b) Determination of ferrous oxide :

50 cc. of the slag solution was heated in a conical flask, and the ferric iron was reduced to ferrous iron by the addition of a few drops of stannous chloride solution while the solution was boiling. The solution was then cooled to room temperature and 20 cc. of mercuric chloride solution were added to remove the excess stannous chloride as a silky white precipitate.

This was followed by the addition of 10 cc. of orthophosphoric–sulphuric acid mixture, and 8 drops of sodium diphenylsulphonate as

internal indicator. The solution was then titrated against standard potassium dichromate solution to an intense purple end point[48]. The total iron determined was considered to exist in the slag in the form of ferrous oxide.

(c) Determination of titania

The slag master solution was diluted in order to render the titanium concentration suitable for atomic absorption analysis.

Three standard solutions of known titanium concentration were used to construct the calibration curve. These standards were prepared by making appropriate dilutions of the titanium stock standard solution mentioned earlier. The titanium concentrations of both the standard and the diluted slag master solutions were made to be in the linear range of titanium determination by atomic absorption analysis. The matrix of the standard solutions was matched to that of the slag solution by making appropriate additions of iron, silicon and calcium from the stock standard solutions of these elements.

All solutions were made to contain 2000 ppm of KCl in order to suppress interferences from other elements.

(d) Determination of calcium oxide :

A similar method was used for CaO determinations to that used for titania. Dilution of the slag master solution was made to place the calcium concentration in the linear range for atomic absorption analysis.

Three standard solutions containing known concentrations of calcium and in the same linear range, were prepared by making suitable dilutions of the calcium stock standard solution, and were used to construct

the calibration curve.

The matrix of the standard solutions was made the same as that of the slag solutions by additions from the titanium, iron and silicon stock standard solutions.

All the solutions for calcium reading by atomic absorption spectrometer contained between 0.1 and 1% of lanthanum oxide to inhibit interference.

It should be mentioned that calcium oxide was determined by atomic absorption spectrometry in the quaternary system $FeO-TiO_2-SiO_2-CaO$ and by difference in the ternary system $FeO-TiO_2-CaO$.

(e) Determination of silica

Silica was determined by difference in all the systems investigated with some checks using the atomic absorption spectrometer.

2.6.4 Chemical Analysis In The System $FeO-TiO_2-SiO_2-MnO$:

For this system two fusions were necessary to determine the final composition of each slag. One fusion with sodium bisulphate followed by dissolution in sulphuric and hydrochloric acids for determination of ferrous oxide in the slag. The second fusion, with sodium tetraborate and sodium carbonate followed by dissolution in hydrochloric acid, was employed for the determination of the other oxides by atomic absorption spectrometry.

(a) Technique of fusion of the slag to determine ferrous oxide :

About 0.03-0.05 gm. of the slag was fused in a platinum crucible with 0.75 gm. of sodium bisulphate. The fused mixture was dissolved in 10 cc. deionized water and 15 cc. of concentrated sulphuric acid. The

solution was transferred quantitatively to a conical flask where 25 cc. of concentrated hydrochloric acid was added. Fusion with sodium bisulphate does not dissolve the silica and for this reason a few drops of hydrofluoric acid were added to the solution to dissolve the silica[49] while the solution was boiling.

(b) Determination of ferrous oxide :

The slag solution prepared in section 2.6.4(a) was titrated against standard solution of potassium dichromate in the same way as in section 2.6.3(b). The method of fusion with sodium bisulphate prior to dissolution in acid, gave a more distinct end point in titration than the fusion with sodium tetraborate and sodium carbonate.

Some experiments were done on prepared slags having known amounts of titania and ferrous oxide and the results showed that by this technique of fusion all the ferrous oxide was extracted and that titania did not form any compounds with ferrous oxide which were difficult to fuse and dissolve by this procedure.

(c) Technique of fusion of the slag to determine other oxides :

The same procedure as in section 2.6.3(a) was followed to fuse and dissolve the slag.

(d) Determination of manganous oxide :

The slag master solution prepared in section 2.6.4(c) was diluted in order to make the manganese concentration lie in the linear range of manganese for atomic absorption analysis.

Three standards prepared in the same way as in the case of

titanium and calcium, and in the same linear range, were used to establish the calibration curve.

Additions to these standards from the silicon, iron and titanium stock standard solution were also made to prevent any matrix interference.

(e) Determination of titania :

Titanium oxide was determined in the solution prepared in section 2.6.4(c) in the same way as in section 2.6.3(c).

(f) Determination of silica :

Silica was determined by difference in this system with some checks using the atomic absorption spectrometer.

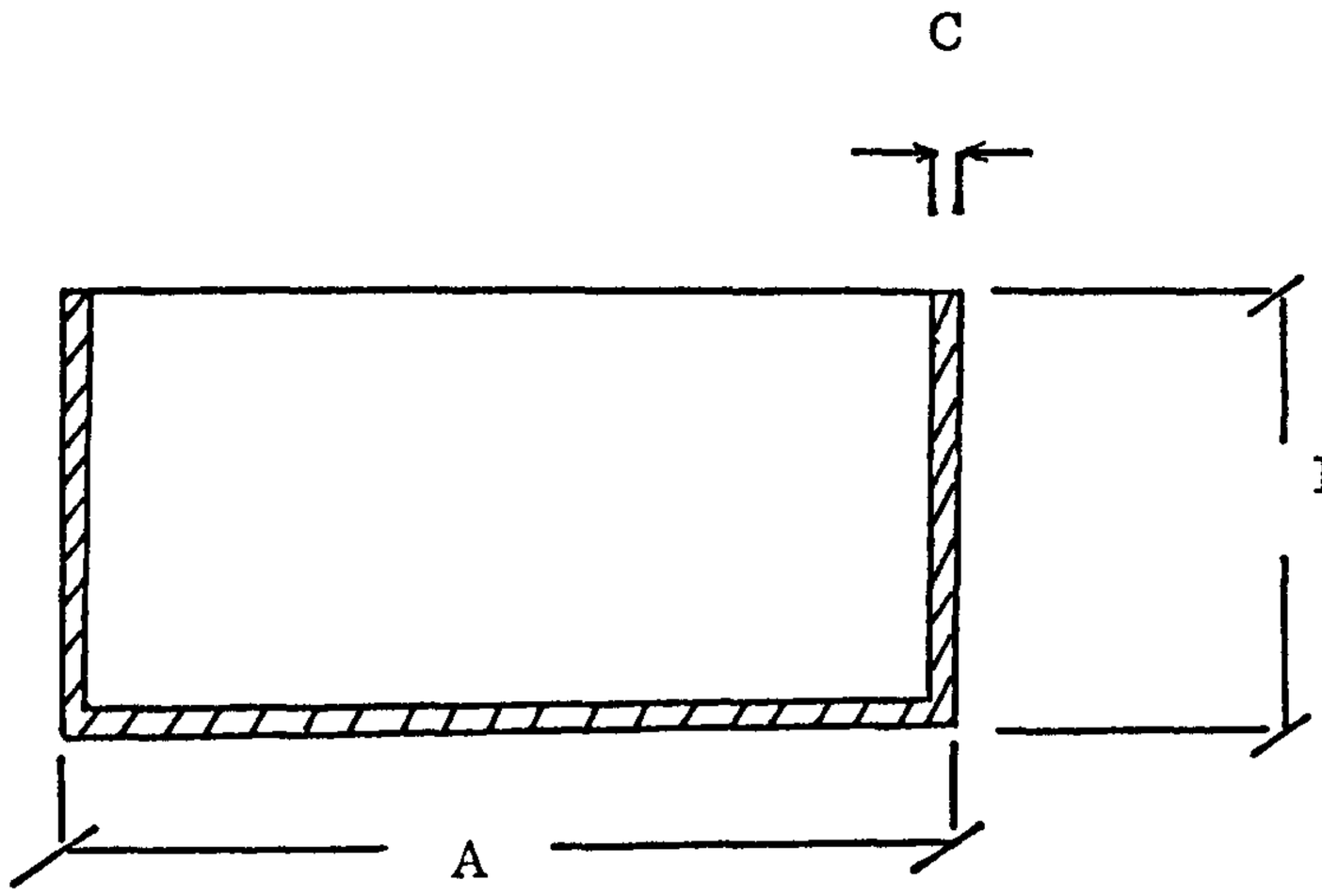

A DIAMETER 12 mm.

B HEIGHT 6 mm.

C WALL THICKNESS $\frac{1}{2}$ mm.

FIGURE (2.1)A. DIMENSIONS OF THE CRUCIBLES.

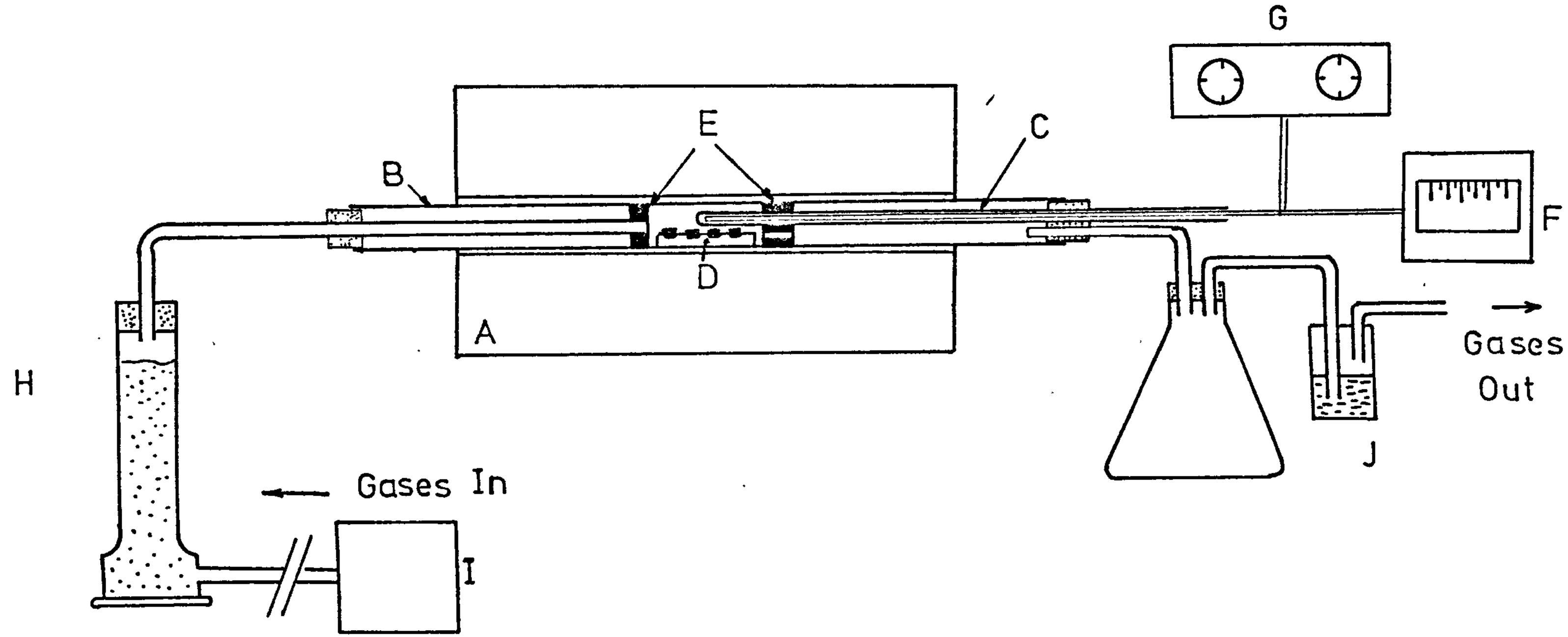

A - Pt-Wound Furnace B - Mullite Tube C - Thermocouple Sheath

D - Alumina Tray with Crucibles E - Radiation Baffle

F - Furnace Controller G - Potentiometer H - Drying Tower

I - Gas Mixing Apparatus J - Bubbler

Fig. (2.1) B - Furnace Apparatus

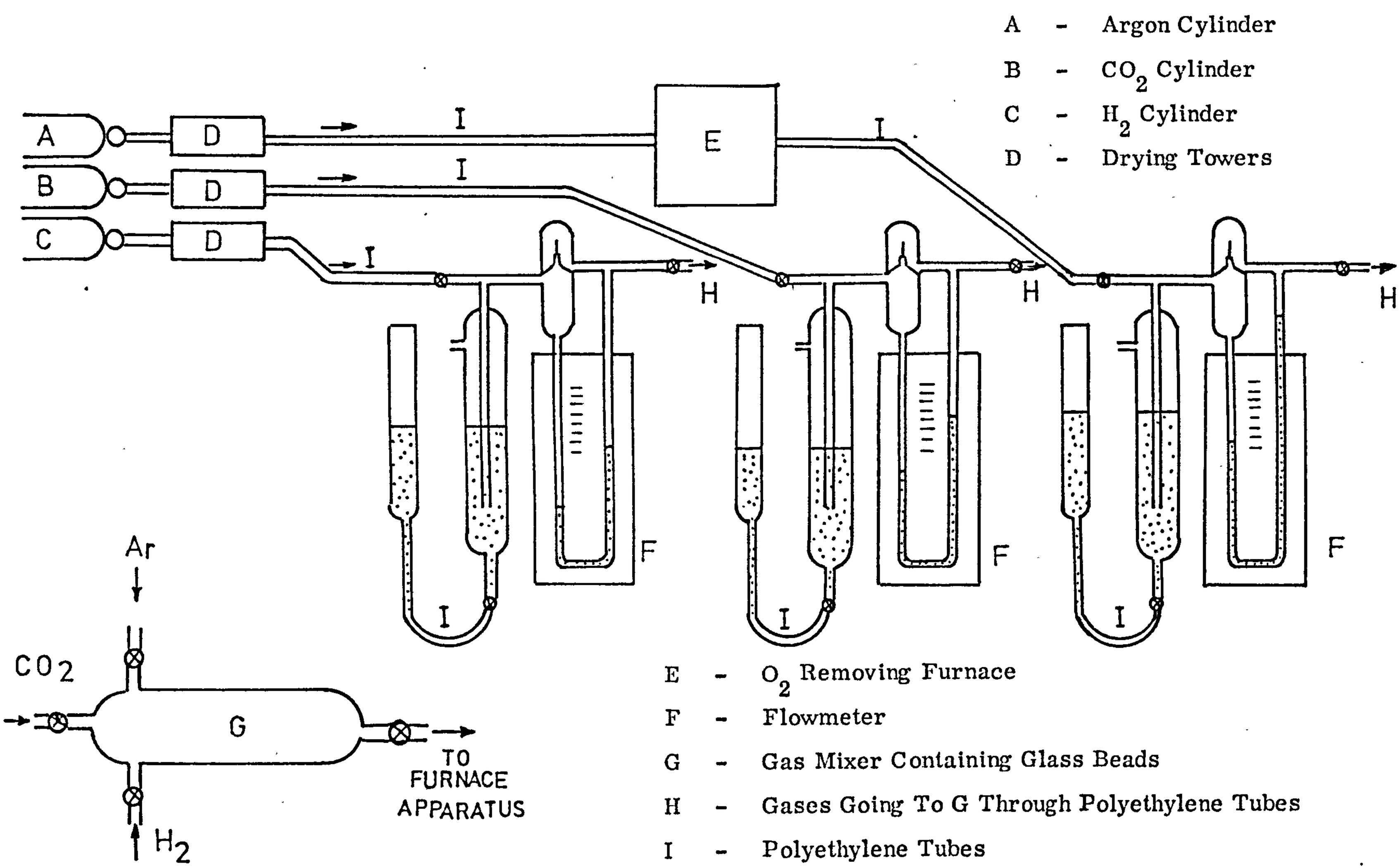

Fig. (2.2) A - Gas Mixing Apparatus.

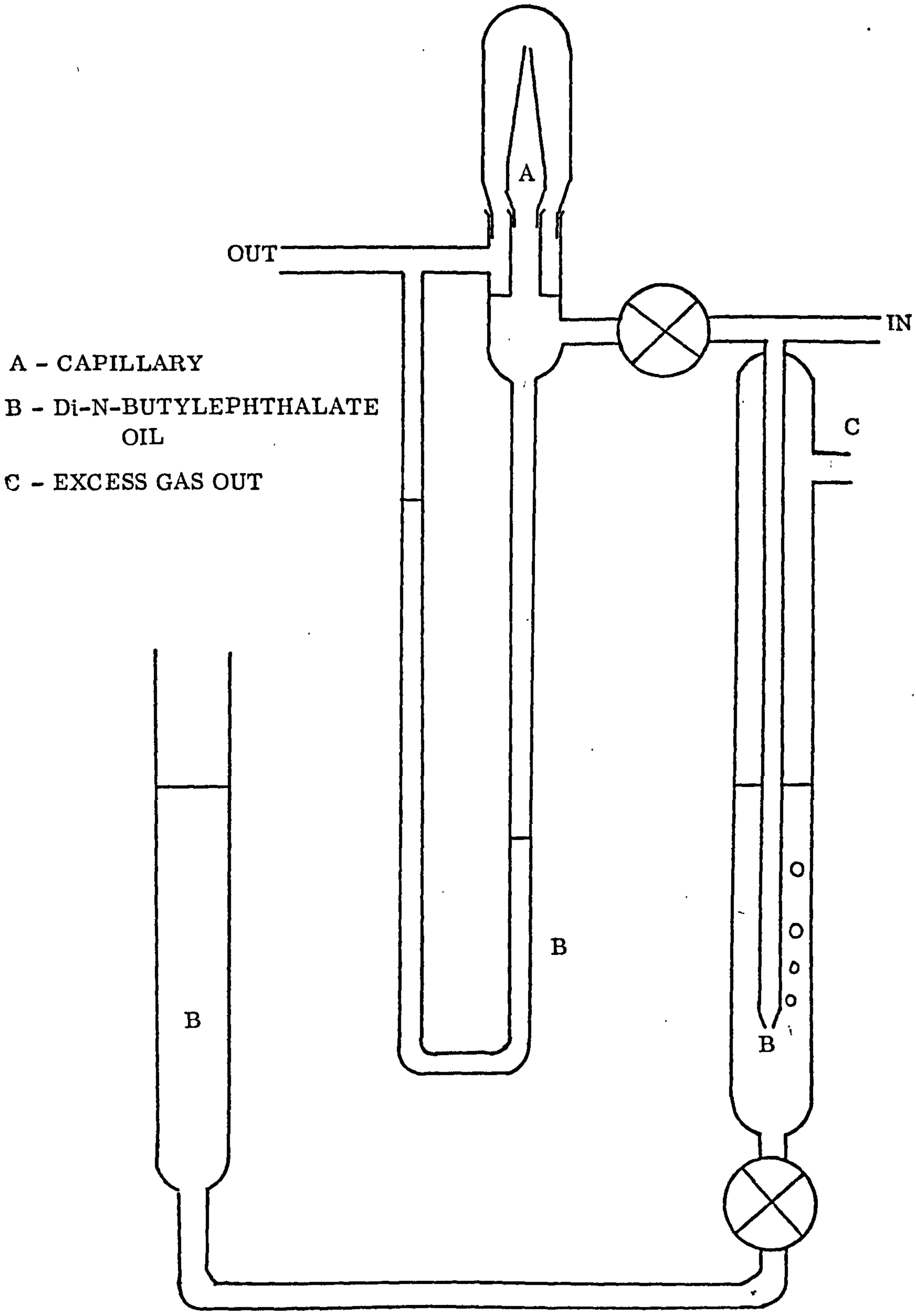

FIGURE (2.2) B. FLOWMETER AND CAPILLARY DESIGN.

CHAPTER 3

DISCUSSION

3. DISCUSSION

3.1 THE BINARY SYSTEMS $FeO-SiO_2$ AND FeO-CaO:

3.1.1 The Binary System $FeO-SiO_2$:

(a) Ferrous oxide activity :

In the course of investigating the ferrous oxide activity in the ternary system $FeO-TiO_2-SiO_2$ at 1475°C, the binary system $FeO-SiO_2$ was checked. The results are presented in Figure (3.1) and in appendix (3) in Tables 9-14.

The ferrous oxide activity obtained is relative to the pure super cooled liquid non-stoichiometric ferrous oxide (wustite) as standard state. The results show a satisfactory agreement with the work of Bodsworth[14] at 1265-1365°C in the FeO activity range of 0.4-0.6.

Schuhmann and Ensio[12] investigated the $FeO-SiO_2$ system at the temperature range 1263-1407°C. They reported that ferrous oxide activity is not dependent on temperature. The present work at 1475°C is re-affirming that ferrous oxide activity in this binary system is not dependent on temperature. The results of the present work are plotted with those of other investigators in Figure (3.2).

The ferrous oxide activity show a positive deviation from ideality at high FeO contents, which is attributed to the non-stoichiometric wustite which is taken as standard state. This is due to the triple charged ferric ions in the wustite phase. It has been shown by Bodsworth and Davidson[50] that if a correction to stoichiometric ferrous oxide as reference state is made, the activity show a negative deviation at all concentrations.

(b) Silica activity :

In order to calculate the silica activity - composition relation in the $FeO-SiO_2$ system at 1475°C, Gibbs-Duhem equation was used. The equation was in the form :-

$$\log \gamma_{SiO_2} = -\frac{N_{FeO}}{N_{SiO_2}} \int_{N_{SiO_2}=1}^{N_{SiO_2}=(saturation)} d \log \gamma_{FeO} - \frac{N_{FeO}}{N_{SiO_2}} \int_{N_{SiO_2}=(saturation)}^{N_{SiO_2}=N_{SiO_2}} d \log \gamma_{FeO} \quad \ldots 3.1$$

This equation gives the activity of silica relative to the pure solid silica as standard state. The method is explained in appendix (2).A. The results are presented in Figure (3.3).

An attempt was made to apply the regular solution model to the results of the $FeO-SiO_2$ system at 1475°C by plotting $\log \gamma_{FeO}$ versus $(1-N_{FeO})^2$ but the results can not be represented by a straight line.

3.1.2 The Binary System FeO-CaO:

(a) Ferrous oxide activity :

Ferrous oxide activity was determined in the binary system FeO-CaO at 1470°C. The results are presented in Figure (3.4) and in appendix (3) in Tables 15-20. The results show a marked deviation from ideality.

Bishop, Grant and Chipman[8] investigated the ferrous oxide activity in the FeO-CaO system in the temperature range of 1530°C to over 1660°C and reported a temperature dependence of the activity of ferrous oxide. The high negative deviation from ideality was explained in terms of the tendency of the ferric ions in the non-stoichiometric wustite to form

oxy-acid complexes such as $Fe_2O_4^{2-}$ and associate with calcium ions[8].

(b) Calcium oxide activity :

It was possible to calculate calcium oxide activity in the FeO-CaO binary system by using the Gibbs-Duhem equation in the form :-

$$\log \gamma_{CaO} = - \frac{N_{FeO}}{N_{CaO}} \int_{N_{CaO}=1}^{N_{CaO}=(saturation)} d \log \gamma_{FeO} - \frac{N_{FeO}}{N_{CaO}} \int_{N_{CaO}=(saturation)}^{N_{CaO}=N_{CaO}} d \log \gamma_{FeO} \quad ....3.2$$

The method of calculation is explained in appendix (2)B, and the results are presented in Figures (3.5). This equation gives the CaO activity relative to the pure solid CaO as standard state.

(c) Application of the regular solution model :

By plotting $\log \gamma_{FeO}$ against $(1-N_{FeO})^2$ for the FeO-CaO binary system results at 1470°C, the results could be represented by a straight line of a slope = -1.473 as shown in Figure (3.6). It was possible to apply a regular solution model to the system and the expressions used for the activity coefficients are in the form :-

$$\log \gamma_{FeO} = b N_{CaO}^2 \qquad 3.3$$

$$\log \gamma_{CaO} = b N_{FeO}^2 \qquad 3.4$$

Equation 3.4 was used to calculate CaO activity relative to the pure liquid CaO as standard state, taking b = -1.473

Considering CaO m.p. 2500°C or 2773°K and ΔG^f at 1470°C or 1743°K = +6687cal.the ratio of $\frac{a_{CaO(l)}}{a_{CaO(s)}}$ was calculated and was found to equal 0.145. Since the Gibbs-Duhem equation gives the activity of CaO relative to the pure solid CaO, the above ratio was used to obtain the CaO

activities relative to the pure liquid supercooled CaO and these were compared to CaO activities obtained using equation 3.4. This comparison is given in Table 3.1. There is a satisfactory agreement between columns (4) and (6) which indicates that the assumption of a regular solution to this binary is a reasonable assumption.

Table (3.1)

a_{FeO}	N_{FeO}	N_{CaO}	$a_{CaO}^{(1)}$	$a_{CaO}^{(2)}$	$a_{CaO}^{(3)}$
0.9	0.922	0.078	0.0044	0.042	0.0060
0.8	0.839	0.161	0.015	0.107	0.0155
0.7	0.786	0.214	0.026	0.192	0.0278
0.603	0.715	0.285	0.050	0.302	0.044
0.5	0.662	0.338	0.07	0.459	0.067
0.402	0.608	0.392	0.112	0.672	0.097

$a_{CaO}^{(1)}$ = CaO activity relative to the pure liquid supercooled CaO as standard state calculated by equation 3.4.

$a_{CaO}^{(2)}$ = CaO activity relative to the pure solid CaO as standard state calculated by Gibbs-Duhem equation.

$a_{CaO}^{(3)}$ = CaO activity relative to the pure liquid supercooled CaO calculated using $a_{CaO(l)} / a_{CaO(s)} = 0.145$.

3.2 THE TERNARY SYSTEM $FeO-TiO_2-SiO_2$.

3.2.1 Introduction :

The ferrous oxide iso-activity curves are shown in Figure (3.7) and are presented in appendix (3) in Tables 9-14. The curves show a marked bowing towards FeO corner. From Figure (3.8) the effect of addition of

TiO_2 to the FeO-SiO_2 binary system is shown for N_{FeO} = 0.8, 0.7, and 0.6. This addition results in the decrease of FeO activity to a minimum beyond which it increases again. Similarly the effect of adding SiO_2 to FeO-TiO_2 binary system is shown in Figure (3.9) for the same values of N_{FeO}. It is also apparent that such an addition lowers FeO activity in these melts.

From Figure (3.8) it is shown that at N_{FeO} = 0.8 the replacement of SiO_2 by TiO_2 decreases FeO activity but from Figure (3.9) and for the same N_{FeO} the replacement of TiO_2 by SiO_2 increases FeO activity. This indicates a slightly stronger association between FeO and TiO_2 than between FeO and SiO_2 at 1475°C.

The effect of addition of silica to FeO-TiO_2 binary on the activity coefficient of FeO is shown in Figure (3.9). It is apparent that for constant FeO:TiO_2 ratio the addition of SiO_2 to the FeO-TiO_2 binary system decreases the FeO activity coefficient. A similar effect results from the addition of TiO_2 to FeO-SiO_2 binary system at constant FeO:SiO_2 ratio as shown in Figure (3.8).

The FeO iso-activity curves are almost symmetrical about the line of $\frac{N_{TiO_2}}{N_{SiO_2}} = 1$. This is mainly due to the location of the immiscibility gap in the system TiO_2-SiO_2 shown in Figure (3.10). The system has an immiscibility gap ranging from 16-90 mole % TiO_2 at 1780°C. The shape of the iso-activity curves is what would be expected from this immiscibility gap i.e. the binary system TiO_2-SiO_2 should show a positive deviation from ideality. The pattern of FeO iso-activity curves in the FeO-TiO_2-SiO_2 implies that the two liquid region on the TiO_2-SiO_2 system links up with that

of the FeO-SiO_2 system side to yield a huge two liquid field extending well into the ternary system FeO-TiO_2-SiO_2 as proved by Bell[45].

In molten slags containing FeO-TiO_2-SiO_2 titania and silica have a repulsive interaction and there is an attractive interaction between FeO and each of TiO_2 and SiO_2. It can be then concluded that in such slags there will be a high iron oxide content for any given FeO activity and therefore high iron losses in any steel making processes involving these slags.

3.2.2 Comparison Between The FeO-TiO_2-SiO_2 And The MnO-TiO_2-SiO_2 Ternary Systems:

The MnO iso-activity curves investigated by Martin[38] are presented in Figure (3.11). The curves are bowed towards MnO corner which means that the additions of SiO_2 to the MnO-TiO_2 binary system or the addition of TiO_2 to MnO-SiO_2 binary system decreases the activity of MnO. It can be concluded then that both ferrous oxide and manganous oxide behave similarly in melts containing TiO_2 and SiO_2.

By comparing the MnO-SiO_2 binary and MnO-TiO_2 binary the MnO has more attractive interaction with silica than it has with titania at 1500°C. But from the FeO-TiO_2 and FeO-SiO_2 binary systems at 1475°C, the ferrous oxide associates more favourably with TiO_2 than with SiO_2. In all the above mentioned binary systems the MnO assumes lower activity than ferrous oxide when equal mole fraction of each of them is considered.

To compare MnO and FeO each in the corresponding ternary containing SiO_2 and TiO_2 the variation of a_{MnO} and a_{FeO} along the line

representing a constant $N_{MnO} = N_{FeO} = 0.69$, is plotted against TiO_2 : SiO_2 ratios. It is obvious from this plot shown in Figure (3.12) that at all TiO_2:SiO_2 ratios σ_{MnO} is less than σ_{FeO} for a given concentration of FeO. This applies throughout the range of concentrations of FeO and MnO examined and it is what should be expected from the stronger association between MnO and either SiO_2 or TiO_2. The variation of γ_{FeO} and γ_{MnO} with TiO_2:SiO_2 ratios is shown in the same figure.

This implies that by the addition of MnO to the SiO_2-TiO_2 binary system the immiscibility gap is closed rather more quickly than by FeO additions. In other words the critical compositions for the formation of the two liquid region occur at lower MnO contents than in the case of FeO, thus allowing the iso-activity curves to move towards the TiO_2-SiO_2 binary join.

3.2.3 Calculation Of Titania Activity In The System Using Ternary Gibbs-Duhem Equations :

It was possible to calculate titania activity using Wagner's[51] integration of Gibbs-Duhem equation. The equation was in the form :-

$$\text{Log}\,\gamma_{TiO_2} = \left[\int_0^1 \frac{\log \gamma_{FeO}}{(1-N_{FeO})^2}\, d N_{FeO}\right]_{y=O} + \left[-y\int_1^{N_{FeO}} \frac{\partial}{\partial y}\, \frac{\log \gamma_{FeO}}{(1-N_{FeO})}\, d N_{FeO}\right.$$

$$\left. - \frac{N_{FeO}\ \log \gamma_{FeO}}{(1-N_{FeO})} + \int_1^{N_{FeO}} \frac{\log \gamma_{FeO}}{(1-N_{FeO})^2}\, d N_{FeO}\right]_y \qquad 3.5$$

The first part of this integration is the b for FeO-TiO_2. The

value of b for this binary was obtained from the experimental results obtained by Smith and Bell[16] at 1475°C. The value calculated from their results was - 0.623 and was taken as the b for FeO-TiO_2. Equation (3.5) gives the value of γ_{TiO_2} at 1475°C relative to the pure super-cooled liquid TiO_2 as standard state. The method followed in evaluating the above integration is explained in appendix (2)C. The results are presented in Figure (3.13) as a series of TiO_2 iso-activity curves. As expected from the direction of bowing of FeO iso-activity curves, the TiO_2 iso-activity curves are bowed away from the TiO_2 corner.

From Figure (3.14) it is clear that the addition of silica to FeO-TiO_2 binary system at constant N_{TiO_2} will increase the activity of TiO_2 and it is also apparent that the addition of SiO_2 to this binary will increase the activity coefficient of TiO_2. Similar relations hold for the addition of TiO_2 to FeO-SiO_2 binary which manifest the strong association of FeO with TiO_2 and SiO_2.

3.3 THE TERNARY SYSTEM FeO-TiO_2-CaO:

3.3.1 Introduction :

The ferrous oxide activity has been determined in this system at 1470°C to in hibit creeping, because high titania slags were susceptible to creeping at 1475°C. It was possible therefore to investigate a wider range of slag compositions high in titania.

The results are presented as a series of iso-activity curves in Figure (3.15) and in appendix (3) in Tables 15-20.

The FeO iso-activity curves are bowed away from the FeO corner

the degree of bowing being greater at high FeO contents, but less marked than the corresponding activity curves in the FeO-TiO_2-SiO_2 system. Each of the FeO iso-activity curves shows a peak of minimum FeO content for every iso-activity curve. By inspecting the CaO-TiO_2 phase diagram in Figure (3.16), the CaO and TiO_2 form a series of compounds of the formula $3CaO.2TiO_2$ melting at 1740°C, $4CaO.3TiO_2$ melting at 1755, and $CaO.TiO_2$ melting at 1915. These compounds form at a $CaO/_{TiO_2}$ (mole ratio) between 1 and 1.5. The shape of the iso-activity curves of FeO in this system is what should be expected from the attractive interaction between CaO and TiO_2 which is also evident in the molten state at 1470°C, allowing FeO to be relatively free and have high activity. The decrease in the bowing of the iso-activity curves at low FeO contents, is mainly due to the fact that FeO will associate more readily with CaO and TiO_2 which are present at high concentration and it will then have a less chance to be present as free oxide and will have a lower activity.

The effect of replacing CaO by TiO_2 on the activity of FeO at constant N_{FeO} is shown in Figure (3.17) for N_{FeO} = 0.6, 0.7, and 0.8. It is clear that this replacement increases the activity of FeO to a maximum followed by a decrease.

In the same way the effect of replacement of TiO_2 by CaO on the activity of FeO at constant N_{FeO} is shown in Figure (3.18) for N_{FeO} values of 0.6, 0.7, and 0.8. This replacement increases FeO activity to a maximum, occurring when replacement is approximately half completed.

Figure (3.17) show the effect of addition of TiO_2 to FeO-CaO

binary system at constant FeO:CaO ratio. It is clear that the activity coefficient of FeO increases with addition of TiO_2 to a maximum value then it decreases again. The same effect is accomplished by adding CaO to FeO-TiO_2 binary system at constant FeO:TiO_2 as shown in Figure (3.18). By comparing the two binary systems FeO-TiO_2 and FeO-CaO as in Figure (3.19) it is clear that the negative deviation from ideality is greater for the FeO-CaO binary system.

The fact that the activity of FeO is increased by addition of CaO to FeO-TiO_2 binary system or by addition of TiO_2 to FeO-CaO binary system can be explained by the stronger attractive interaction between CaO-TiO_2 than between FeO and either of them. By further increase of TiO_2 or CaO concentration in the ternary melt the activity of FeO will decrease again due to the association between it and either or both of them.

3.3.2 Calculation Of Titania Activity In The System Using Ternary Gibbs-Duhem Equation :

By applying Wagner's[51] integration of Gibbs-Duhem equation, the calculation of titania activities has been attempted. The equation used was in the form:-

$$\log \gamma_{TiO_2} = \left[\int_0^1 \frac{\log \gamma_{FeO}}{(1-N_{FeO})^2} \, d N_{FeO} \right]_{y=0} + \left[-y \int_1^{N_{FeO}} \frac{\partial}{\partial y} \frac{\log \gamma_{FeO}}{(1-N_{FeO})^2} \, d N_{FeO} \right] - \frac{N_{FeO} \log \gamma_{FeO}}{(1-N_{FeO})} + \int_1^{N_{FeO}} \frac{\log \gamma_{FeO}}{(1-N_{FeO})^2} \, d N_{FeO} \Bigg]_y \qquad 3.6$$

The first part of this equation is the b $FeO-TiO_2$ used in the $FeO-TiO_2-SiO_2$ system. The activity of titania calculated by equation 3.6 is relative to the pure supercooled liquid titania.

The method of calculation and the calculated activities are shown in appendix (2)D.

The results are presented as a series of TiO_2 iso-activity curves in Figure (3.20). The curves are bowed towards TiO_2 corner which indicates that the replacement of FeO by CaO at constant N_{TiO_2}, decreases TiO_2 activity to a minimum then it increases again. This is shown in Figure (3.21) for constant N_{TiO_2}= 0.3, 0.35, and 0.4. The effect of addition of CaO to the $FeO-TiO_2$ binary system at constant TiO_2/ FeO on FeO activity coefficient is shown in the same figure. This addition leads to a decrease in the activity coefficient of TiO_2 in the $FeO-TiO_2-CaO$ ternary melt.

3.3.3 Calculation Of Calcium Oxide Activity In The System Using Ternary Gibbs-Duhem Equation :

As in the case of titania, the activity of calcium oxide in this system was calculated using Wagner's integration of Gibbs-Duhem equation in the form :-

$$\log \gamma_{CaO} = \left[\int_0^1 \frac{\log \gamma_{FeO}}{(1-N_{FeO})^2} \, d N_{FeO} \right]_{y=0} + \left[(1-y) \int_0^{N_{FeO}} \frac{\partial}{\partial y} \frac{\log \gamma_{FeO}}{(1-N_{FeO})^2} \, d N_{FeO} \right.$$

$$\left. - \frac{N_{FeO} \log \gamma_{FeO}}{1-N_{FeO}} + \int_1^{N_{FeO}} \frac{\log \gamma_{FeO}}{(1-N_{FeO})^2} \, d N_{FeO} \right]_y \qquad 3.7$$

The first part of this integration is the b FeO-CaO which was obtained by plotting $\log \gamma_{FeO}$ against $(1-N_{FeO})^2$ for the experimental results of FeO activity in the FeO-CaO binary system obtained in the present work.

The method used in calculating CaO activity is given in appendix (2)D. Equation 3.7 gives the activity of calcium oxide in this ternary melt relative to the pure supercooled liquid CaO as the standard state.

The results are presented in Figure (3.22) as a series of CaO iso-activity curves. Figure (3.23) shows that replacing FeO by TiO_2 at constant N_{CaO} decreases calcium oxide activity to a minimum after which it increases again. Addition of TiO_2 to the FeO-CaO binary system at constant $CaO/_{FeO}$ decreases the FeO activity coefficient as shown in the same figure.

3.3.4 Application Of The Regular Solution Model:

In section 3.1.2C, b FeO-CaO was calculated to be-1.473 at $1470^{o}C$. In section 3.2.3, b for $FeO-TiO_2$ of the results of Smith and Bell[16] was used. It was therefore of interest to determine whether or not the system also shows a regular solution behaviour. The expressions for the γ of component (1) in a ternary system of components (1, 2, and 3) is in the form :-

$$\log \gamma_1 = b_{12}^{K} N_2^2 + b_{13} N_3^2 + (b_{12} + b_{13} - b_{23}) N_2 N_3 \qquad 3.8$$

For FeO, CaO and TiO_2 respectively, the expressions are in the form :-

$$\log \gamma_{FeO} = b_{FeO-TiO_2} N_{TiO_2}^2 + b_{FeO-CaO} N_{CaO}^2$$

$$+ (b_{FeO-TiO_2} + b_{FeO-CaO} - b_{CaO-TiO_2}) N_{CaO} \cdot N_{TiO_2} \qquad 3.9$$

$$\log \gamma_{TiO_2} = b_{TiO_2\text{-}FeO}\ N^2_{FeO} + b_{TiO_2\text{-}CaO}\ N^2_{CaO}$$

$$+ (b_{TiO_2\text{-}FeO} + b_{TiO_2\text{-}CaO} - b_{FeO\text{-}CaO})\ N_{FeO}.N_{CaO} \quad 3.10$$

$$\log \gamma_{CaO} = b_{CaO\text{-}TiO_2}\ N_{TiO_2} + b_{CaO\text{-}FeO}\ N_{FeO}$$

$$+ (b_{CaO\text{-}TiO_2} + b_{CaO\text{-}FeO} - b_{FeO\text{-}TiO_2})\ N_{FeO}.N_{TiO_2} \quad 3.11$$

The $b_{CaO\text{-}TiO_2}$ was found by a method of trial and error, and the value of -4.7 was found to give the best agreement between the FeO experimentally determined activities and those calculated by regular solution model shown together in Figure (3.24). The agreement can be described as good.

The TiO_2 and CaO iso-activity curves obtained by regular solution approach are presented in Figure (3.25) and (3.26).

By using b for each binary equations 3.9, 3.10 and 3.11 thus become :-

$$\log \gamma_{FeO} = -0.623\ N^2_{TiO_2} - 1.473\ N^2_{CaO} + 2.604\ N_{TiO_2}.N_{CaO} \quad 3.12$$

$$\log \gamma_{TiO_2} = -0.623\ N^2_{FeO} - 4.7\ N^2_{CaO} - 3.857\ N_{FeO}.N_{CaO} \quad 3.13$$

$$\log \gamma_{CaO} = -1.473\ N^2_{FeO} - 4.7\ N^2_{TiO_2} + 5.55\ N_{FeO}.N_{TiO_2} \quad 3.14$$

3.4 THE EFFECT OF ADDITION OF BASIC OXIDES TO THE $FeO\text{-}TiO_2\text{-}SiO_2$ TERNARY SYSTEM ON FERROUS OXIDE ACTIVITY :

In order to investigate the effect of basic oxides on ferrous oxide activity, its iso-activity curves were determined in the system $FeO\text{-}TiO_2\text{-}SiO_2$ containing either MnO or CaO at constant levels as explained in section 2.1.

3.4.1 The Effect Of MnO Addition , "The Quaternary System $FeO-TiO_2-SiO_2-MnO$" :

The ferrous oxide iso-activity curves have been determined at $1475^{o}C$ in the $FeO-TiO_2-SiO_2-MnO$ system. The results are presented as a series of iso-activity curves on a pseudo-ternary diagrams,each corresponding to constant N_{MnO}. The results are shown in Figures (3.27) - (3.29) and are presented in appendix (3) in Tables 21-34. It should be noticed that at high MnO contents some FeO iso-activity curves are eliminated from the diagram. It is apparent that exactly the same pattern of curves bowed towards the FeO corner is maintained when MnO is present. From the foregoing comparison between $FeO-TiO_2-SiO_2$ and $MnO-TiO_2-SiO_2$ ternary systems in section 3.2.2 it should be expected that the addition of MnO to the $FeO-TiO_2-SiO_2$ ternary at $1475^{o}C$ will simply lead to MnO associating more strongly with SiO_2 and TiO_2 than FeO and consequently this leading to the liberation of FeO in the melt. In other words its activity and activity coefficient will increase.

This effect is shown in Figures (3.30)-(3.31). In these figures the increase of FeO activity with addition of MnO is shown for TiO_2:SiO_2 ratios of 0.25 and 1 and for the same N_{FeO}.

The effect of MnO additions in increasing the activity coefficient of FeO along a line representing constant $N_{FeO} = 0.69$ in the planes of $N_{MnO} = 0$ to $N_{MnO} = 0.2408$ is plotted against all TiO_2 : SiO_2 ratios as shown in Figure (3.32).

From the TiO_2-SiO_2 phase diagram in Figure (3.10) the miscibility gap ranges from 16 to 90 mole percent TiO_2 at $1780^{o}C$ i.e., it is

slightly nearer the TiO_2 side of the diagram. This effect is clear in all the levels of MnO at high FeO activities, and because of the slightly higher affinity of FeO for TiO_2 than for SiO_2, the iso-activity curves are pushed up from the TiO_2 rich side of the diagram than on the SiO_2 rich side.

3.4.2 The Effect Of CaO Addition ,"The Quaternary System $FeO-TiO_2-SiO_2-CaO$" :

Ferrous oxide iso-activity curves were determined in the system $FeO-TiO_2-SiO_2-CaO$ at 1470°C. The results are presented as a series of iso-activity curves on pseudo-ternary diagrams in Figures (3.33)-(3.36) and in appendix (3) in Tables 35-53. The same pattern of FeO iso-activity curves bowing towards FeO corner is maintained at CaO content of 5.6 mole % only. At this level,the FeO contents of the iso-activity curves are lower than those of the corresponding curves in the basic ternary, and consequently the curves are bowed less. By further addition of CaO to the basic ternary the iso-activity curves change the direction of bowing to the reverse direction. This indicates that the addition of CaO increases FeO activity and activity coefficient as in the case of MnO addition, but to a higher degree. The effect of CaO addition on increasing FeO activity is shown in Figures (3.37)-(3.38) for $TiO_2 : SiO_2$ ratios of 0.25 and 1. The variation of the FeO activity coefficient along a straight line representing a constant N_{FeO} with $TiO_2 : SiO_2$ ratio is shown in Figure (3.39).

3.4.3 Comparison Between The Effect Of CaO And MnO Additions To The Basic Ternary $FeO-TiO_2-SiO_2$ And $FeO-TiO_2$ Binary On Ferrous Oxide Activity :

In order to compare the relative effect of MnO addition and CaO

addition to the ternary FeO-TiO_2-SiO_2, the variation of the activity coeff-icient with TiO_2 : SiO_2 ratio for a constant N_{FeO}= 0.69 and for equal mole % of either MnO or CaO is shown in Figure (3.40). CaO increases FeO activity coefficient more than MnO additions, this applies for all mole fractions of N_{FeO}.

To compare the ferrous oxide activity in the ternary system FeO-TiO_2-MnO[17] at 1475°C in Figure (3.41) and in the ternary system FeO-TiO_2-CaO at 1470°C of the present work, a line representing constant N_{FeO}= 0.6 was chosen since it is the only line which intersects experimentally determined activity curves in both systems.

The comparison between the two systemscan be regarded as adding either MnO or CaO to the binary FeO-TiO_2.

The activity coefficient of FeO in the system containing MnO is higher than that in the system containing CaO as shown in Figure (3.42).

This can be explained by considering the association between CaO which is a strong basic oxide and FeO, and comparing it with the association between MnO, which is less basic than CaO and FeO. From the regular solution model application Martin[38] found that b of FeO-MnO = -0.5 and from the present work b of FeO-CaO = -1.473. This indicates that CaO-FeO association is greater than MnO-FeO association which is the probable reason for decreasing FeO activity in the ternary system FeO-TiO_2-CaO than its activity in the ternary system FeO-TiO_2-MnO.

3.4.4 Industrial Significance And Conclusion :

The production of iron from high titania ores will become an

important practice for producing iron in the next decade or two. It is possible that high titania ores will be directly fed into steel making units rather than the blast furnace due to sticking problems under very reducing conditions. Thus, ilmenite ores with high TiO_2 contents could be added to either electric arc furnaces or basic oxygen furnaces possibly after some pre-reduction.

The operating practice in Canada "Quebec Iron and Titanium Corporation" for example, consists in feeding ilmenite ore and coal into electric arc furnaces, reacting these at temperatures in excess of 1550°C, and tapping out a high-carbon iron and a slag containing about 72% TiO_2 (Sorelslag).

The study of the physical properties of these slags have revealed results of industrial significance and it is now well established that once these slags have melted they become remarkably fluid. On the other hand since viscosity is related to the structural units of the slag as explained in section 2.3.4, the titania structure is entirely different from the polymerized silica structure. Also the indication from the miscibility gap in the TiO_2-SiO_2 binary phase diagram supports this assumption. Although the electrical conductivity measurements of high TiO_2 show high values unusual of ionic conductors, the measurements of sulphide capacity indicate that the assumption that TiO_2 is dissociated into Ti^{4+} and O^{2-} ions may not be seriously in error.

The division between acid and basic melts is usually taken as the composition at which just sufficient oxygen ions are donated by the cations

to satisfy all the oxygen-ion bonds of the acidic polymers. An increase in the basic oxide concentration results in the presence of the free oxygen ions and the melt become basic. Conversally if the basic oxide concentration is reduced some of the polymer ions become unsaturated and degenerate into more complex groupings. Some oxides are amphoteric like alumina and ferric oxide i.e., in acid or weakly basic melts it may ionize acting as a base, where as in more strongly basic melts it behaves as an acidic oxide.

This division between acidic and basic melts implies that more acid melts would be non oxidizing and it is highly probable that oxy-acid polymers exist at neutral compositions and it is also probable that free un-attached oxygen ions are also present in more acid melts.

Some investigators[18][19][20][21] showed that TiO_2 behaves as acid oxides but due to the lack of thermodynamic properties of many of the slag mixtures of importance to acid steel making, the exact nature of TiO_2 structure cannot be determined from the thermodynamic approach. It is believed that the structure of high TiO_2 slags will not be clearly understood until a more general theory pertaining to the semi-conducting properties of slags is developed.

The thermodynamic properties determined in this work are useful in the production of iron from high TiO_2 ores. For example the high losses of iron predicted in slags containing SiO_2 and TiO_2 can be lowered by basic additions as explained in section 3.4.3, the partitioning of solute elements between the molten steel and the slag containing TiO_2, SiO_2 and MnO can be controlled. For practical purposes TiO_2 can be regarded as an

oxide which would play a satisfactory role in desulphurization and dephosphorization and as an alternative flux to CaF_2 to facilitate melting CaO while avoiding the formation of di-calcium silicate.

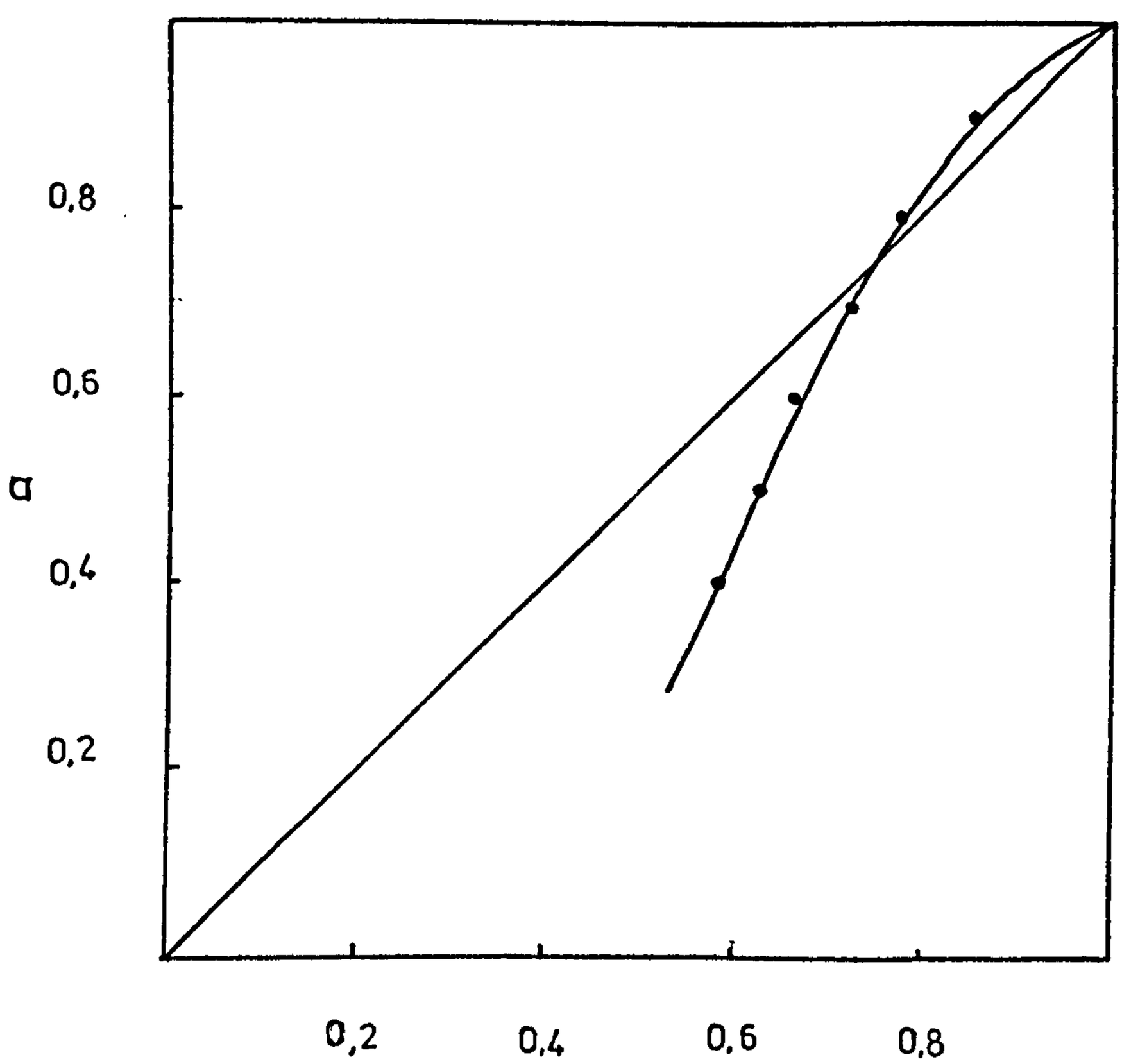

Fig. (3.1) Ferrous Oxide Activity-Composition Relation In The System FeO-SiO_2 At $1475^{o}C$.

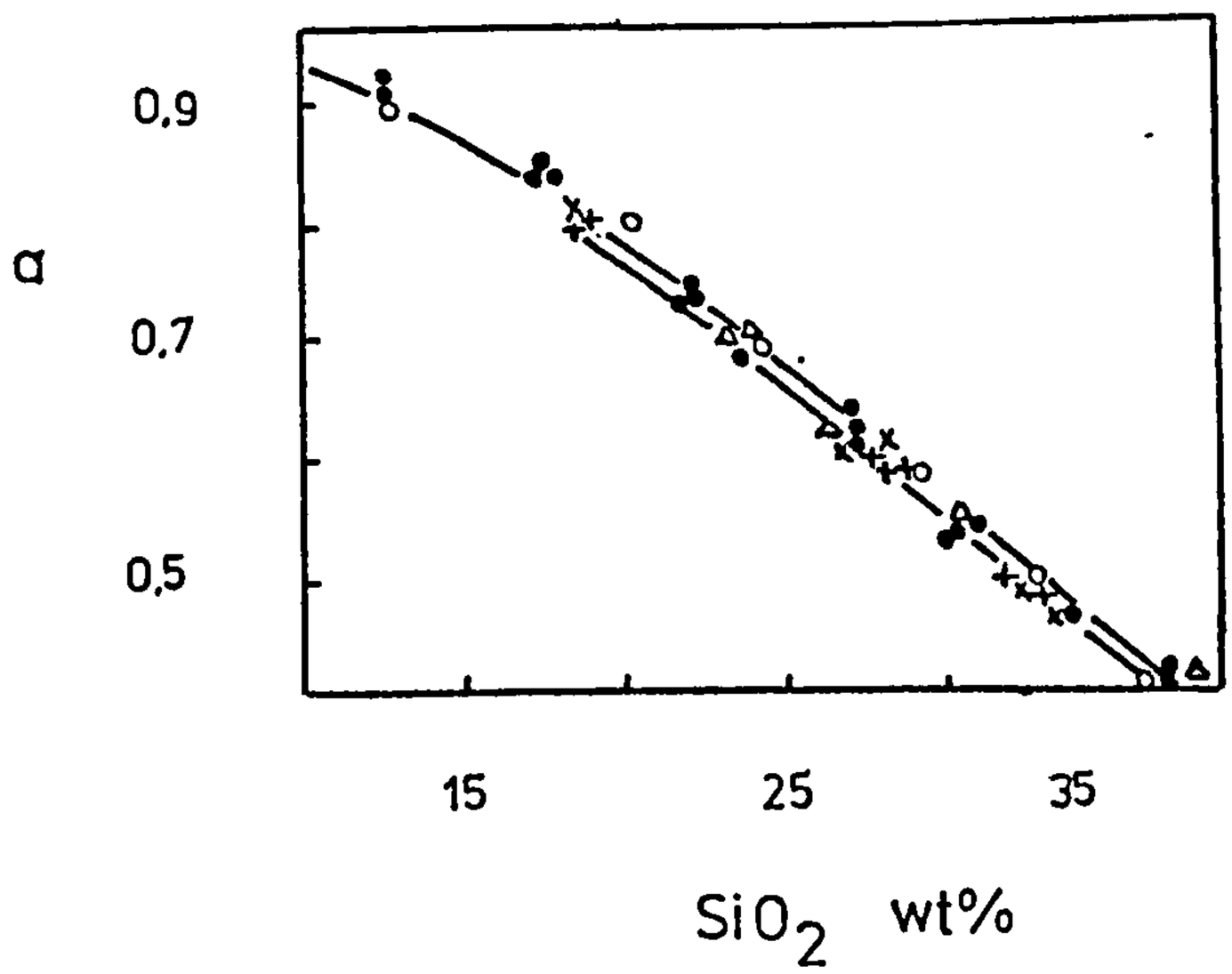

Fig. (3.2) The Results Of FeO Activity In FeO-SiO_2 System Obtained By Other Investigators Compared To The Present Work.

▲ 1265°C
\+ 1305°C C. Bodsworth
x 1365°C
• Schuman And Ensio 1263-1407°C
o Present Work At 1475°C

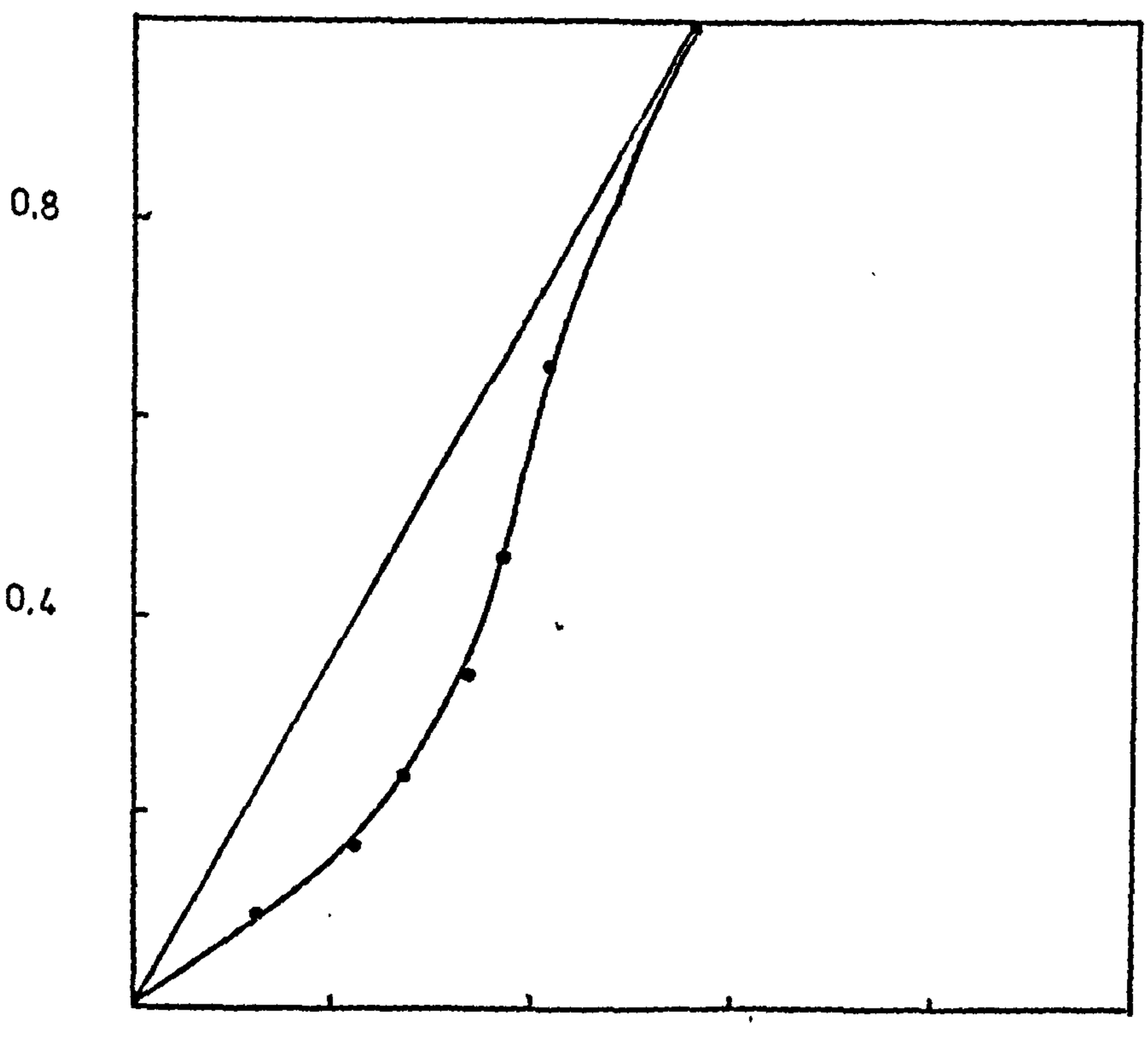

Fig. (3.3) Silica Activity-Composition Relation In The System FeO-SiO_2 At 1475 ^{o}C Calculated By Gibbs-Duhem Equation.

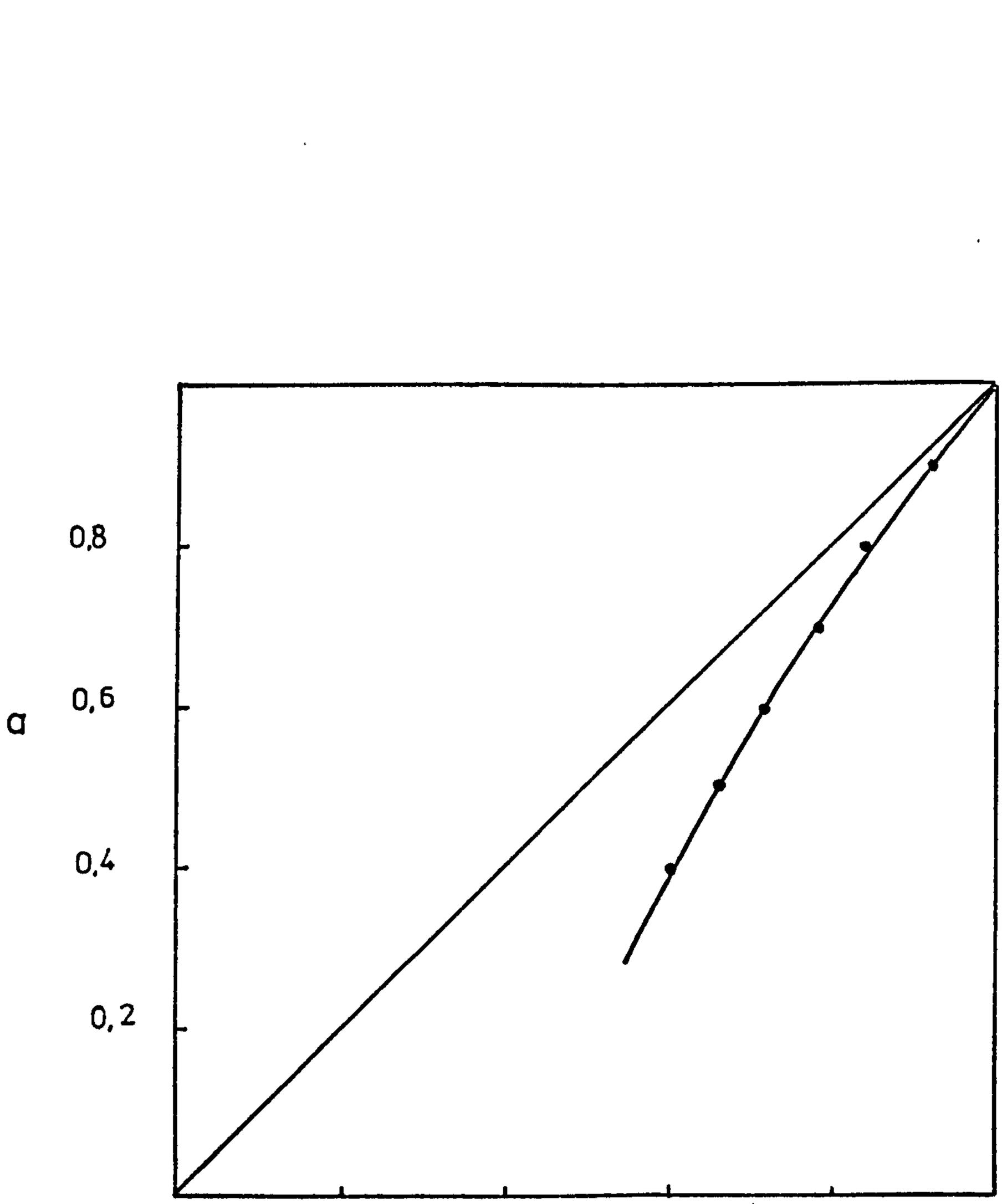

Fig. (3.4) Ferrous Oxide Activity-Composition Relation In The System FeO-CaO At 1470 ^{0}C.

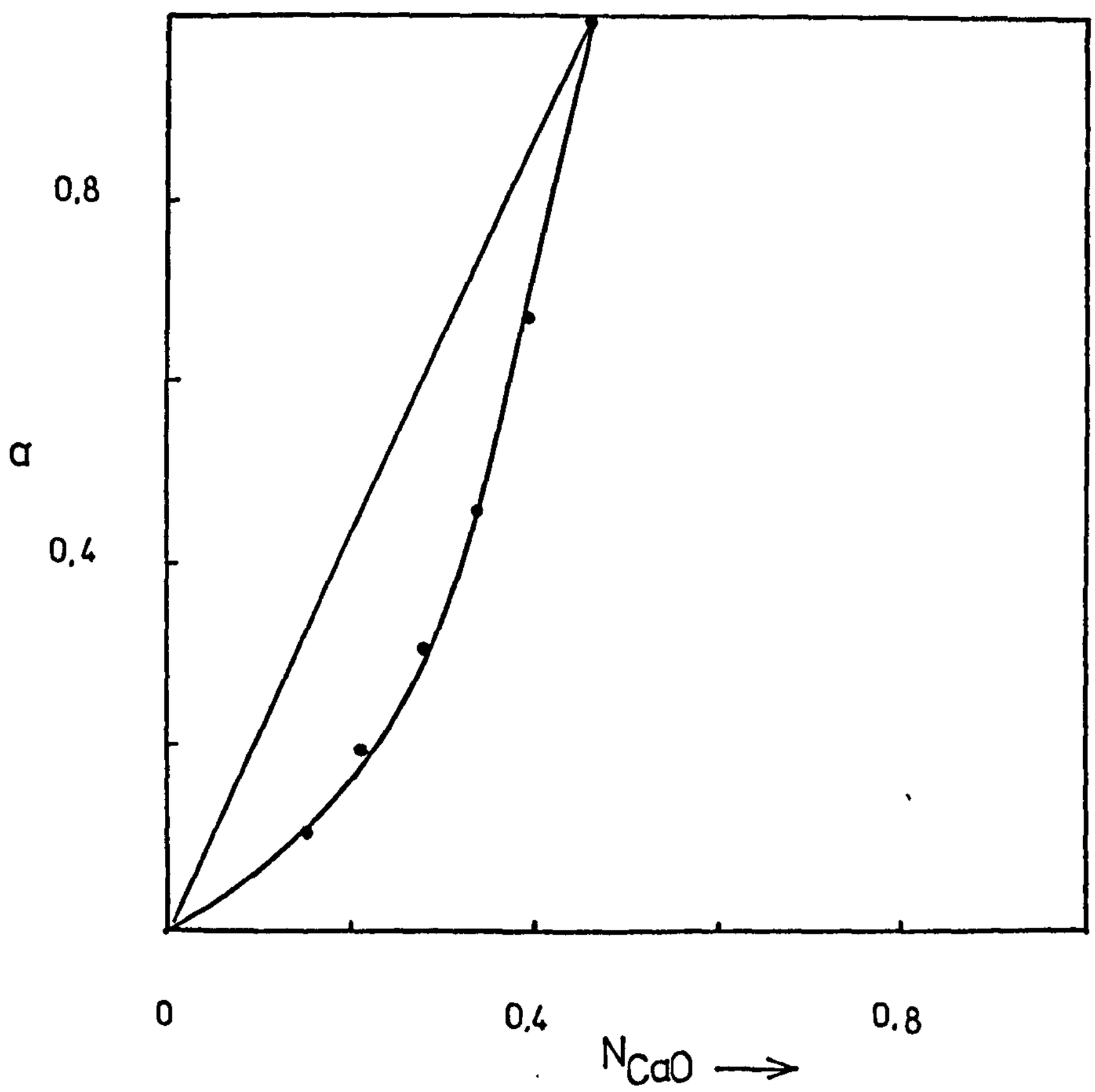

Fig. (3.5) Calcium Oxide Activity-Composition Relation In The System FeO-CaO At 1470°C Calculated By Gibbs-Duhem Equation.

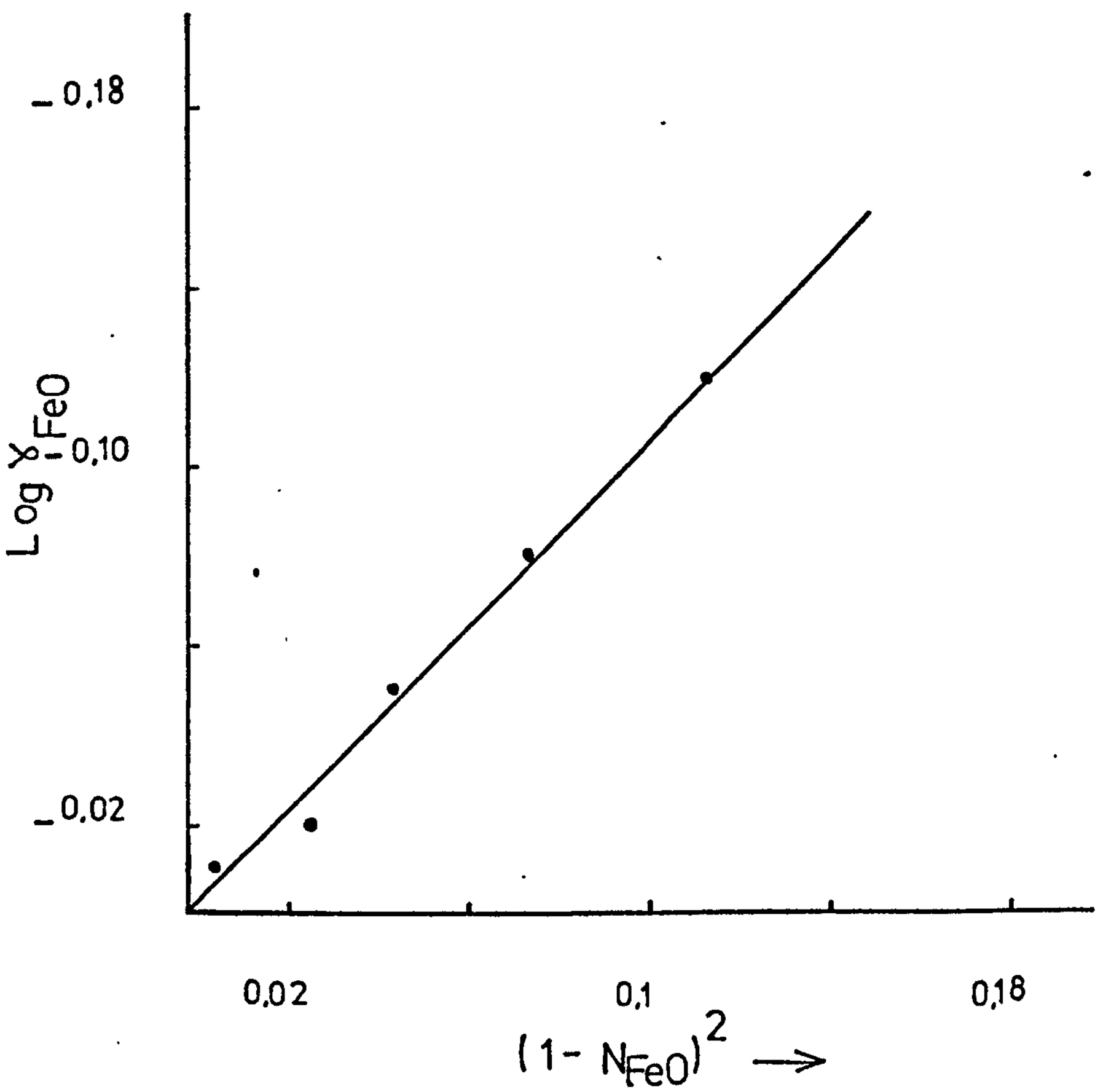

Fig. (3.6) The Plot Of Log γ_{FeO} Versus $(1-N_{FeO})^2$ For The Experimental Results Of The Binary System FeO-CaO At 1470°C.

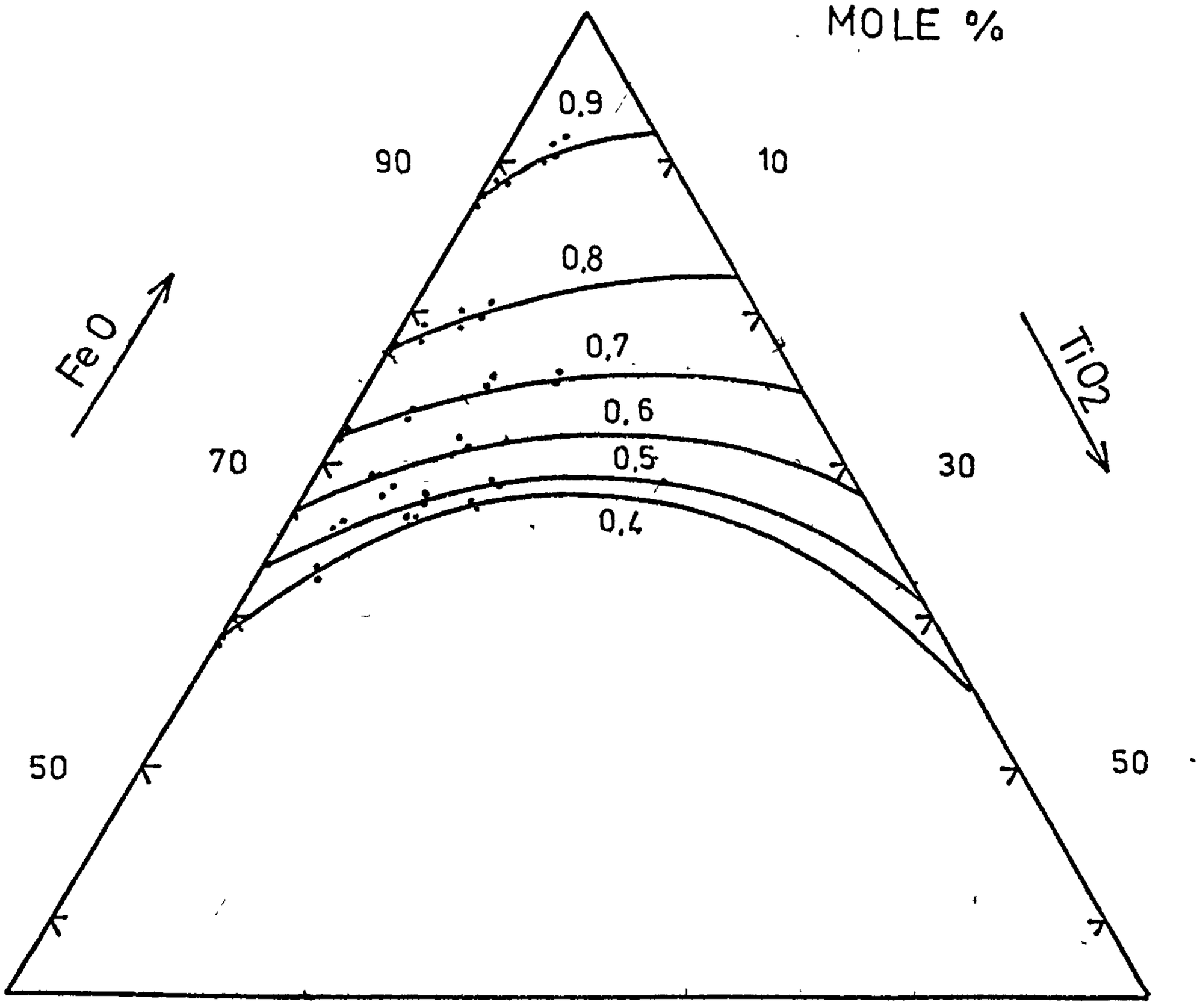

Fig. (3.7) FeO Iso-Activity Curves In The System $FeO-TiO_2-SiO_2$ at $1475^{o}C$.

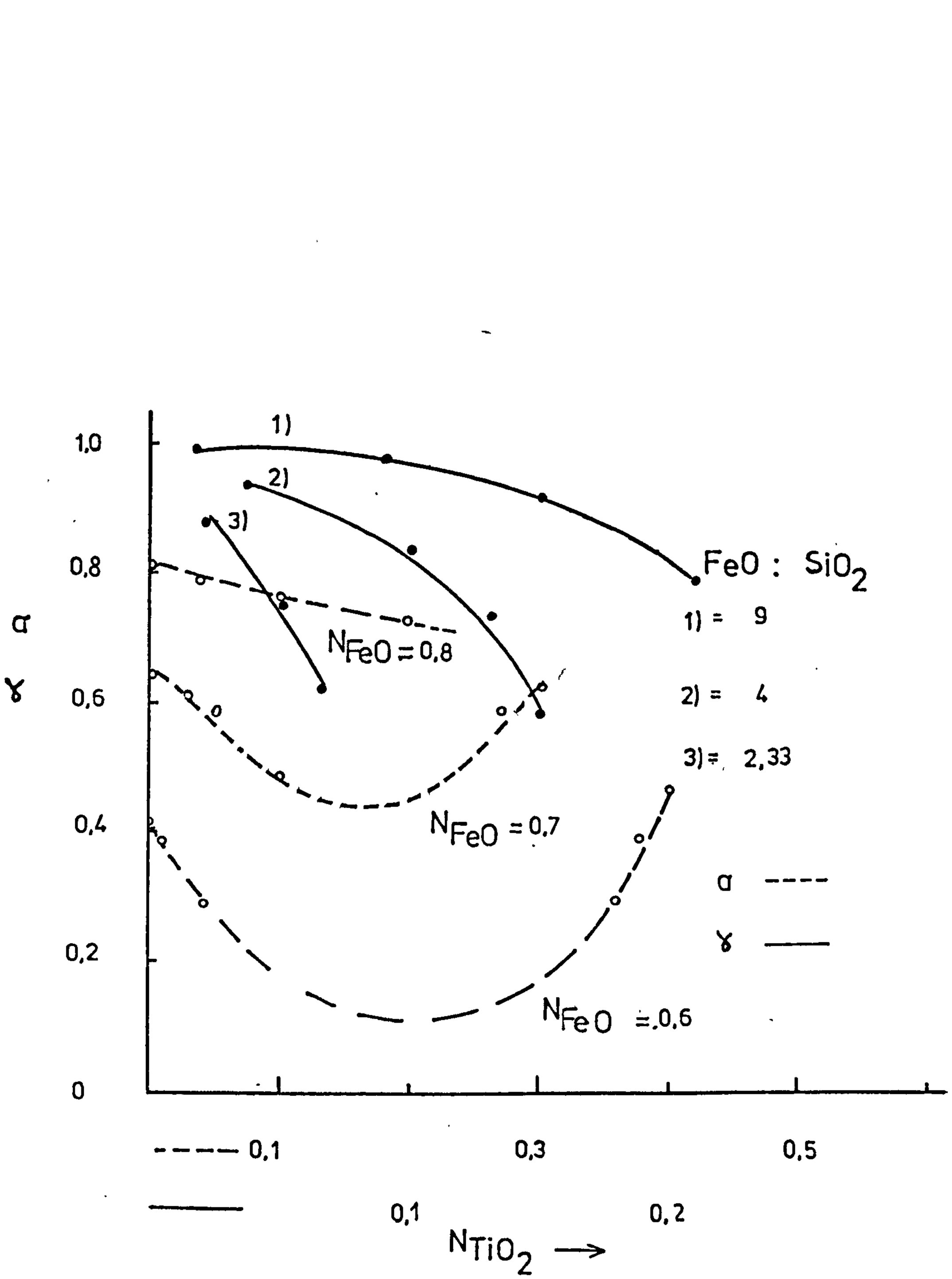

Fig. (3.8) The Effect Of Replacement Of SiO_2 By TiO_2 On FeO Activity At Constant N_{FeO}, And The Variation Of The Activity Coefficient Of FeO With The Addition Of TiO_2 To FeO-SiO_2 Binary At Constant FeO:SiO_2 ratio.

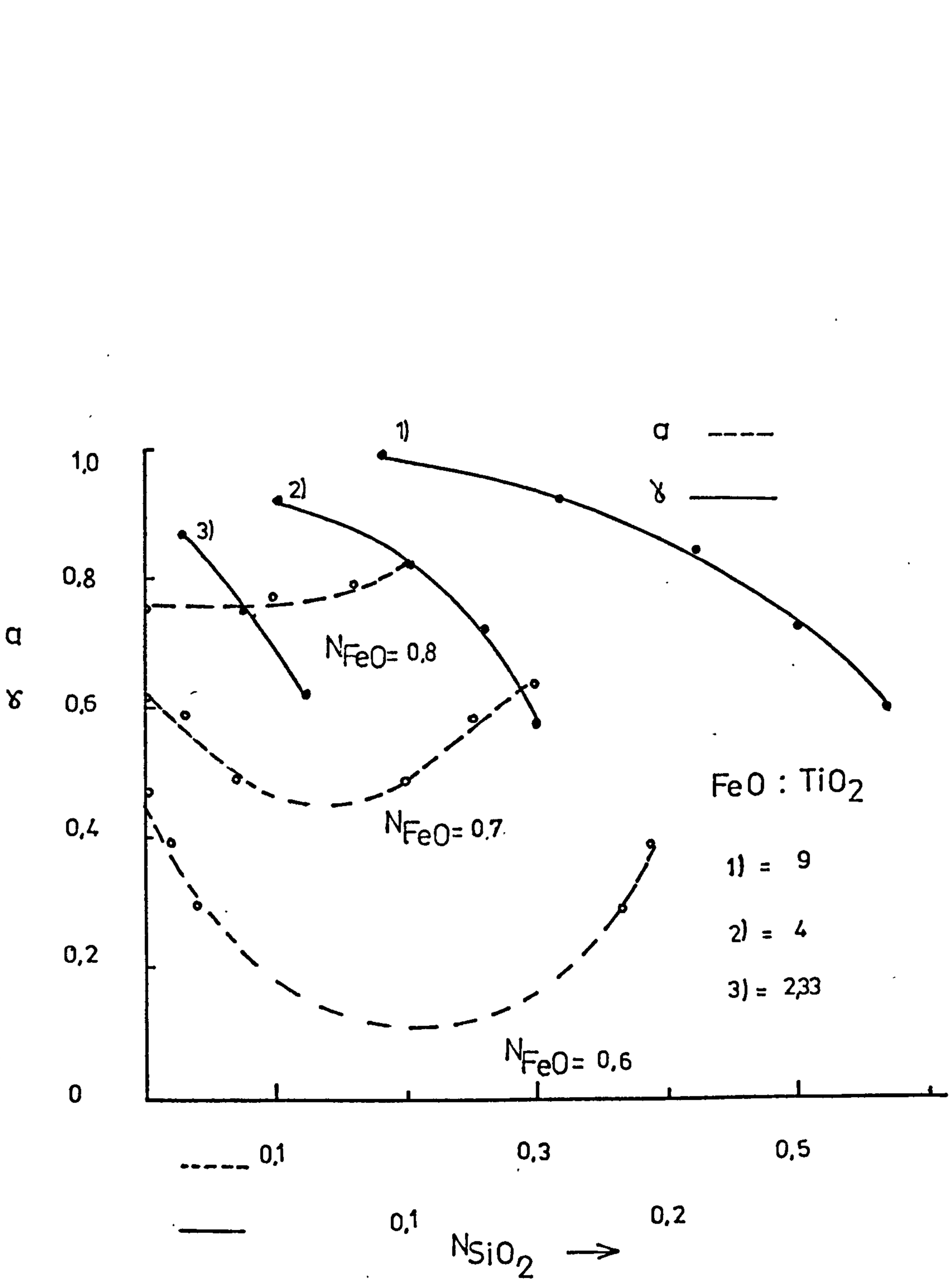

Fig. (3.9) The Effect Of Replacement Of TiO_2 By SiO_2 On FeO Activity At Constant N_{FeO}, And The Variation Of The Activity Coefficient Of FeO With Addition Of SiO_2 to FeO-TiO_2 Binary At Constant FeO:TiO_2 Ratio.

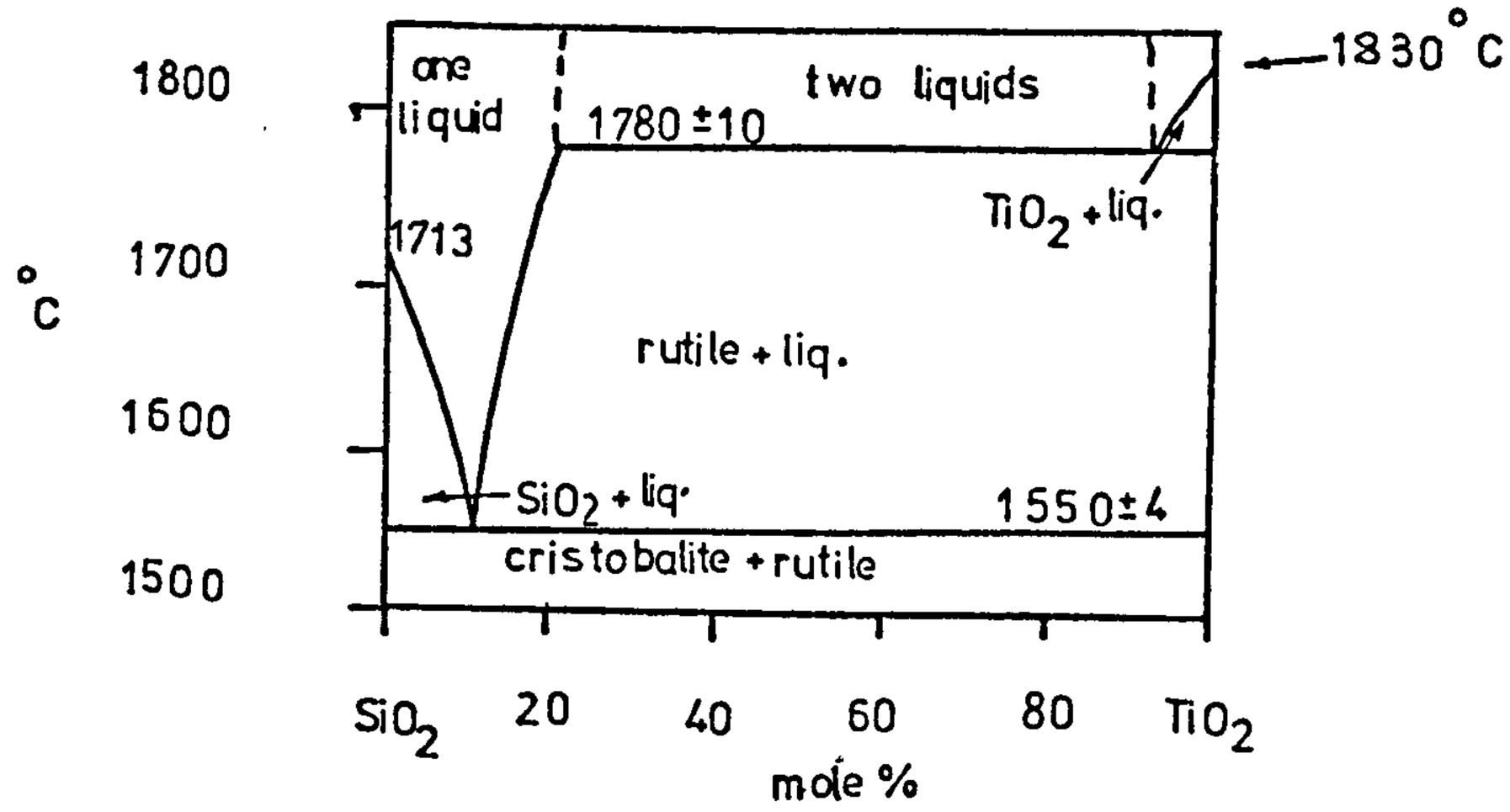

Fig. (3.10) SiO_2-TiO_2 Phase Diagram

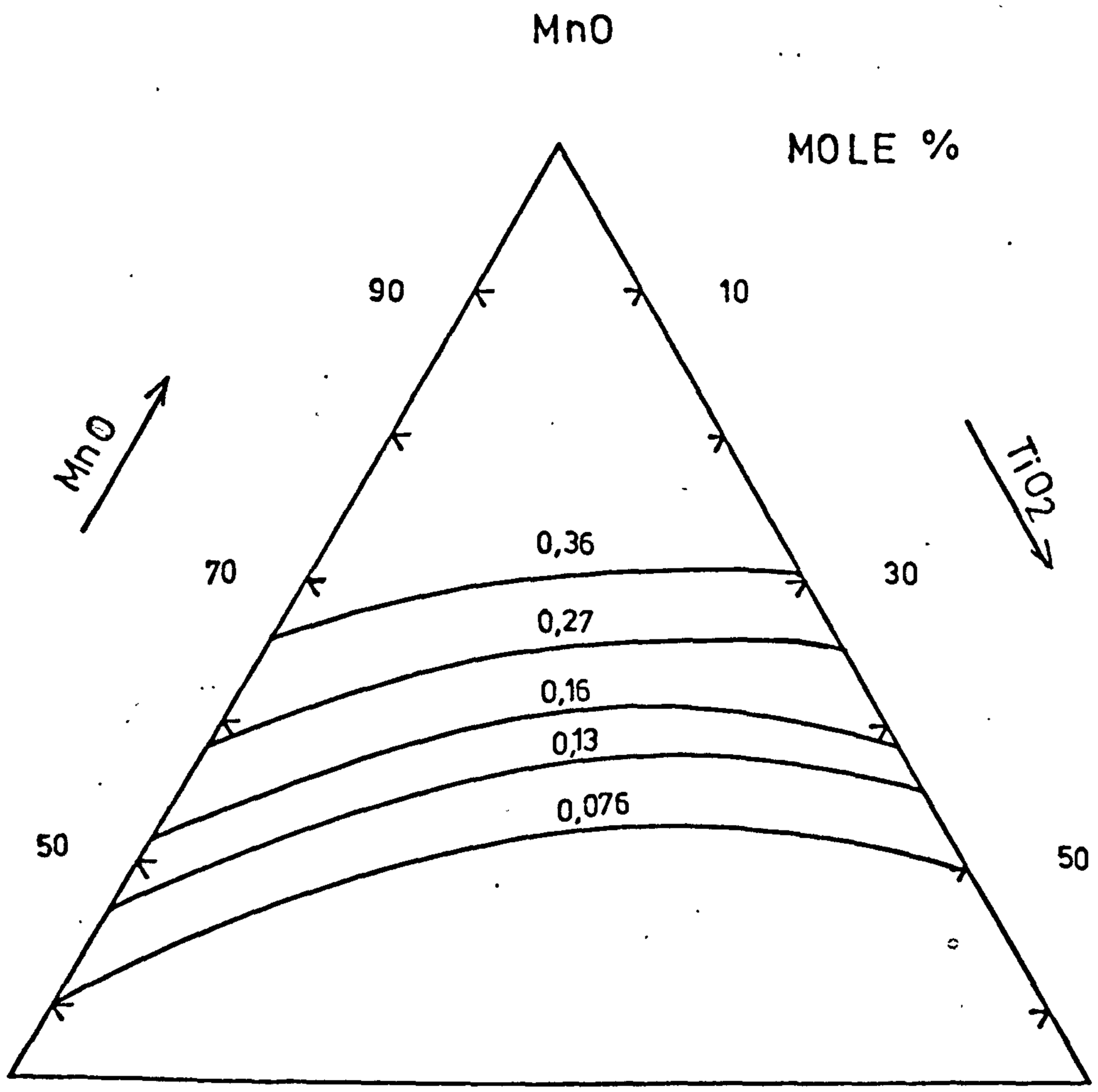

Fig. (3.11) MnO Iso-Activity Curves In The System $MnO-TiO_2-SiO_2$ At $1500^{o}C$ (38).

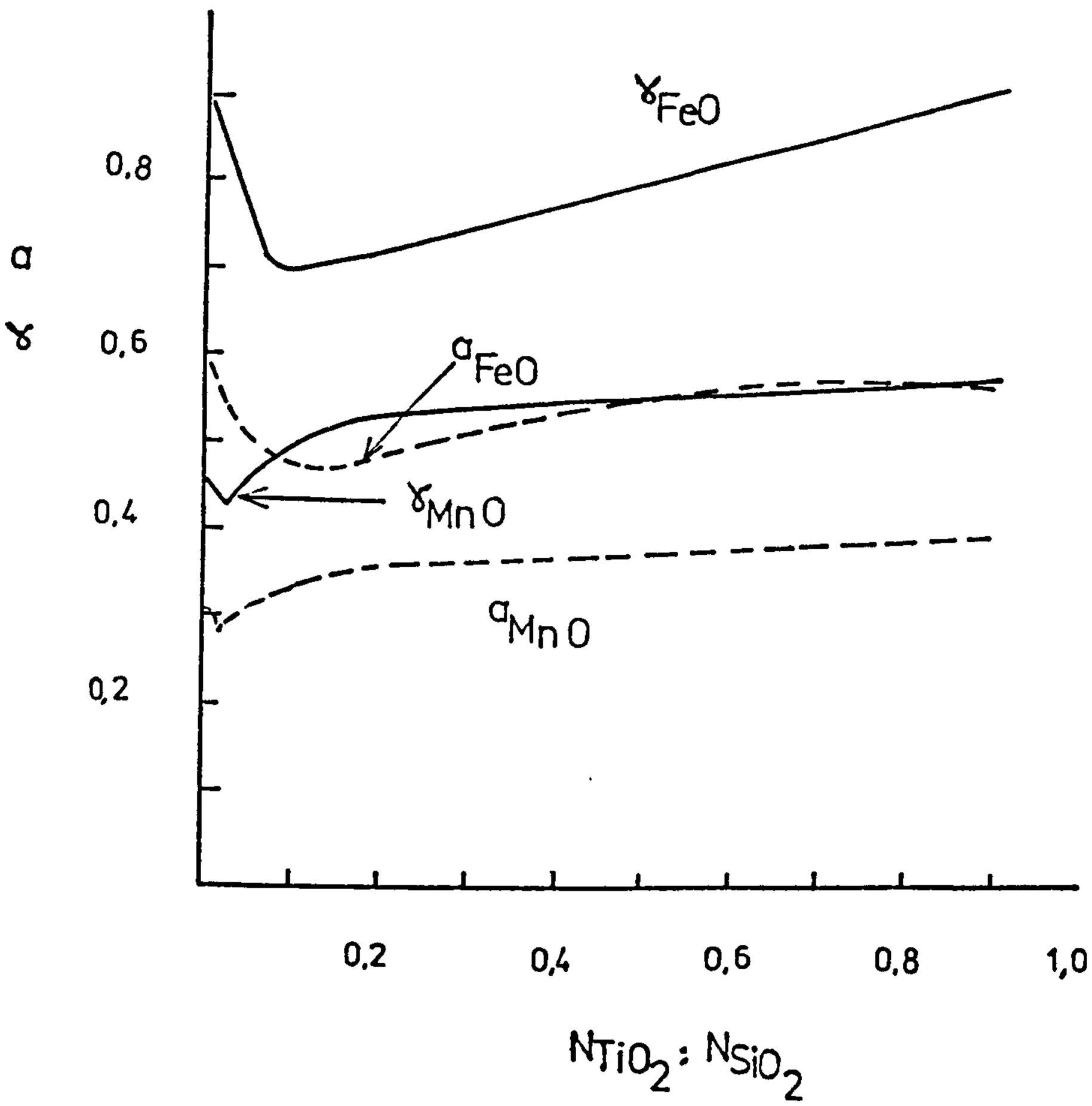

Fig. (3.12) The Variation Of FeO And MnO Activity Coefficient For $N_{FeO} = N_{MnO} = 0.69$ With TiO_2: SiO_2 Ratio In The Ternary Systems $FeO-TiO_2-SiO_2$ And $MnO-TiO_2-SiO_2$.

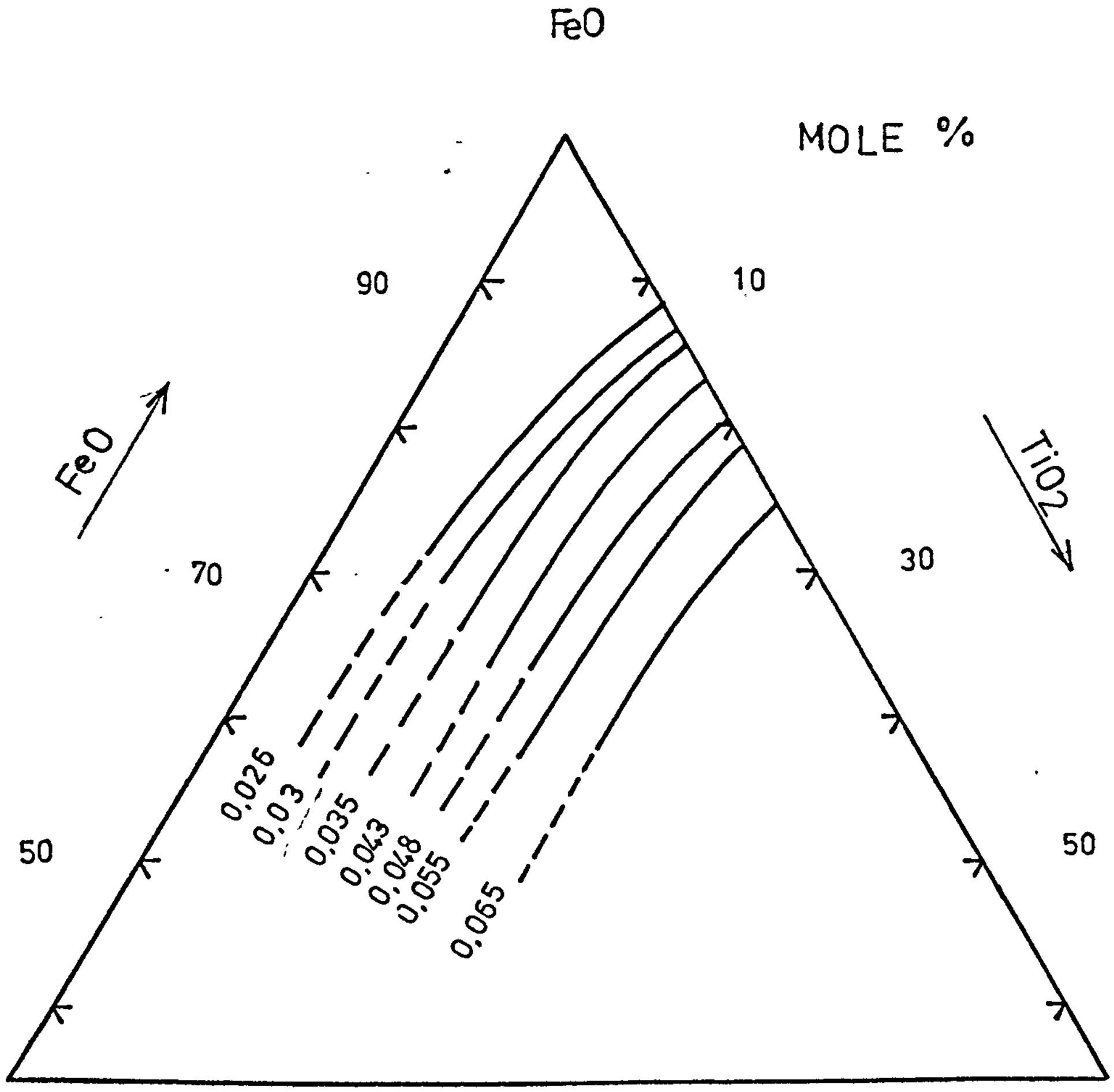

Fig. (3.13) TiO_2 IsoActivity Curves In The System $FeO-TiO_2-SiO_2$ At 1475°C Calculated By Gibbs-Duhem Equation.

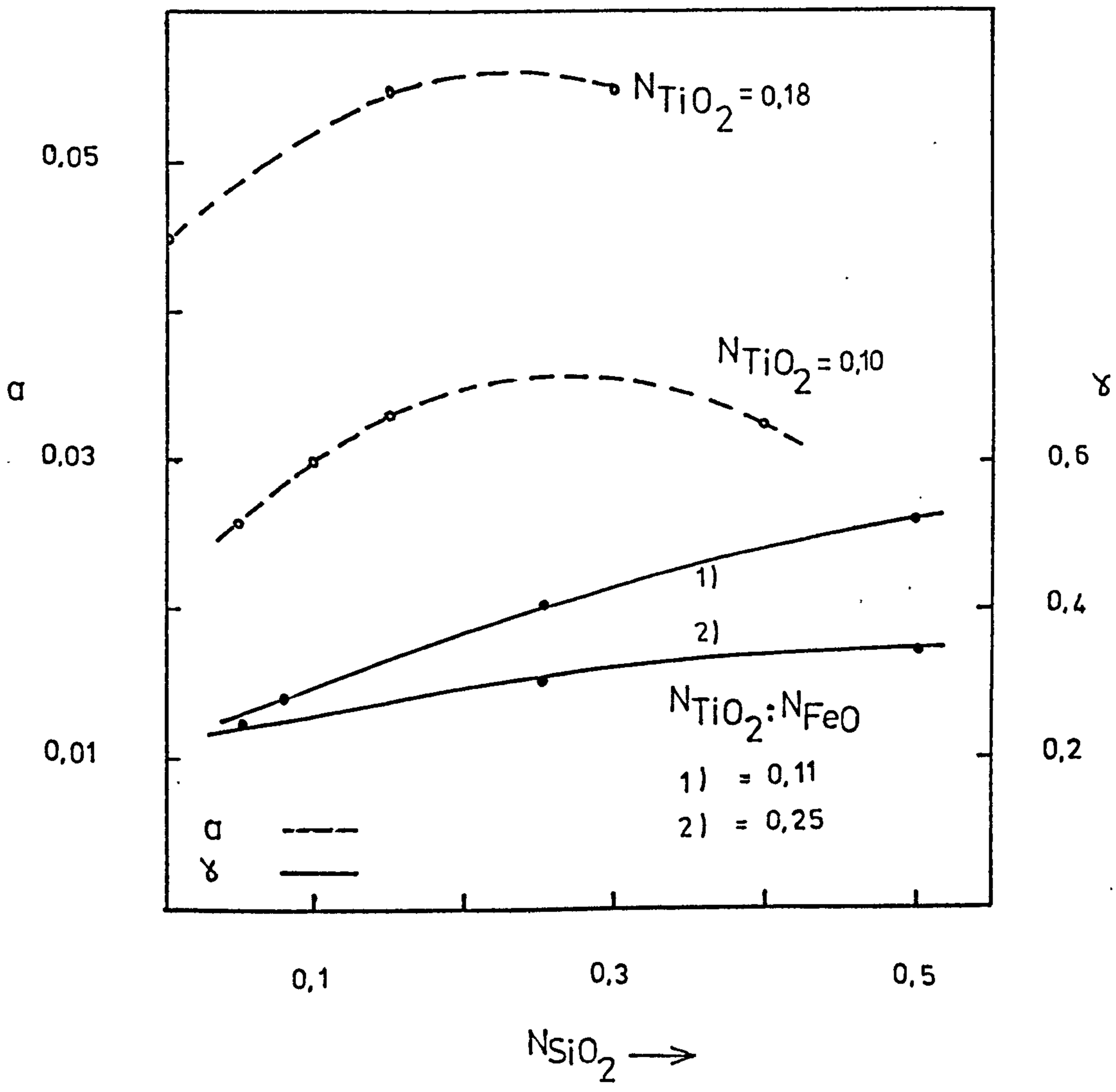

Fig. (3.14) The Effect Of Replacement Of FeO By SiO_2 On TiO_2 Activity At Constant N_{TiO_2}, And The Variation Of The Activity Coefficient Of TiO_2 With The Addition Of SiO_2 To FeO-TiO_2 Binary At Constant TiO_2 : FeO Ratio.

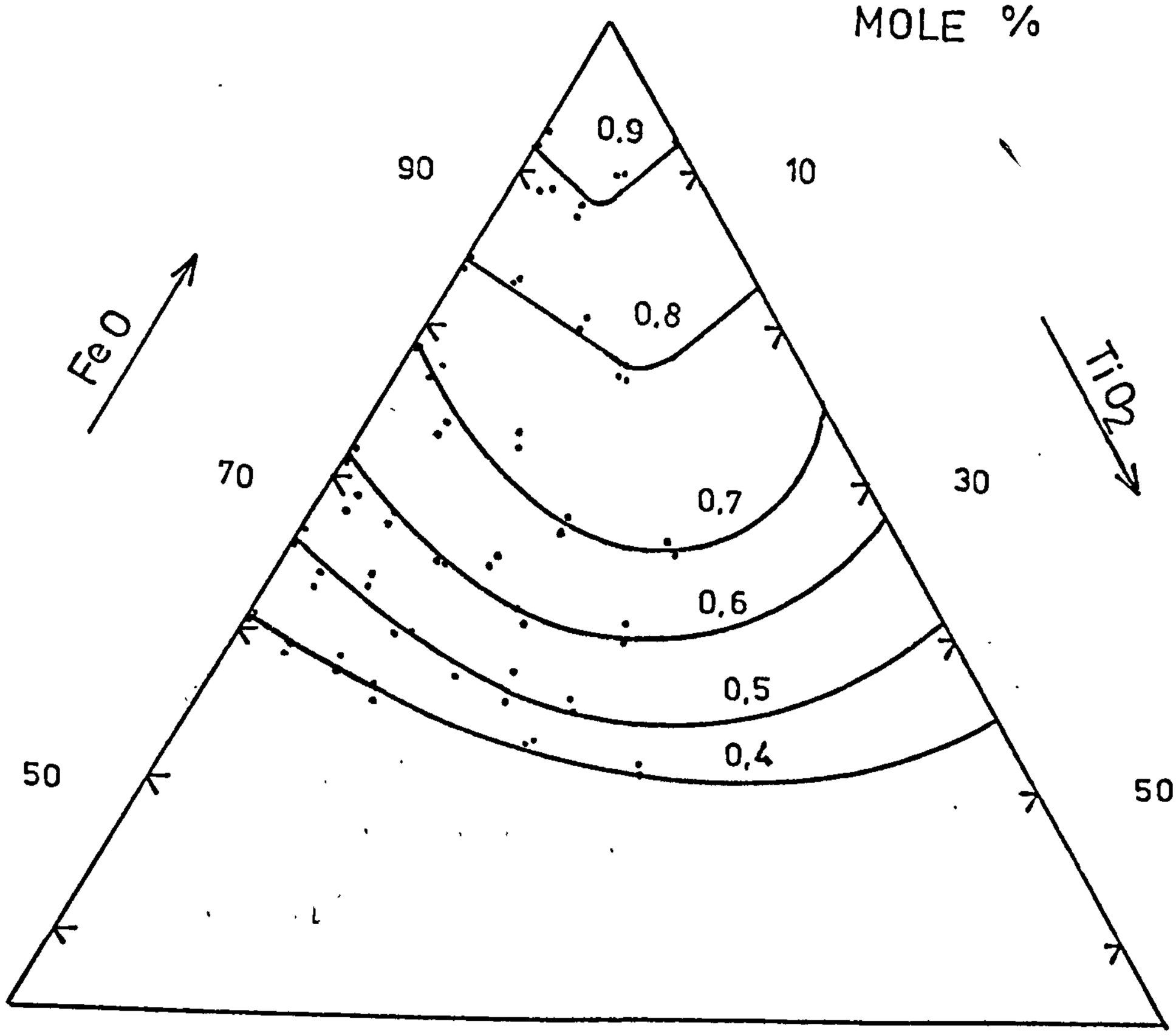

Fig. (3.15) FeO Iso-Activity Curves In The System $FeO-TiO_2-CaO$ At $1470^{o}C$.

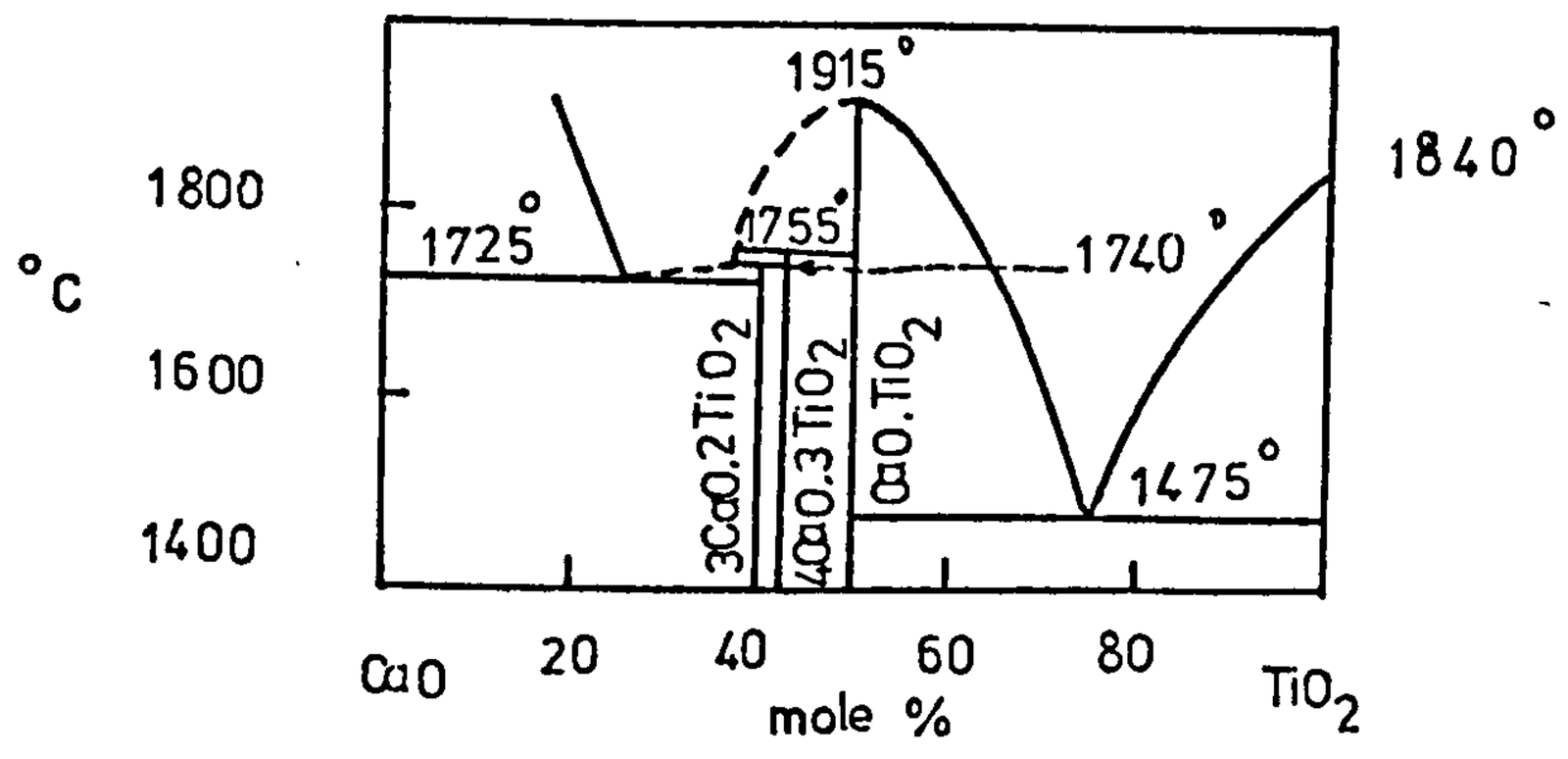

Fig. (3.16) The CaO-TiO_2 Phase Diagram

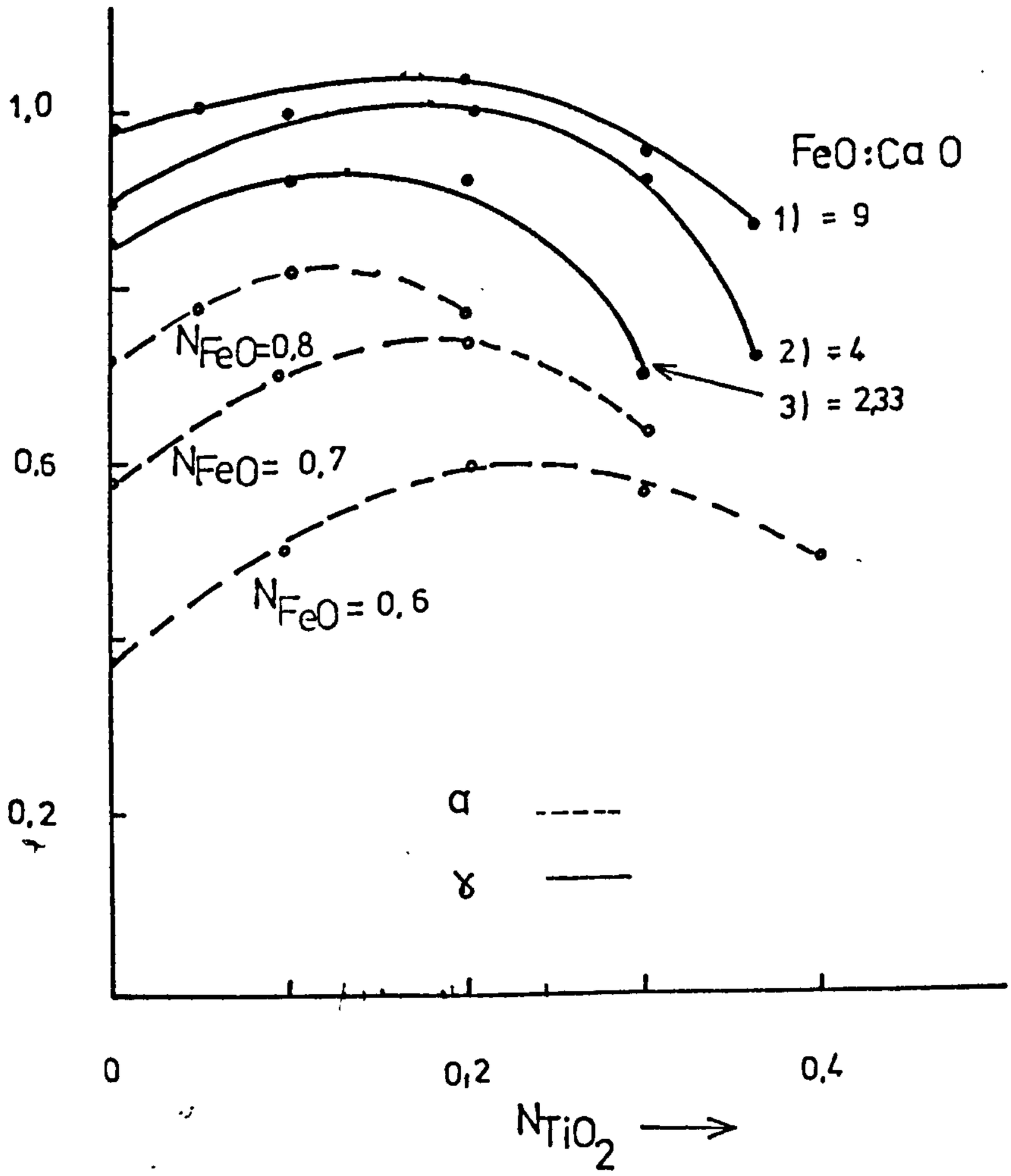

Fig. (3.17) The Effect Of Replacement Of CaO By TiO_2 On FeO Activity At Constant N_{FeO}, And The Variation Of The Activity Coefficient Of FeO With Addition Of TiO_2 To FeO-CaO Binary At Constant FeO : CaO Ratio.

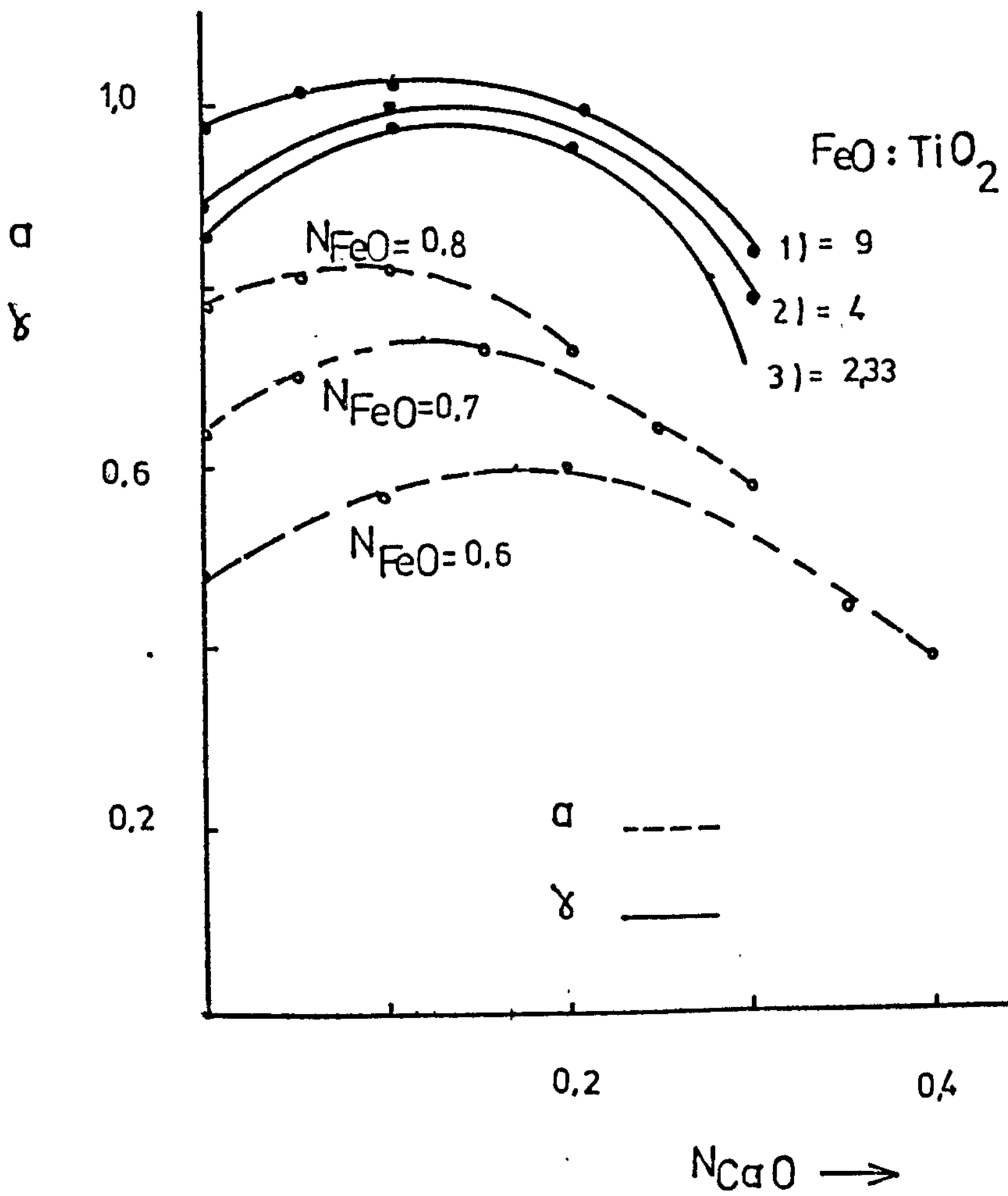

Fig. (3.18) The Effect Of Replacement Of TiO_2 By CaO On FeO Activity At Constant N_{FeO}, And The Variation Of The Activity Coefficient Of FeO With The Addition Of CaO To FeO-TiO_2 Binary At Constant FeO : TiO_2 Ratio.

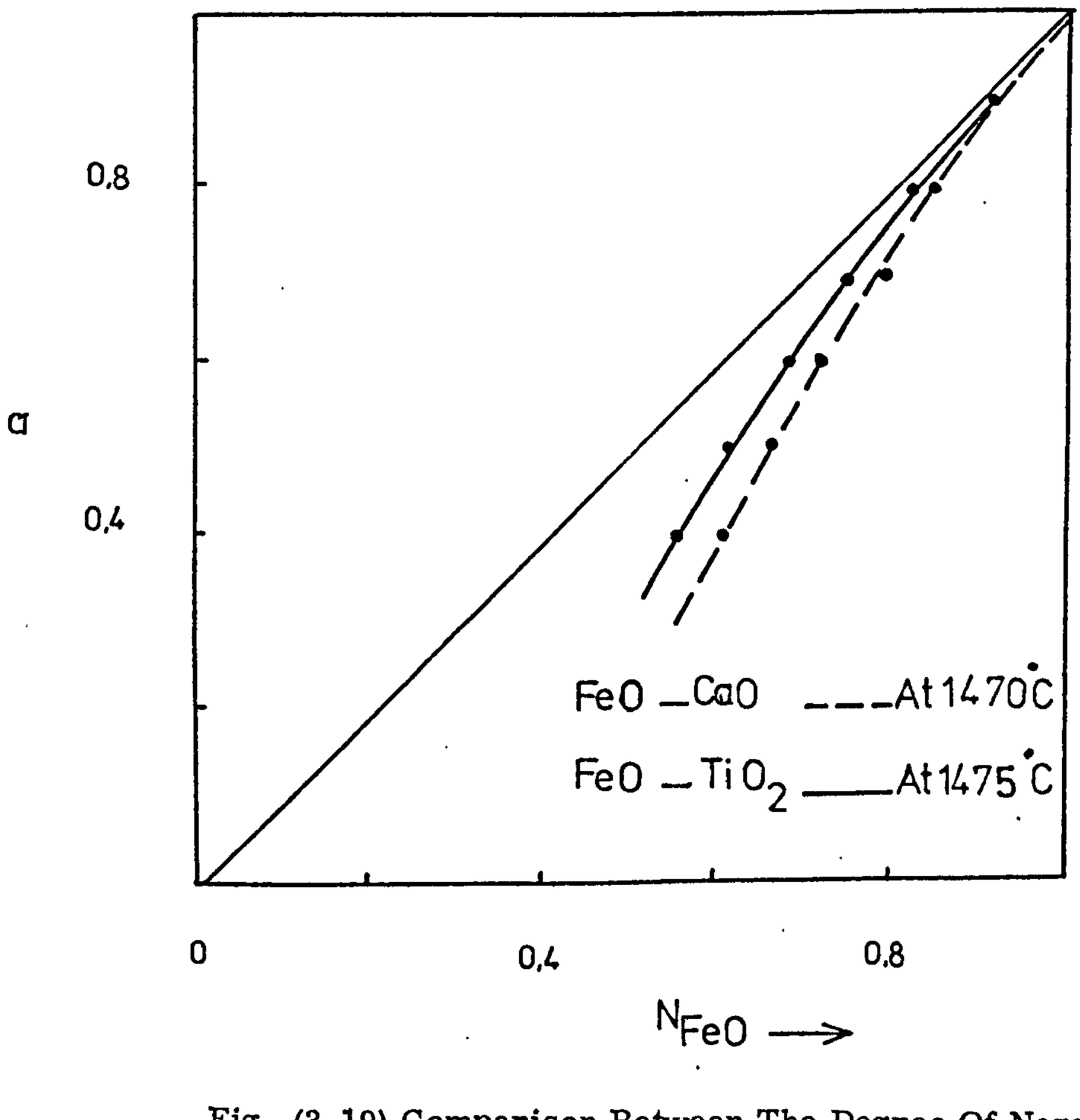

Fig. (3.19) Comparison Between The Degree Of Negative Deviation From Ideality In The Binary Systems FeO-TiO_2 And FeO-CaO.

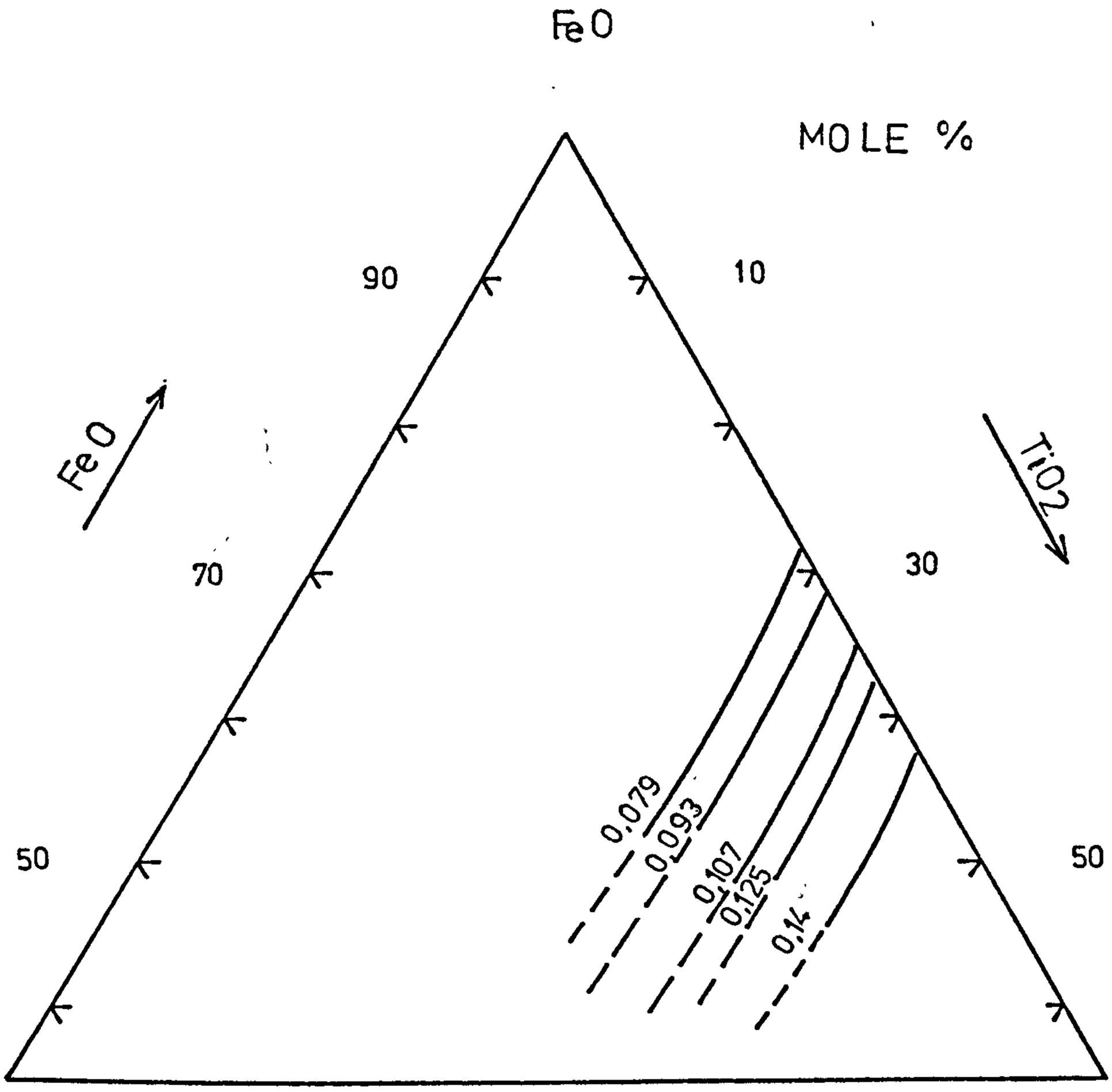

Fig. (3.20) TiO_2 Iso-Activity Curves In The System FeO-TiO_2-CaO At 1470°C Calculated By Gibbs-Duhem Equation.

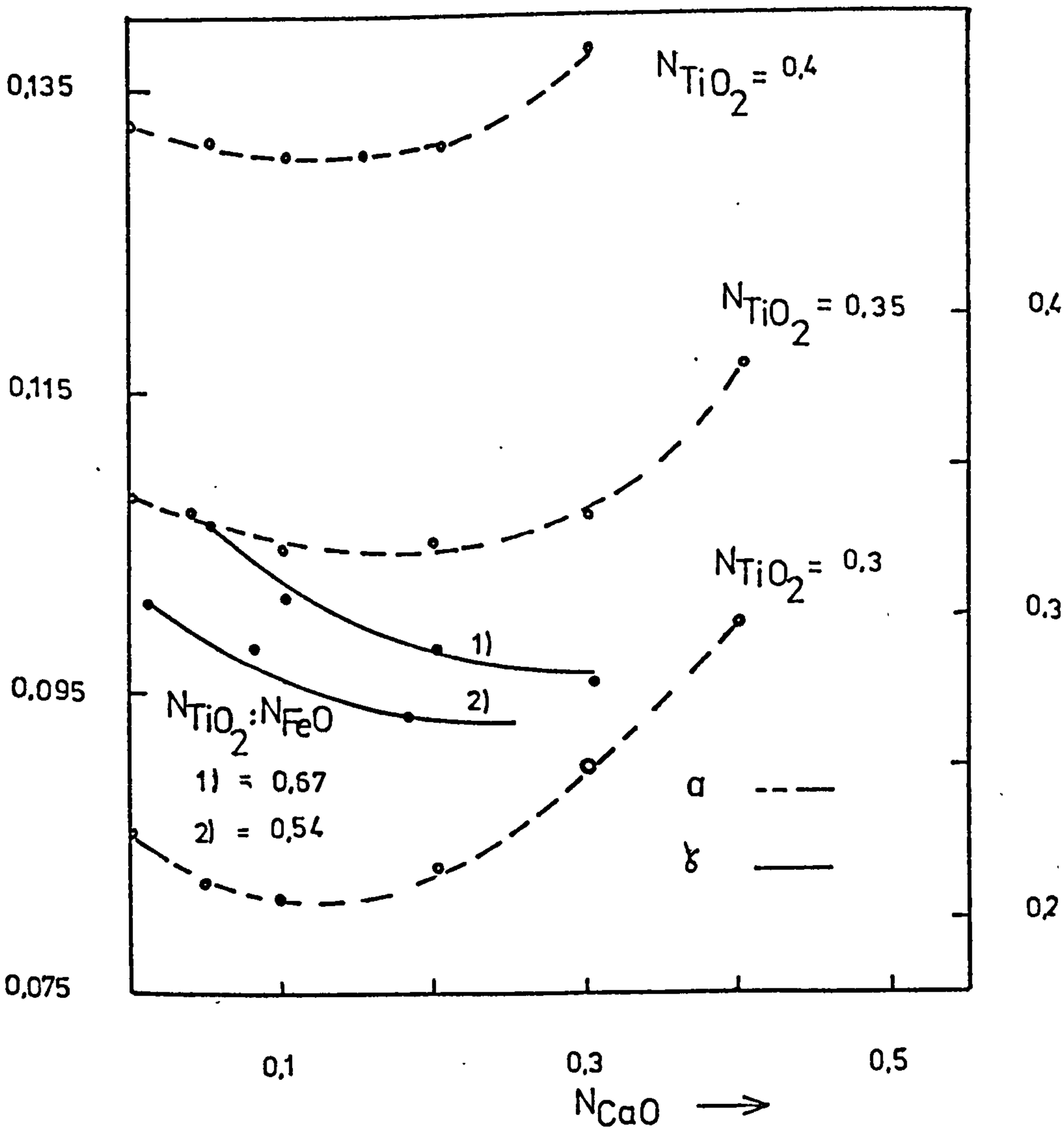

Fig. (3.21) The Effect Of Replacement Of FeO By CaO On TiO_2 Activity At Constant N_{TiO_2} And The Variation Of The Activity Coefficient Of TiO_2 With Addition Of CaO To FeO-TiO_2 Binary At Constant TiO_2 : FeO Ratio.

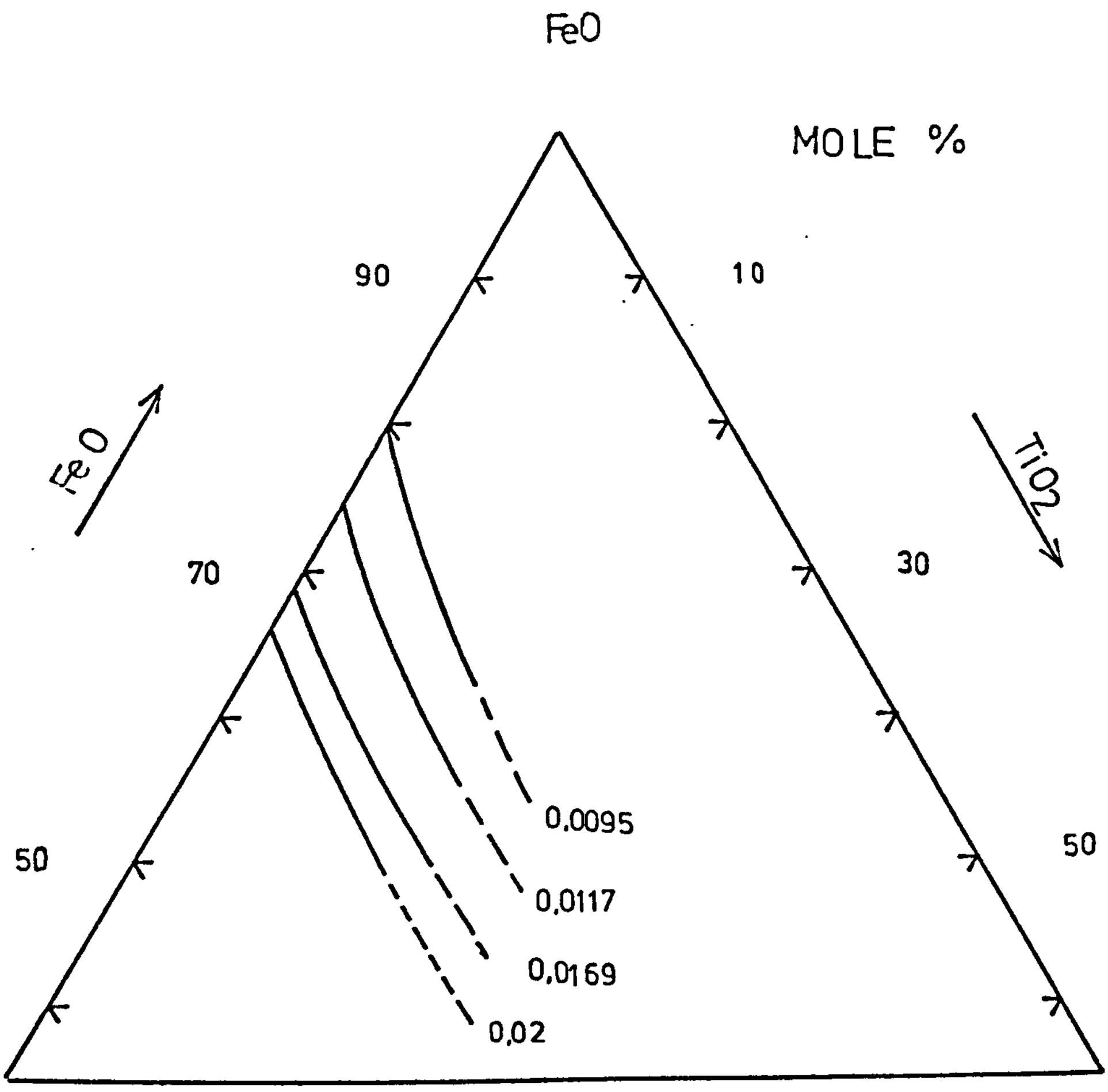

Fig. (3.22) CaO Iso-Activity Curves In The System FeO-TiO_2-CaO At 1470°C Calculated By Gibbs-Duhem Equation.

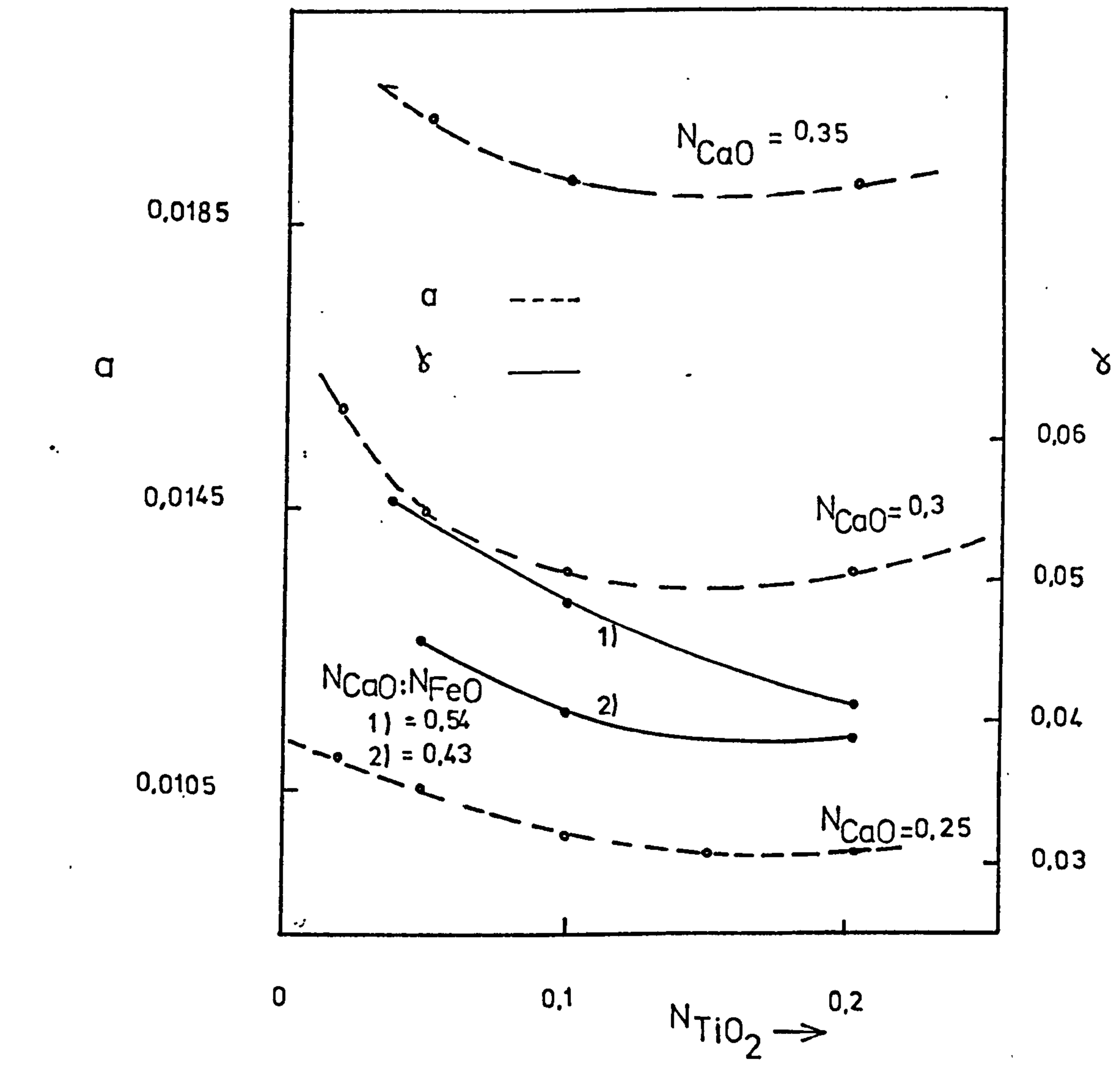

Fig. (3.23) The Effect Of Replacement Of FeO By TiO_2 On CaO Activity At Constant N_{CaO}, And The Variation Of The Activity Coefficient Of CaO With The Addition Of TiO_2 To FeO-CaO Binary At Constant CaO : FeO Ratio.

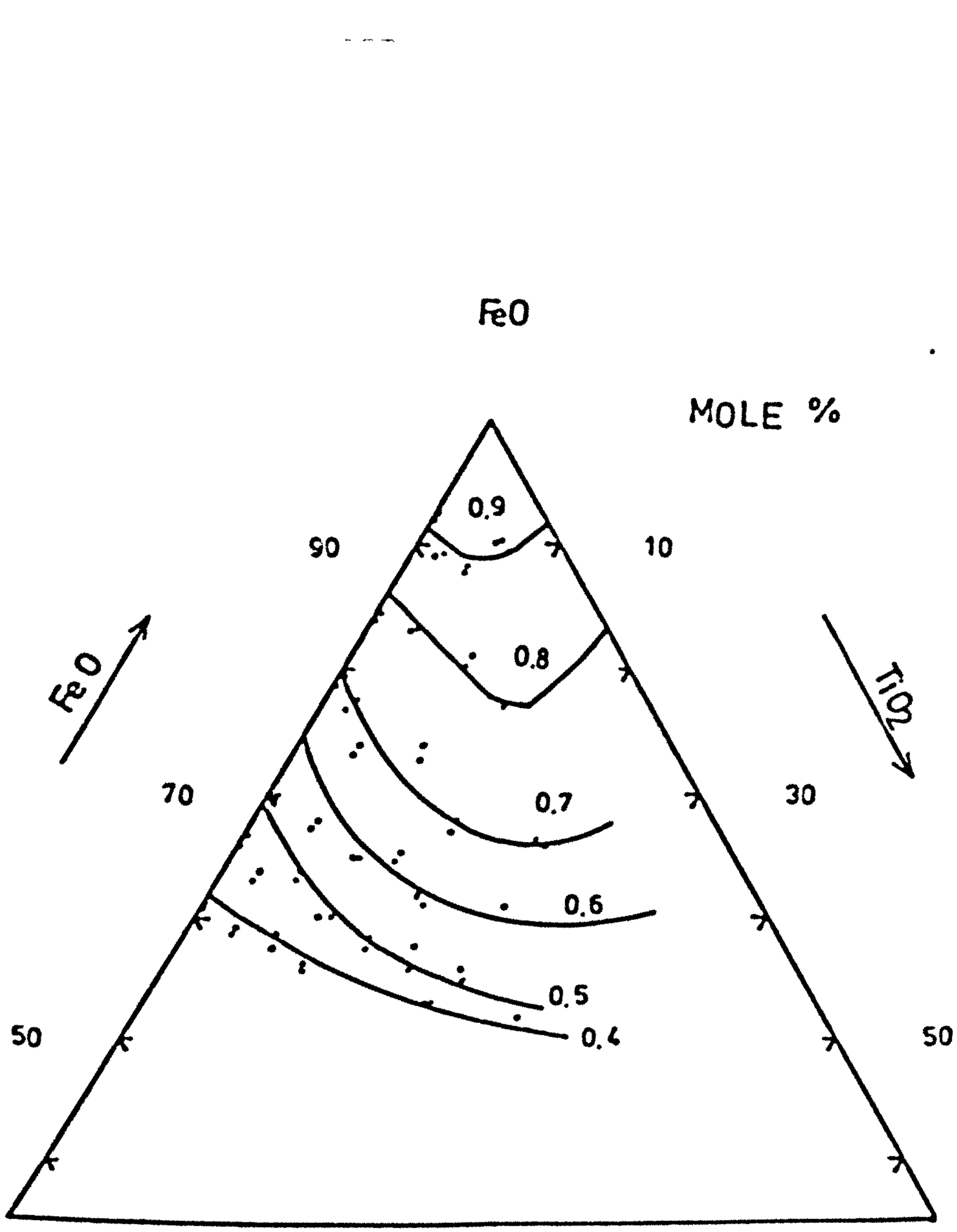

Fig. (3.24) FeO Iso-Activity Curves In The System FeO-TiO_2-CaO At 1470°C Calculated By Regular Solution Model.[2]

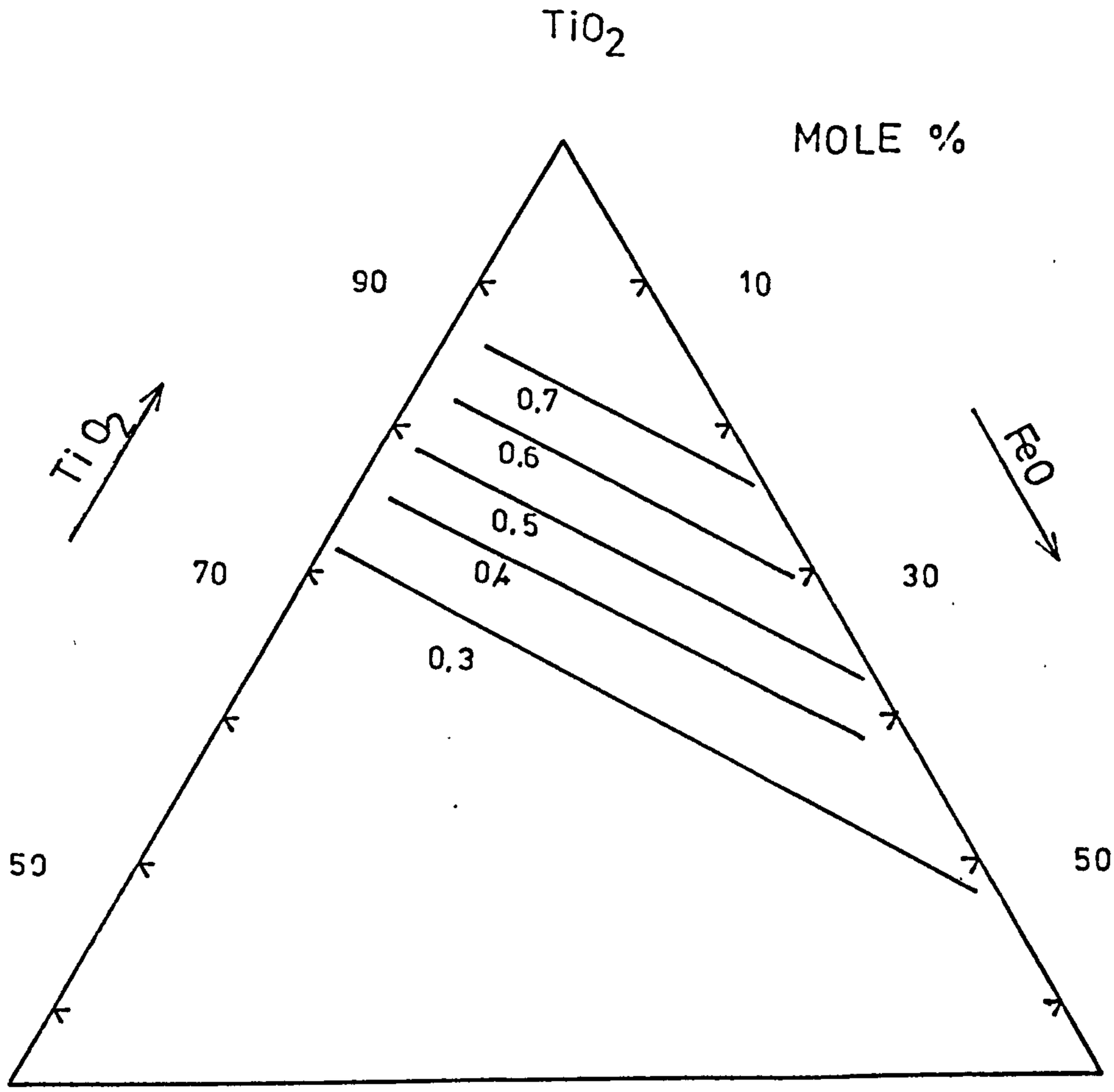

Fig. (3.25) TiO_2 Iso-Activity Curves In The System $FeO-TiO_2-CaO$ At 1470°C Calculated By Regular Solution Model.

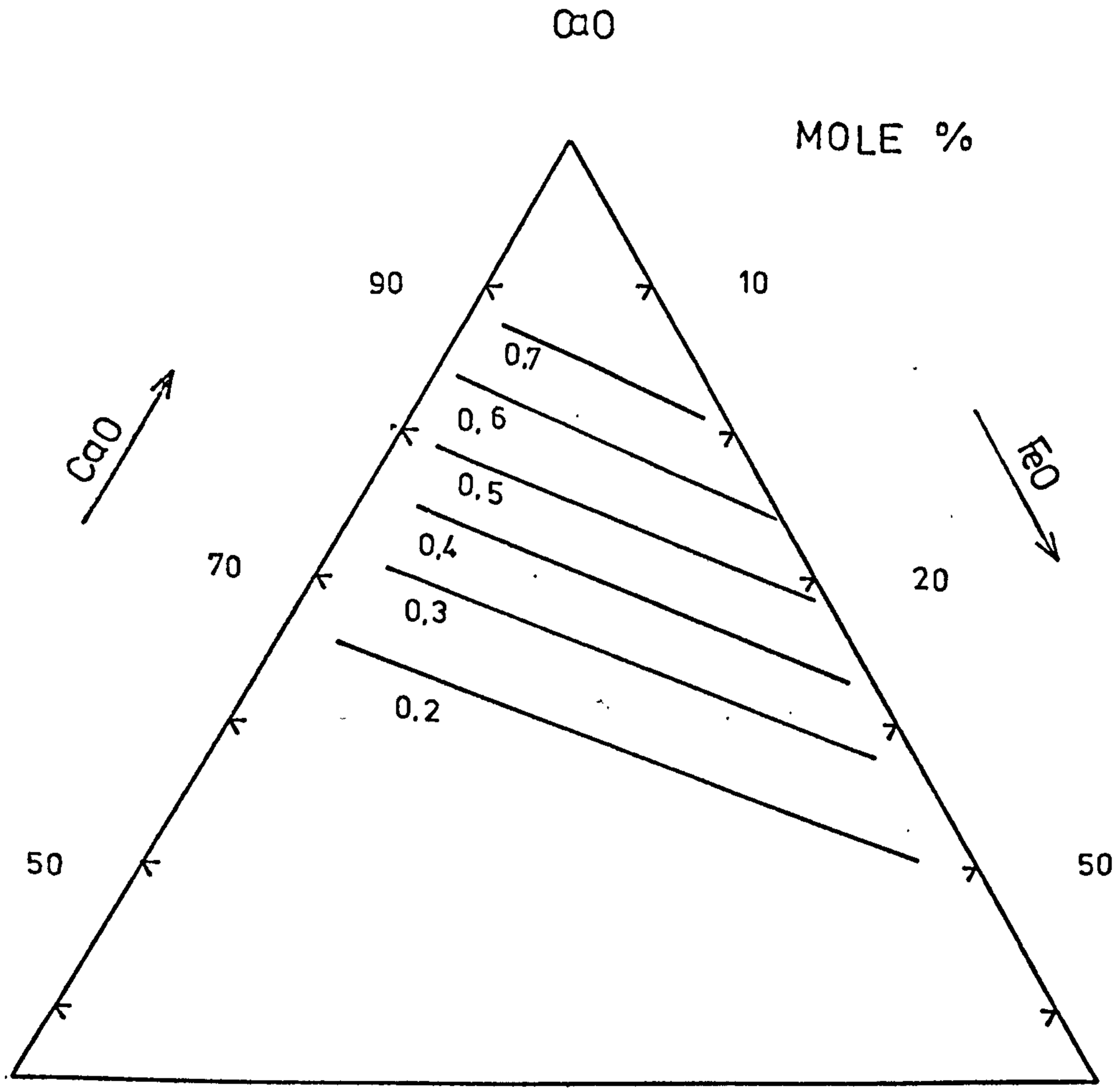

Fig. (3.26) CaO Iso-Activity Curves In The System $FeO-TiO_2-CaO$ At $1470^{o}C$ Calculated By Regular Solution Model.

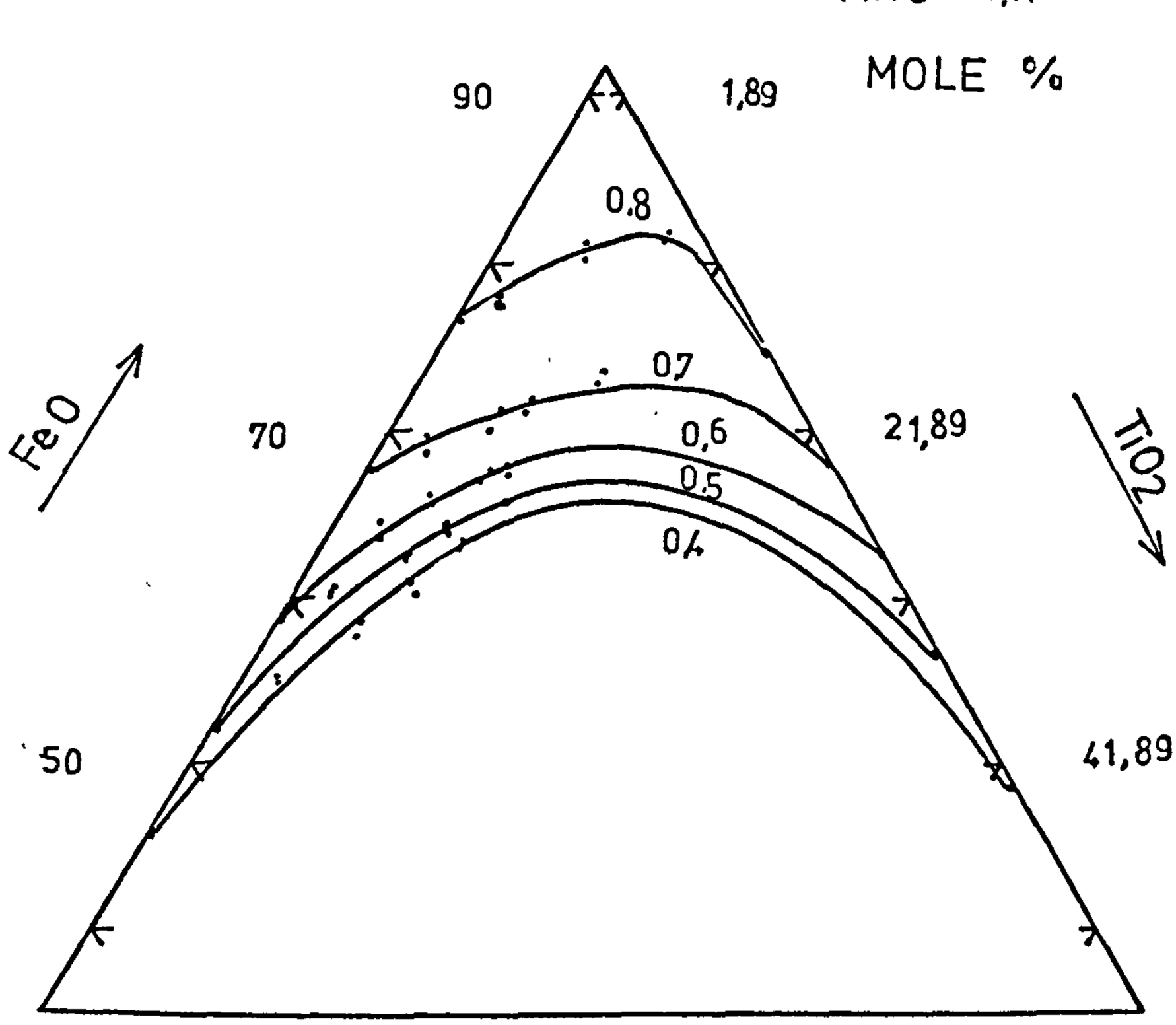

Fig. (3.27) FeO Iso-Activity Curves In The System $FeO-TiO_2-SiO_2-MnO$ At $1475^{o}C$.

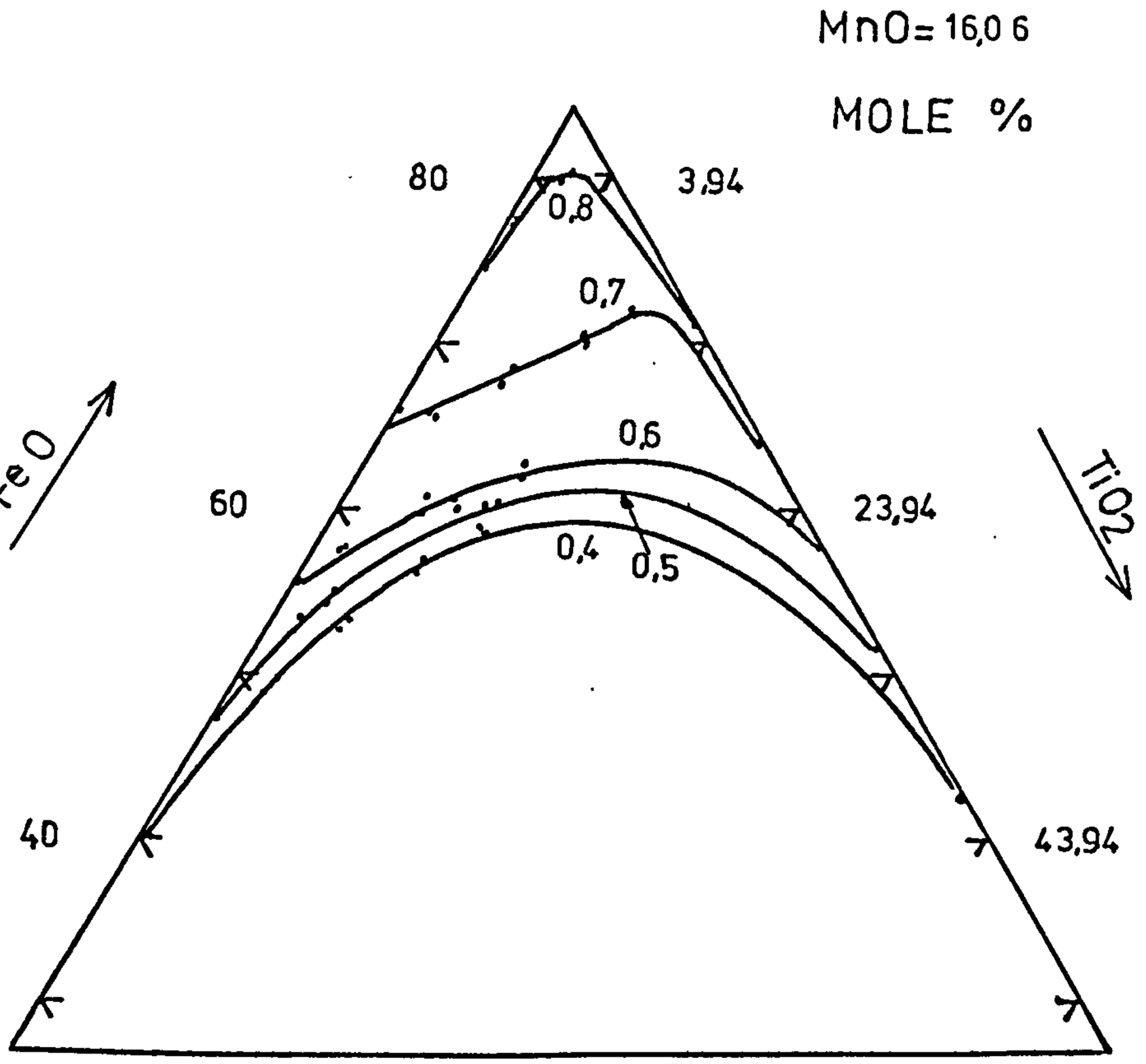

Fig. (3.28) FeO Iso-Activity Curves In The System $FeO-TiO_2-SiO_2-MnO$ At $1475^{o}C$.

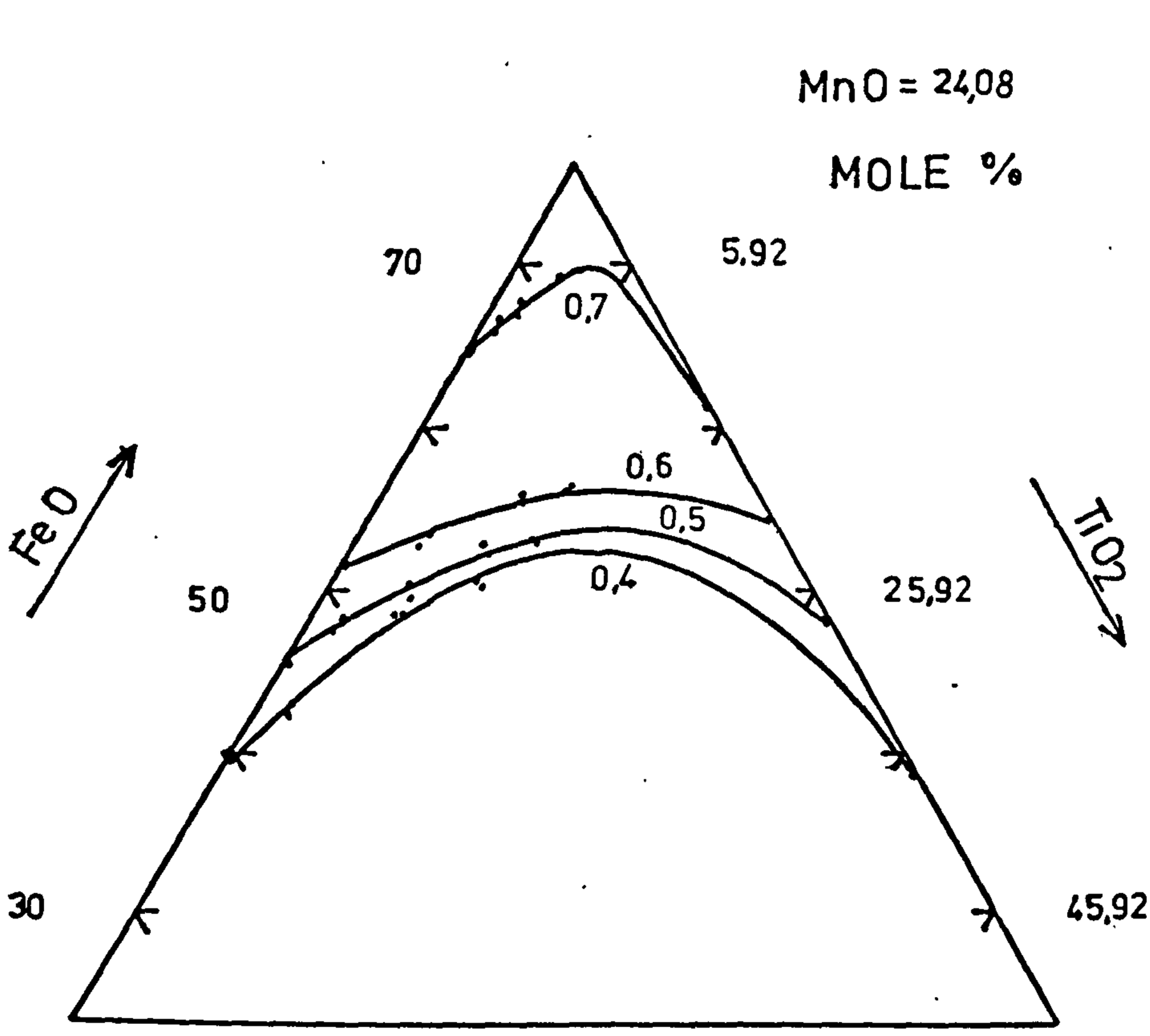

Fig. (3.29) FeO Iso-Activity Curves In The System $FeO-TiO_2-SiO_2-MnO$ At 1475 ^{o}C.

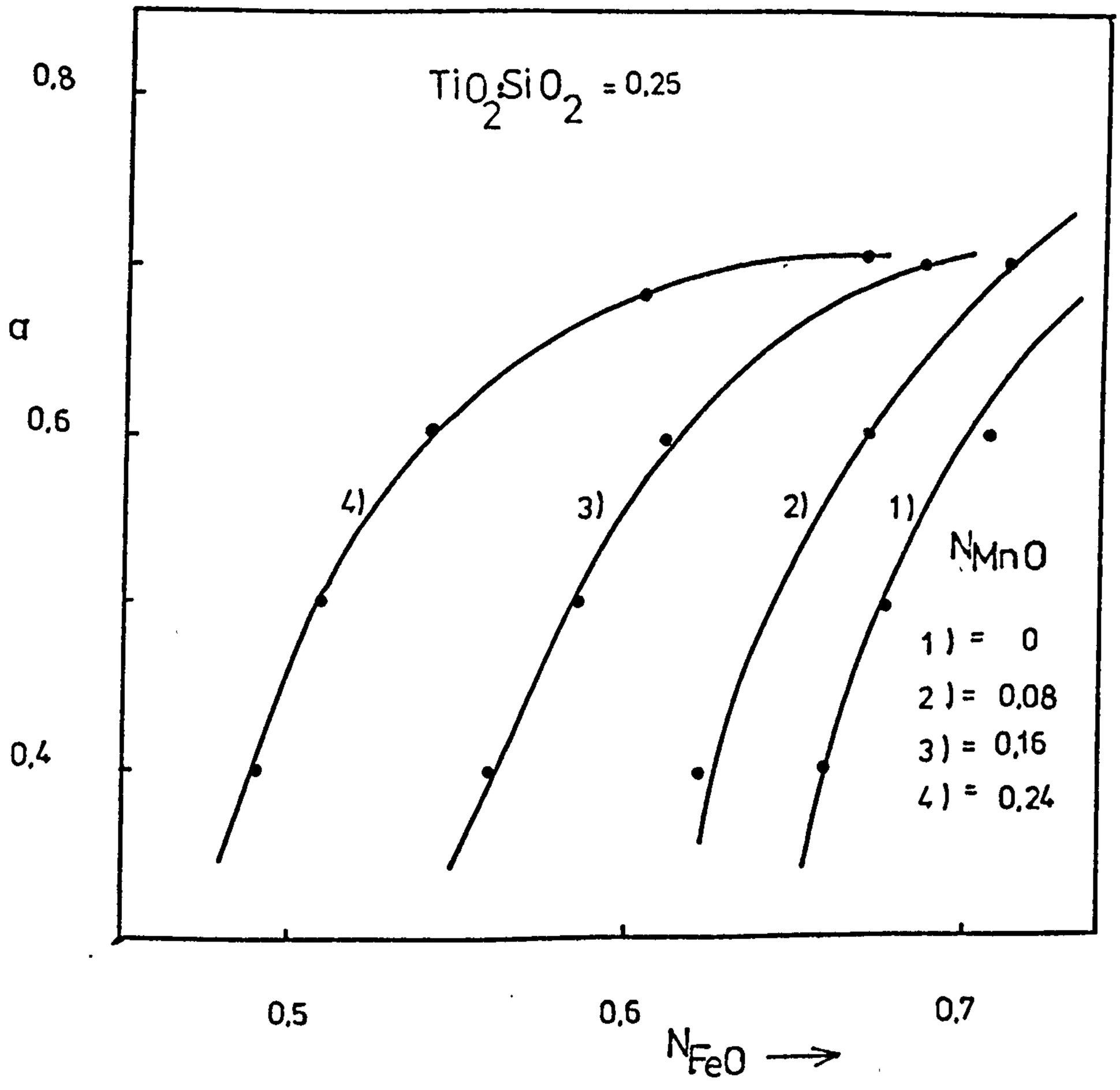

Fig. (3.30) The Effect Of Addition Of MnO To $FeO-TiO_2-SiO_2$ Ternary System On FeO Activity At Constant TiO_2 : SiO_2 = 0.25.

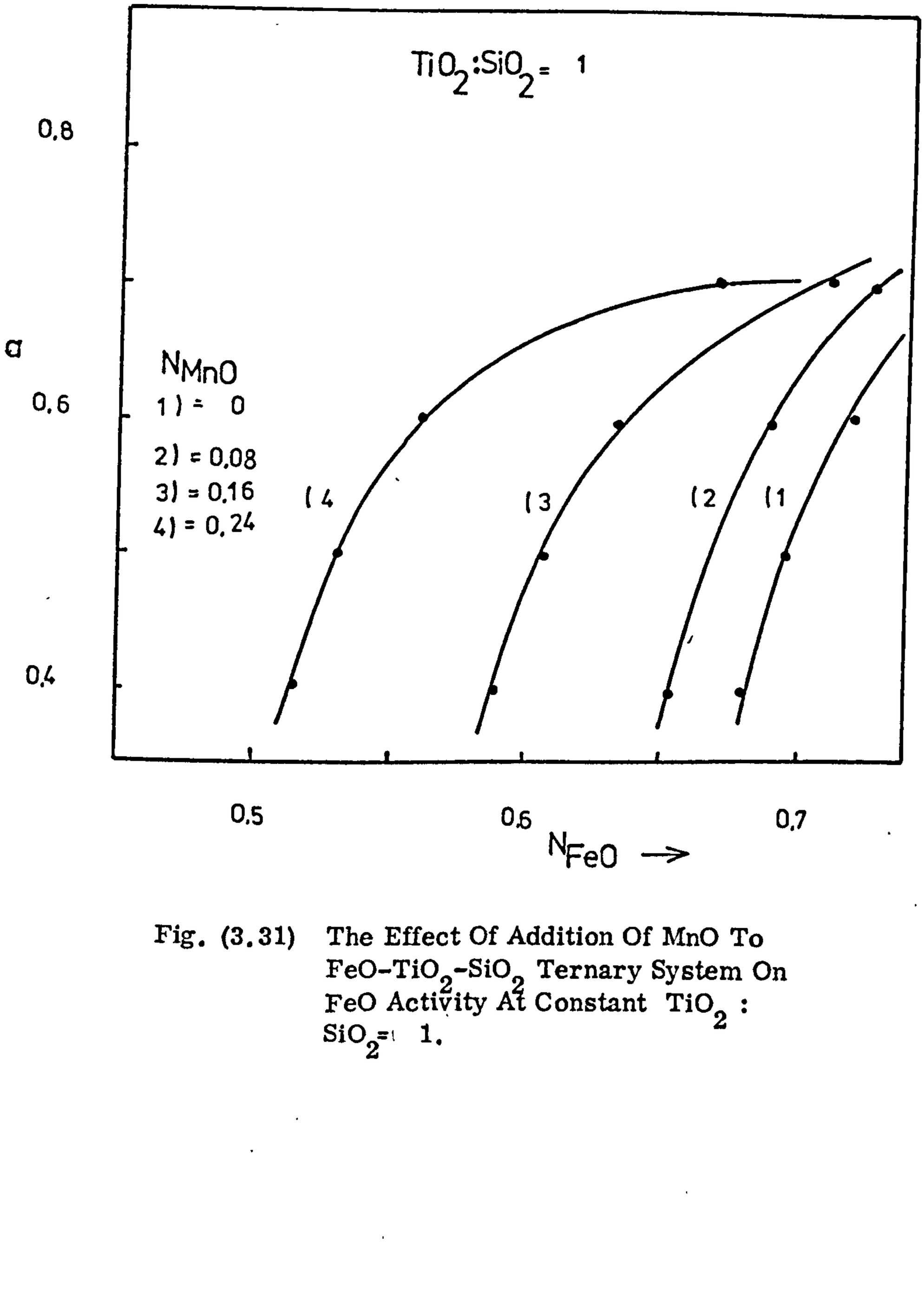

Fig. (3.31) The Effect Of Addition Of MnO To $FeO-TiO_2-SiO_2$ Ternary System On FeO Activity At Constant TiO_2 : SiO_2 = 1.

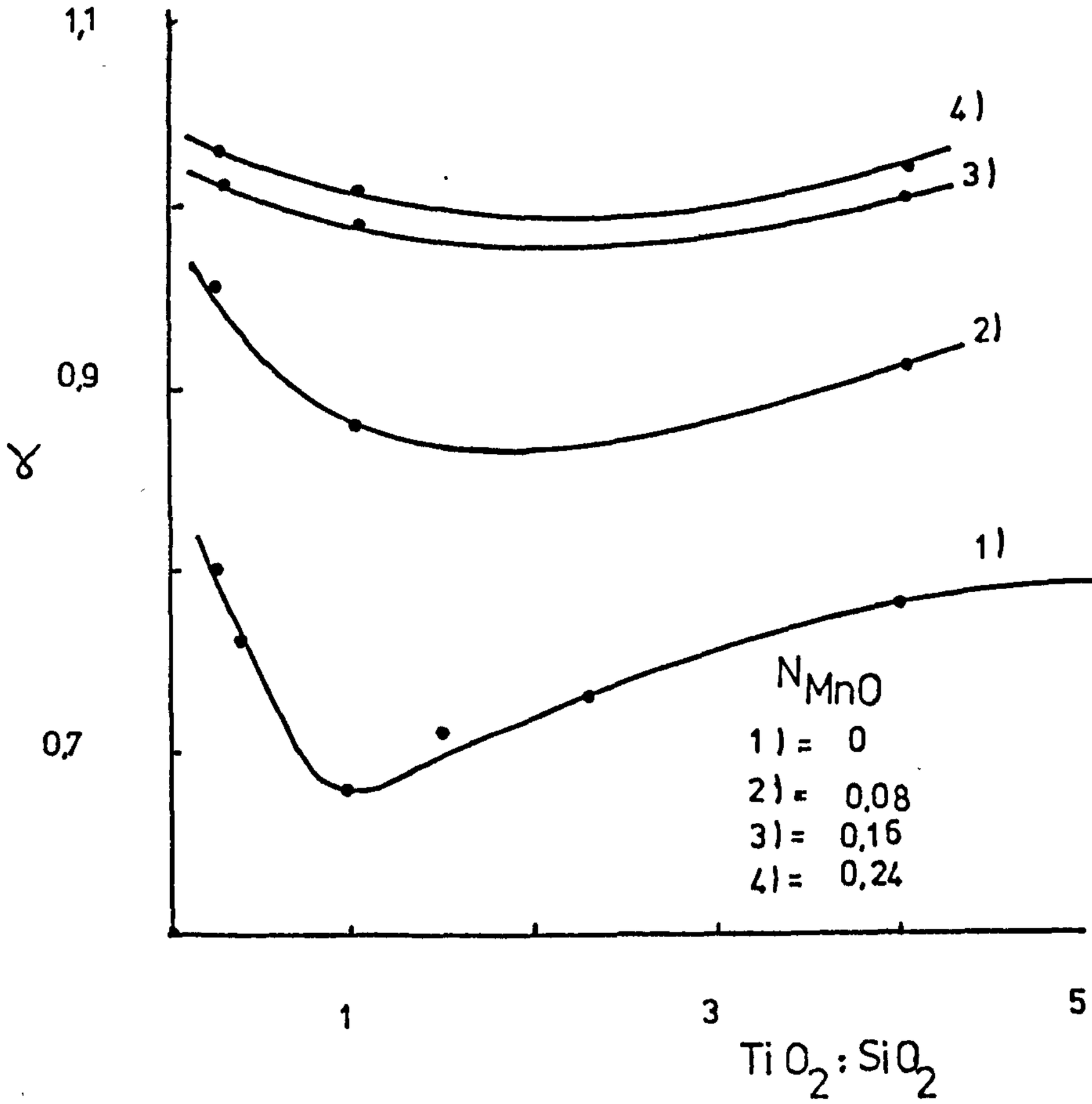

Fig. (3.32) The Effect Of Addition Of MnO To $FeO-TiO_2-SiO_2$ System On γ_{FeO} For Various $TiO_2 : SiO_2$ And $N_{FeO} = 0.69$.

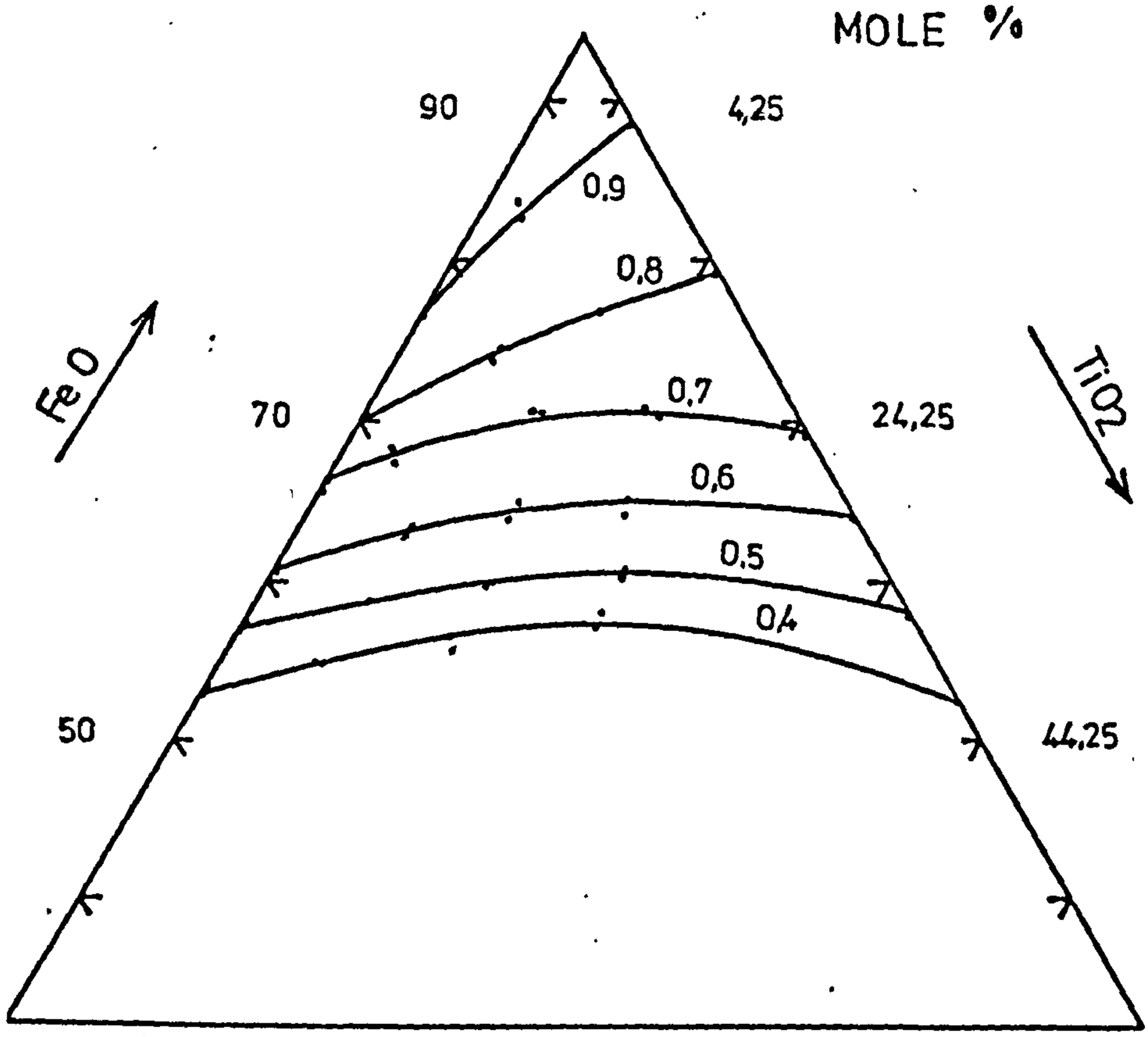

Fig. (3.33) FeO Iso-Activity Curves In The System $FeO-TiO_2-SiO_2-CaO$ At $1470^{o}C$.

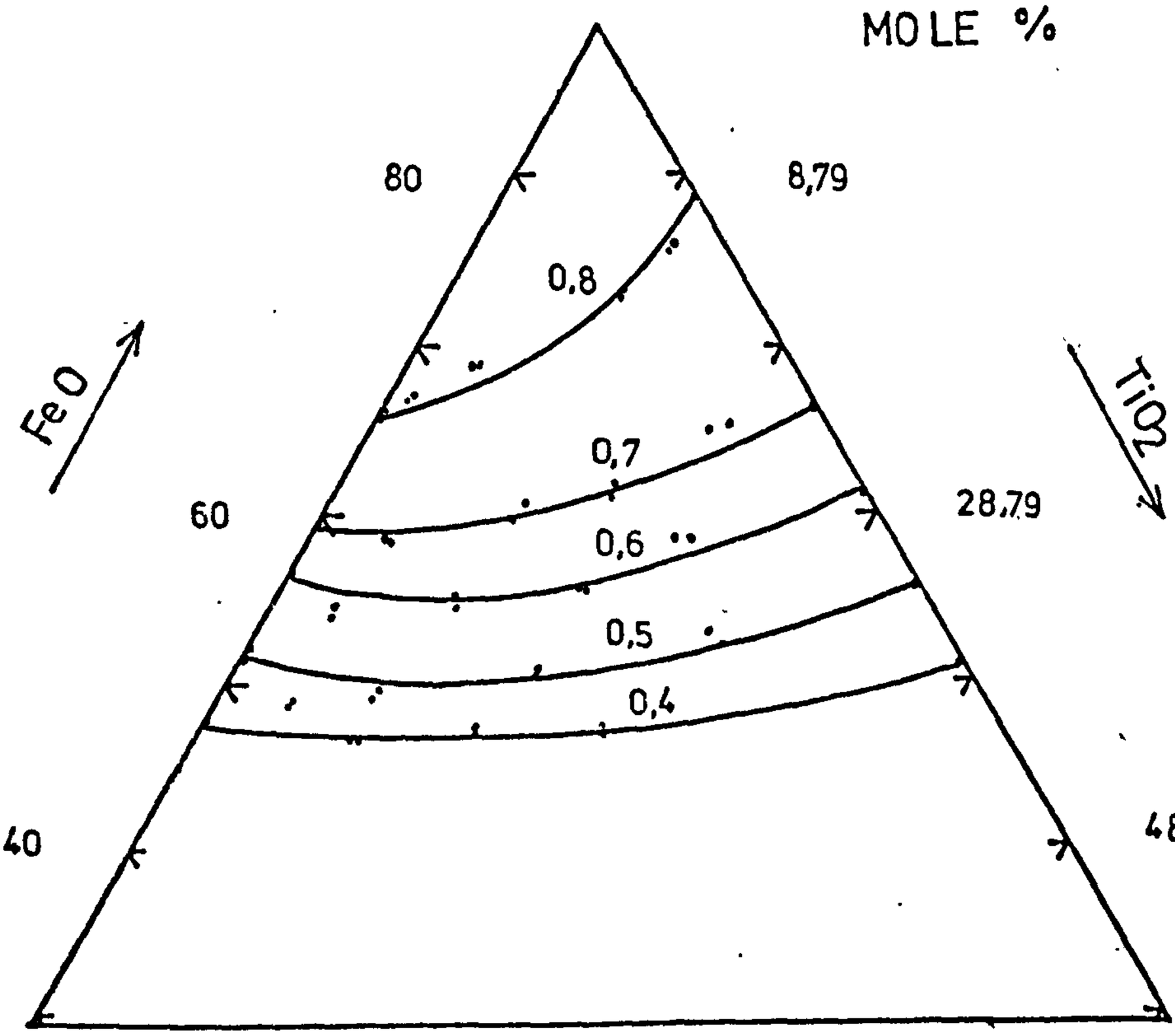

Fig. (3.34) FeO Iso-Activity Curves In The System $FeO-TiO_2-SiO_2-CaO$ At 1470°C.

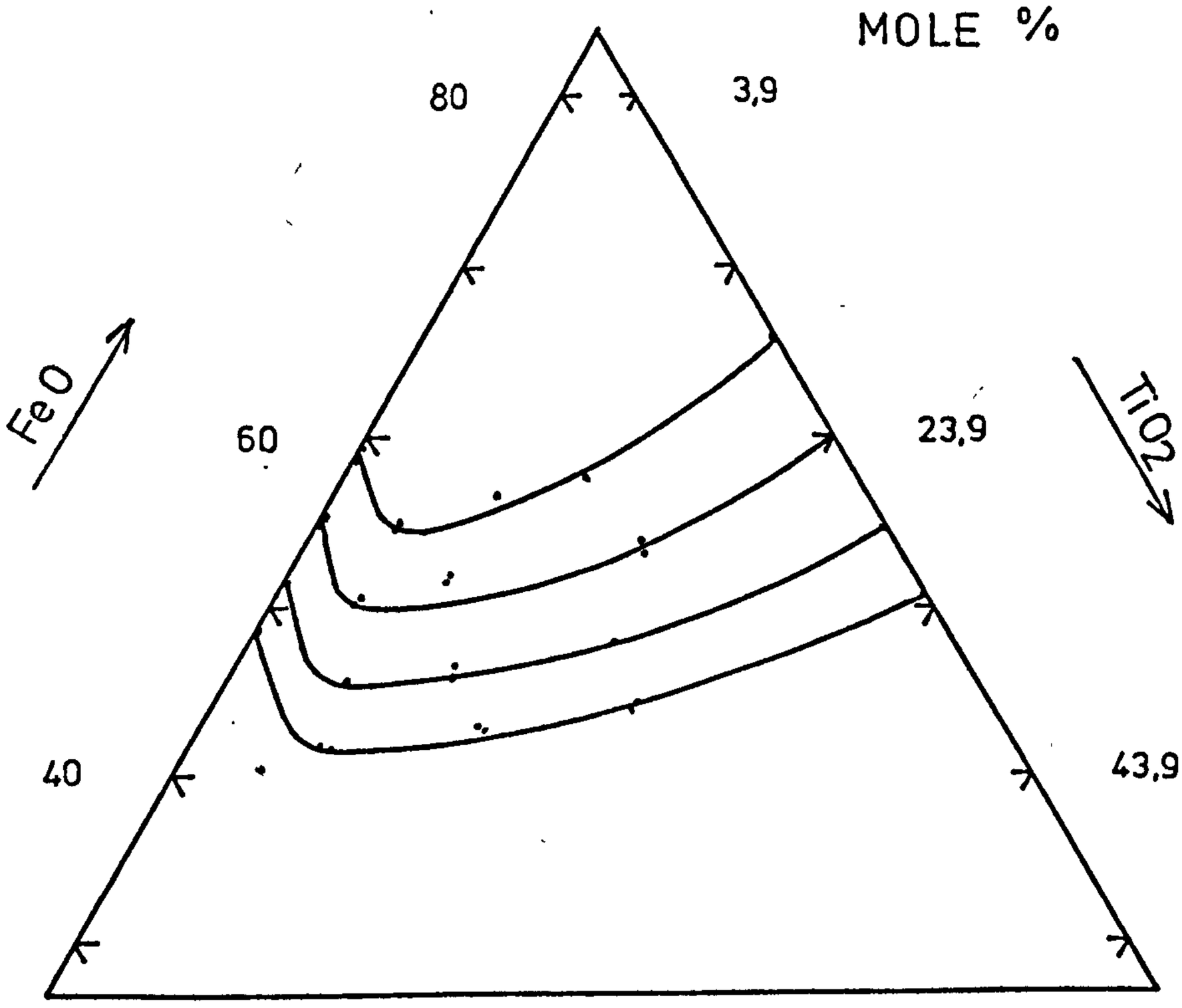

Fig. (3.35) FeO Iso-Activity Curves In The System $FeO-TiO_2-SiO_2-CaO$ At 1470 ^{o}C.

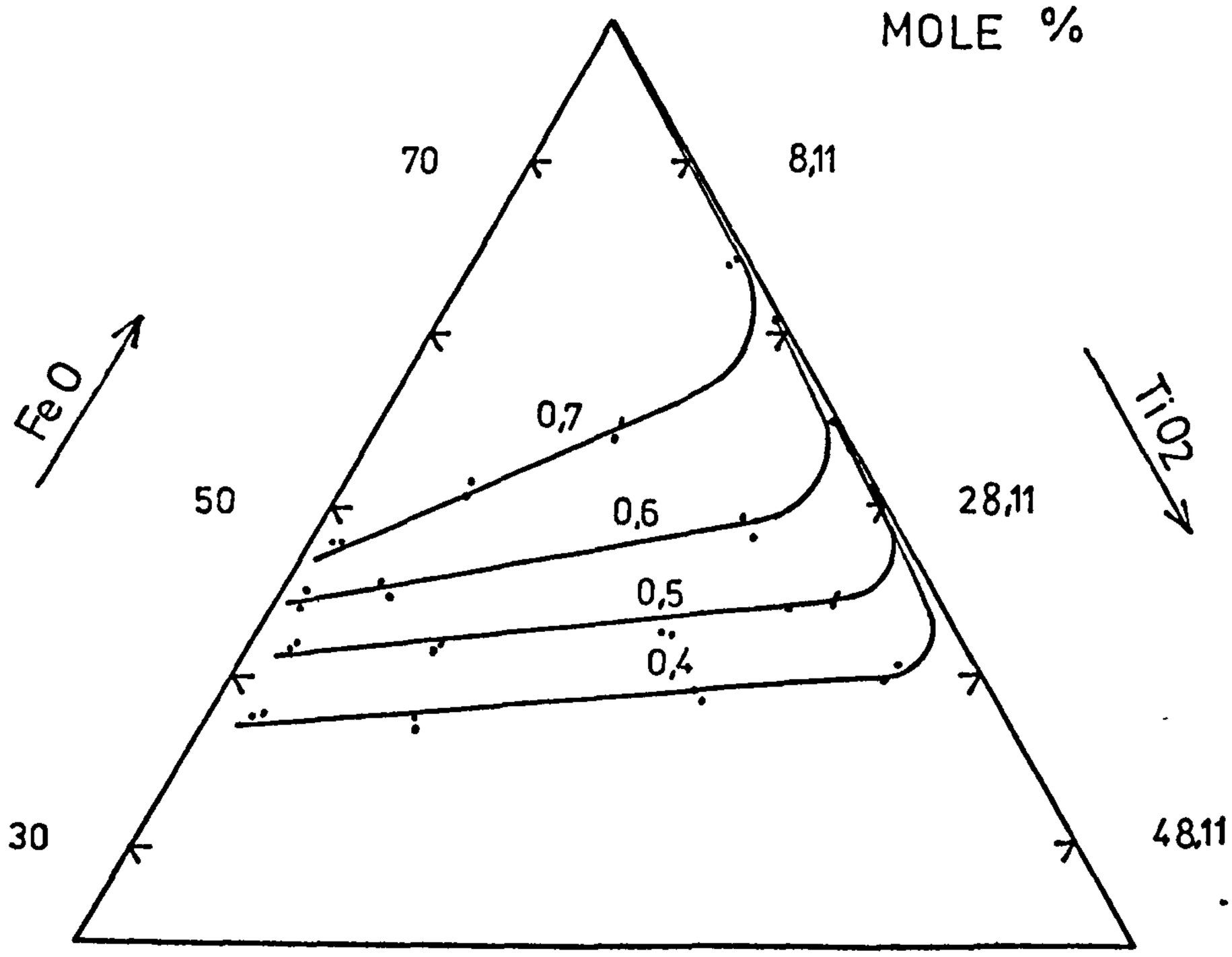

Fig. (3.36) FeO Iso-Activity Curves In The System $FeO-TiO_2-SiO_2-CaO$ At $1470^{o}C$.

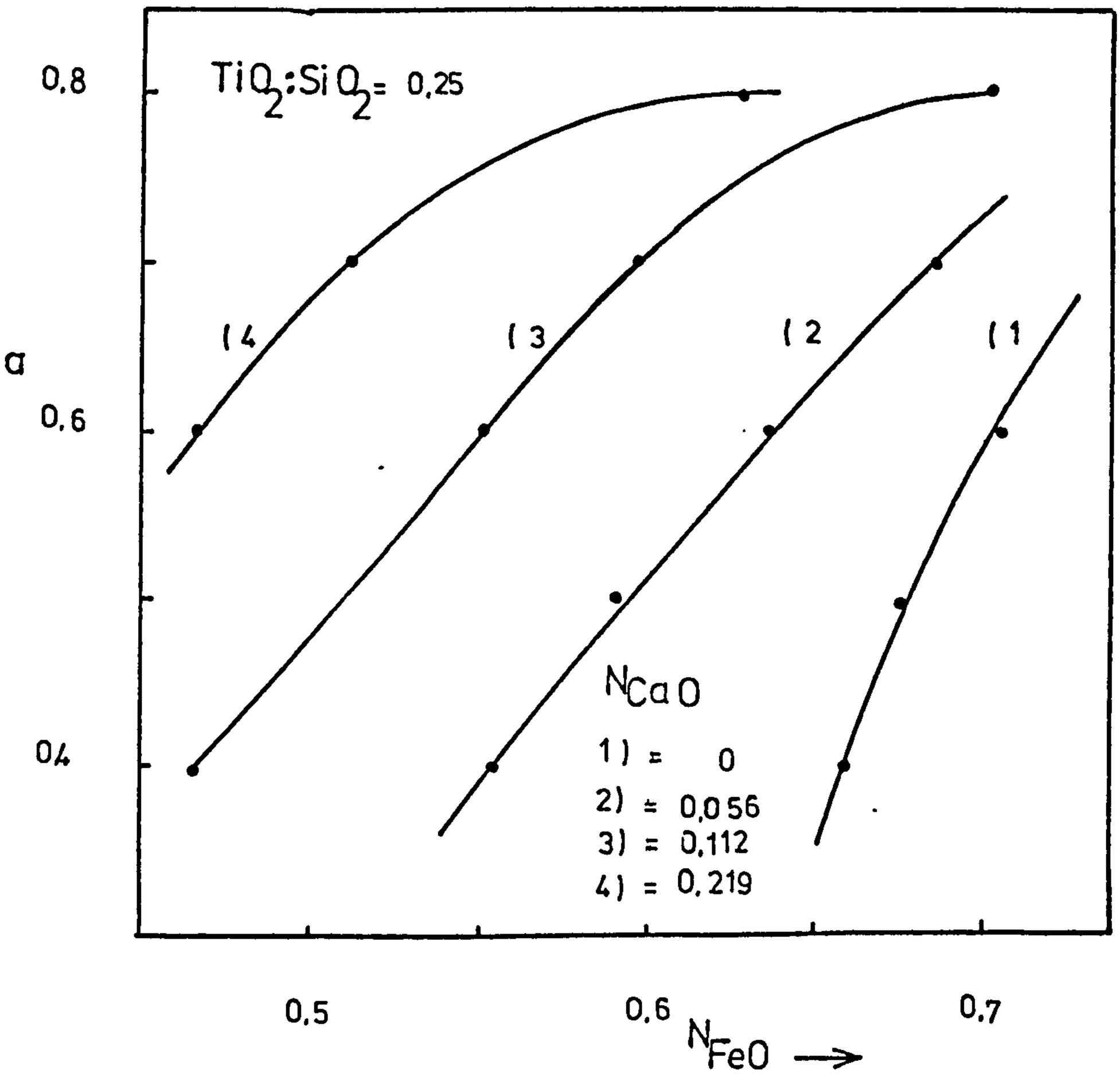

Fig. (3.37) The Effect Of Addition Of CaO To $FeO-TiO_2-SiO_2$ Ternary System On FeO Activity At Constant $TiO_2 : SiO_2$ = 0.25.

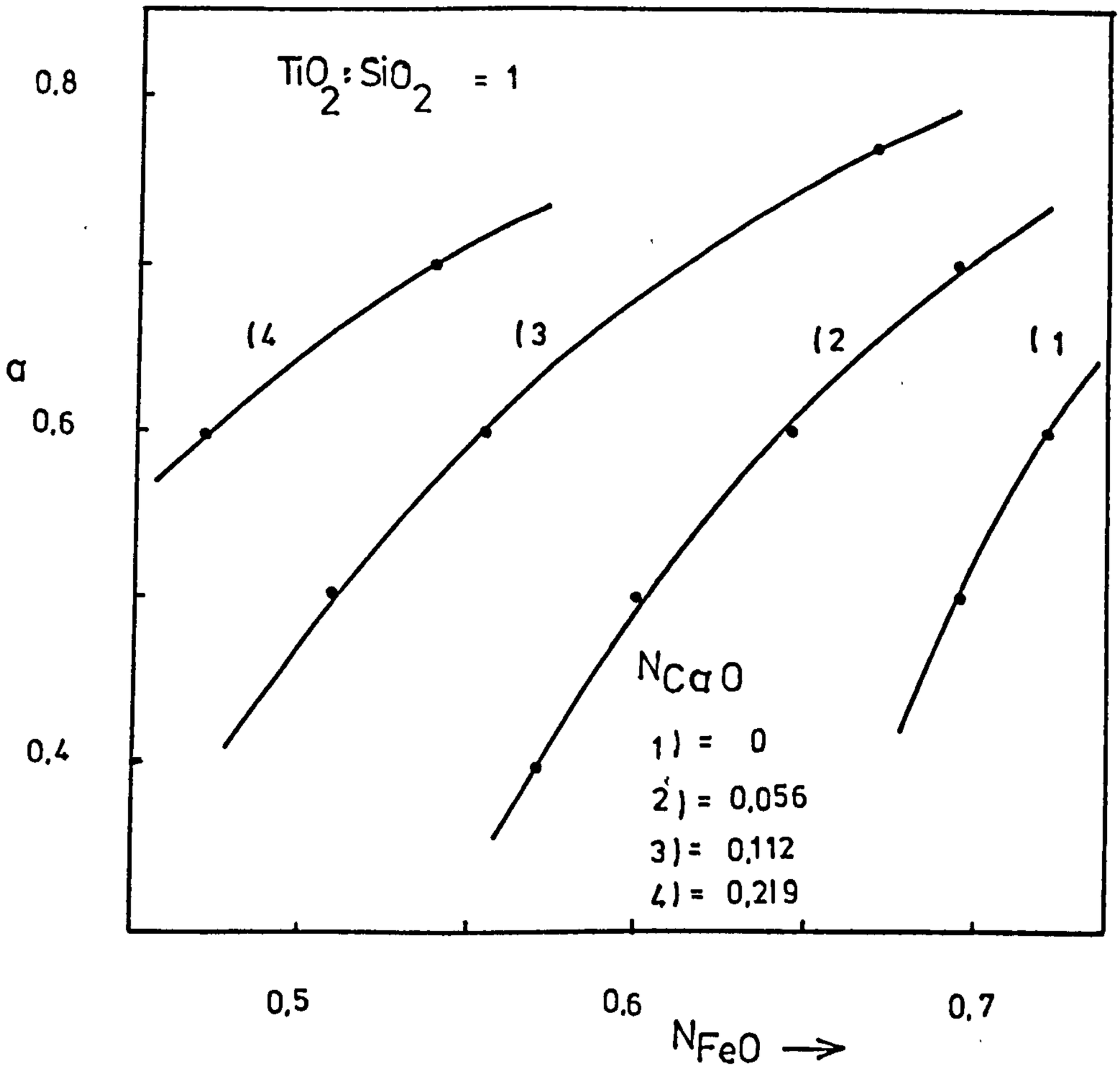

Fig. (3.38) The Effect Of Addition Of CaO To $FeO-TiO_2-SiO_2$ Ternary System On FeO Activity At Constant $TiO_2 : SiO_2$ = 1.

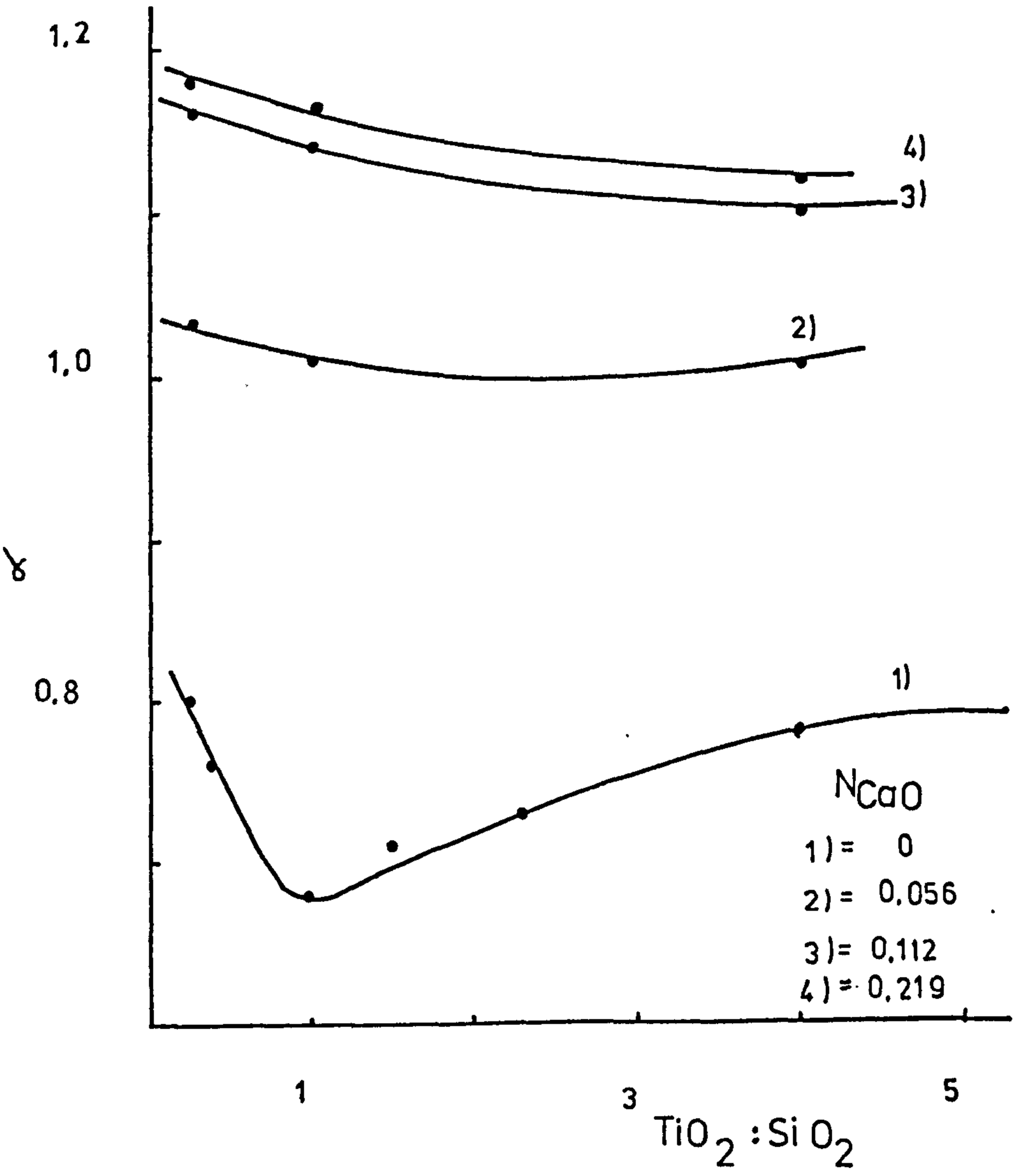

Fig. (3.39) The Effect Of Addition Of CaO To $FeO-TiO_2-SiO_2$ System On γ_{FeO} For Various $TiO_2 : SiO_2$ And $N_{FeO} = 0.69$.

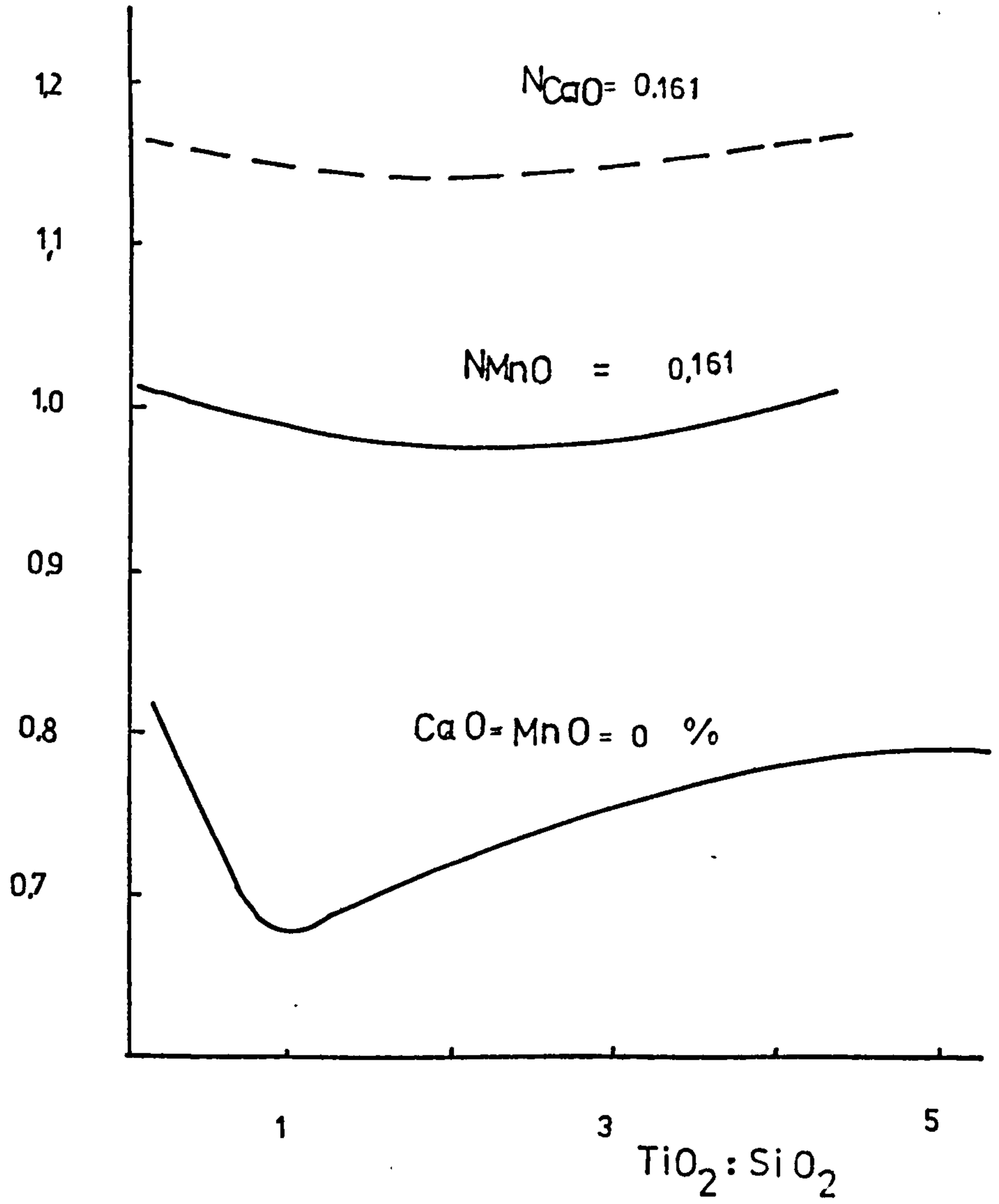

Fig. (3.40) Comparison Between The Effect Of MnO And CaO Addition To The $FeO-TiO_2-SiO_2$ System On γ_{FeO} For CaO = MnO And N_{FeO} = 0.69.

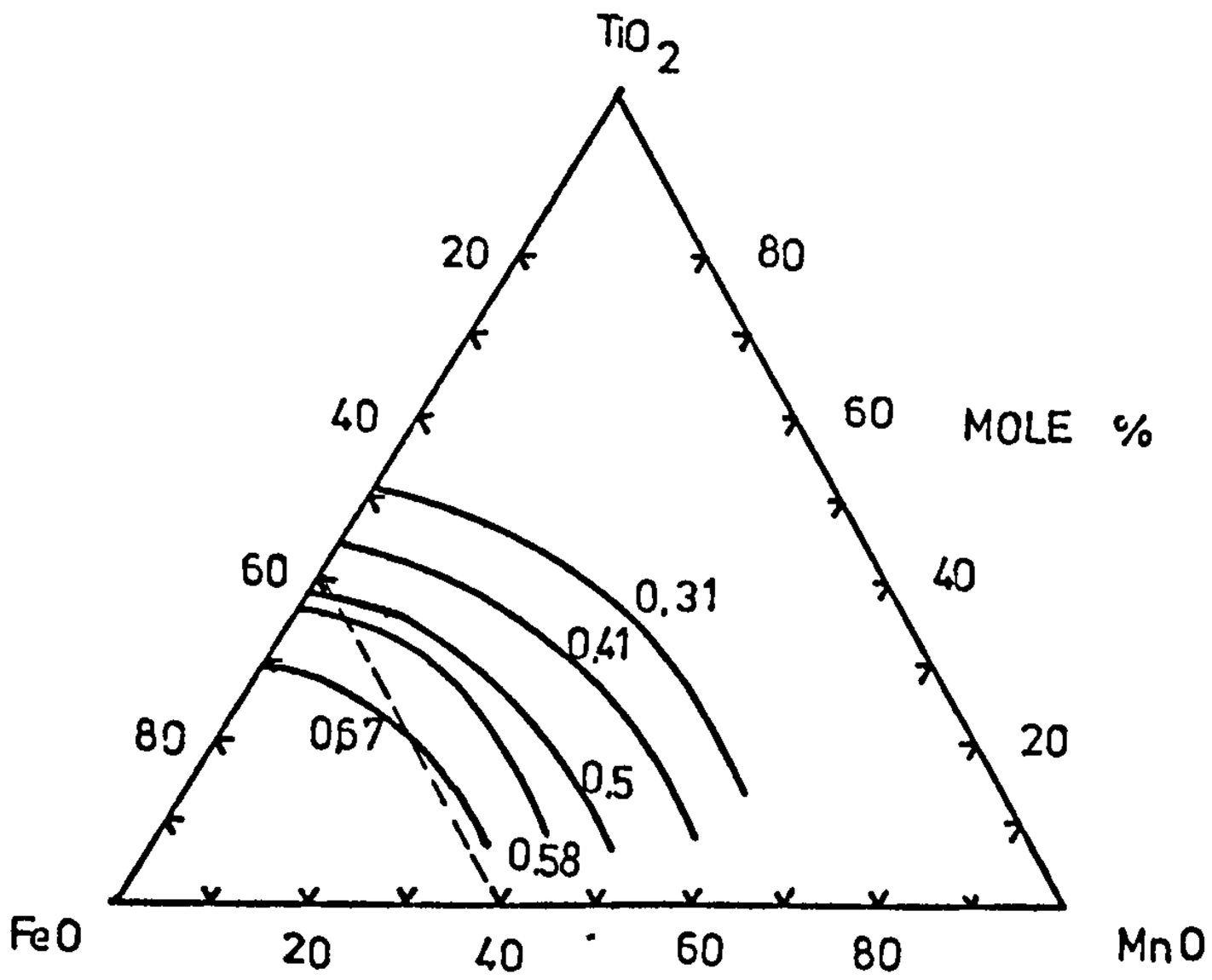

Fig. (3.41) FeO Iso-Activity Curves In The System $FeO-TiO_2-MnO$ At $1475^{o}C$.

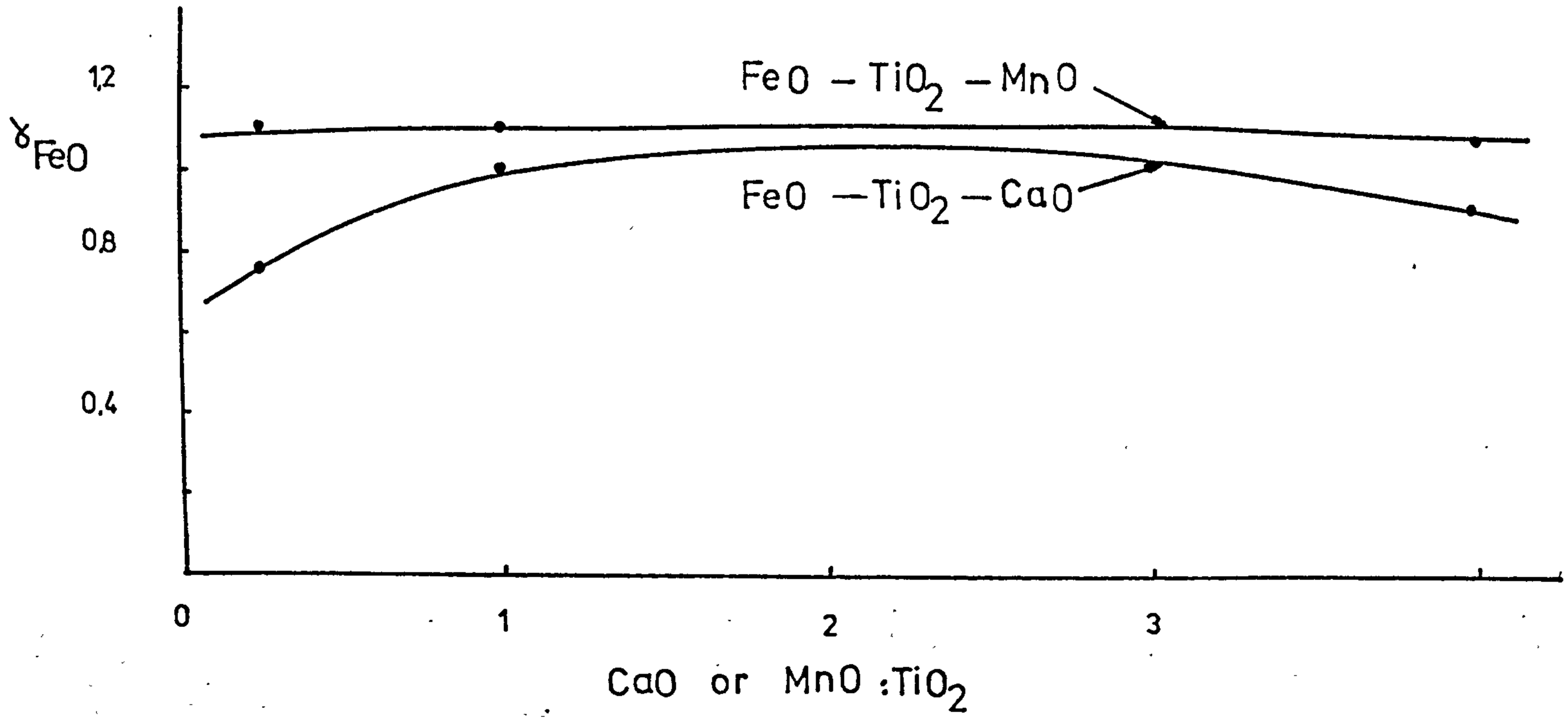

Fig. (3.42) Comparison Between The Effect Of CaO And MnO Addition To The Binary System FeO-TiO_2 On γ FeO.

APPENDICES

APPENDIX (1)

Calculation Of The Ferrous Oxide Activity From The Composition Of The Gas Mixture :

The gases used to equilibrate the different slags contained carbon dioxide, hydrogen and argon. Argon was 50% by volume and the ratio of carbon dioxide to hydrogen differed according to the ferrous oxide activity desired in the slag. The partial pressures of the ingoing carbon dioxide and hydrogen are assigned CO_2^i and H_2^i.

CO_2^i will decompose at the furnace temperature and the equilibrium is described by equation (1)

$$CO_2 \rightleftharpoons CO + \tfrac{1}{2} O_2 \qquad (1)$$

Hydrogen with the ingoing gases will react with the oxygen produced in equation (1) and will form H_2O according to the equilibrium

$$H_2 + \tfrac{1}{2} O_2 \rightleftharpoons H_2O \qquad (2)$$

The equilibrium between the gases, the slag and the iron crucible is represented by equation (3)

$$\underset{(s)}{Fe} + \tfrac{1}{2} \underset{(g)}{O_2} \rightleftharpoons \underset{(l)}{FeO} \qquad (3)$$

By summing equation (1) + (2) equation (4) is obtained

$$CO_2 + H_2 \rightleftharpoons CO + H_2O \qquad (4)$$

The remaining	The produced
CO_2 & H_2	CO H_2O

The equilibrium constants of the four equations are taken as

APPENDIX (1)

Calculation Of The Ferrous Oxide Activity From The Composition Of The Gas Mixture :

The gases used to equilibrate the different slags contained carbon dioxide, hydrogen and argon. Argon was 50% by volume and the ratio of carbon dioxide to hydrogen differed according to the ferrous oxide activity desired in the slag. The partial pressures of the ingoing carbon dioxide and hydrogen are assigned CO_2^i and H_2^i.

CO_2^i will decompose at the furnace temperature and the equilibrium is described by equation (1)

$$CO_2 \rightleftharpoons CO + \tfrac{1}{2} O_2 \qquad (1)$$

Hydrogen with the ingoing gases will react with the oxygen produced in equation (1) and will form H_2O according to the equilibrium

$$H_2 + \tfrac{1}{2} O_2 \rightleftharpoons H_2O \qquad (2)$$

The equilibrium between the gases, the slag and the iron crucible is represented by equation (3)

$$\underset{(s)}{Fe} + \tfrac{1}{2} \underset{(g)}{O_2} \rightleftharpoons \underset{(l)}{FeO} \qquad (3)$$

By summing equation (1) + (2) equation (4) is obtained

$$CO_2 + H_2 \rightleftharpoons CO + H_2O \qquad (4)$$

The remaining	The produced
CO_2 & H_2	CO H_2O

The equilibrium constants of the four equations are taken as

K_1, K_2, K_3 and K_4 respectively, and the partial pressures of the remaining and produced gases in equation (4) are taken as $\overline{P}_{CO_2}$, $\overline{P}_{H_2}$, $\overline{P}_{CO}$ and $\overline{P}_{H_2O}$.

From equation (1) and (2) it can be concluded that the partial pressure of the produced CO in equation (1) equals the partial pressure of H_2O produced in equation (2). If this partial pressure is considered P then :-

$$\overline{P}_{CO} = \overline{P}_{H_2O} = P \qquad (5)$$

Also the remaining CO_2, H_2 partial pressures are related to the pressures of the ingoing CO_2, H_2 by the following equations

$$\overline{P}_{CO_2} = P_{CO_2}^{i} - P \qquad (6)$$

$$\overline{P}_{H_2} = P_{H_2}^{i} - P \qquad (7)$$

The equilibrium constant of equation (4) is :-

$$K_4 = \frac{\overline{P}_{CO} \cdot \overline{P}_{H_2O}}{\overline{P}_{CO_2} \cdot \overline{P}_{H_2}} \qquad (8)$$

Equation (8) can then be written as

$$K_4 = \frac{P.P}{(P_{CO_2}^{i} - P)(P_{H_2}^{i} - P)} = \frac{P^2}{(P_{CO_2}^{i} - P)(P_{H_2}^{i} - P)} \qquad (9)$$

by expanding

$$(K_4 - 1)P^2 - K_4(P_{CO_2}^{i} + P_{H_2}^{i})P + K_4 P_{CO_2}^{i} P_{H_2}^{i} \qquad (10)$$

The solution of this equation to get a value of P is :-

$$P = \frac{K_4(P_{CO_2}^{i} + P_{H_2}^{i}) \pm \sqrt{K_4^2(P_{CO_2}^{i} + P_{H_2}^{i}) - 4K_4(K_4 - 1)P_{CO_2}^{i} P_{H_2}^{i}}}{2(K_4 - 1)} \qquad (11)$$

K_1, K_2, K_3 and K_4 respectively, and the partial pressures of the remaining and produced gases in equation (4) are taken as $\overline{P}_{CO_2}$, $\overline{P}_{H_2}$, $\overline{P}_{CO}$ and $\overline{P}_{H_2O}$.

From equation (1) and (2) it can be concluded that the partial pressure of the produced CO in equation (1) equals the partial pressure of H_2O produced in equation (2). If this partial pressure is considered P then :-

$$\overline{P}_{CO} = \overline{P}_{H_2O} = P \qquad (5)$$

Also the remaining CO_2, H_2 partial pressures are related to the pressures of the ingoing CO_2, H_2 by the following equations

$$\overline{P}_{CO_2} = P^i_{CO_2} - P \qquad (6)$$

$$\overline{P}_{H_2} = P^i_{H_2} - P \qquad (7)$$

The equilibrium constant of equation (4) is :-

$$K_4 = \frac{\overline{P}_{CO} \cdot \overline{P}_{H_2O}}{\overline{P}_{CO_2} \cdot \overline{P}_{H_2}} \qquad (8)$$

Equation (8) can then be written as

$$K_4 = \frac{P.P}{(P^i_{CO_2} - P)(P^i_{H_2} - P)} = \frac{P^2}{(P^i_{CO_2} - P)(P^i_{H_2} - P)} \qquad (9)$$

by expanding

$$(K_4 - 1)P^2 - K_4(P^i_{CO_2} + P^i_{H_2})P + K_4 P^i_{CO_2} P^i_{H_2} \qquad (10)$$

The solution of this equation to get a value of P is :-

$$P = \frac{K_4(P^i_{CO_2} + P^i_{H_2}) \pm \sqrt{K_4^2(P^i_{CO_2} + P^i_{H_2}) - 4K_4(K_4 - 1)P^i_{CO_2} P^i_{H_2}}}{2(K_4 - 1)} \qquad (11)$$

Once the value of P is obtained equation (1) is used to obtain the oxygen potential of the gas mixture from the ratio of $\frac{P_{CO_2}}{P_{CO}}$ as follows :-

$$K_1 = \frac{\overline{P_{CO} \cdot P_{O_2}^{\frac{1}{2}}}}{\overline{P_{CO_2}}} \qquad (12)$$

$$\text{then} \qquad P_{O_2}^{\frac{1}{2}} = K_1 \cdot \frac{\overline{P_{CO_2}}}{\overline{P_{CO}}}$$

Then using equation (5), (6)

$$P_{O_2}^{\frac{1}{2}} = K_1 \frac{P_{CO_2}^{i} - P}{P} \qquad (13)$$

From equation (3)

$$K_3 = \frac{a_{FeO}}{P_{O_2}^{\frac{1}{2}}}$$

$$a_{FeO} = K_3 \cdot P_{O_2}^{\frac{1}{2}} \qquad (14)$$

Then substituting the value of $P_{O_2}^{\frac{1}{2}}$ of equation (13) in (14)

$$a_{FeO} = K_1 \cdot K_3 \cdot \frac{P_{CO_2}^{i} - P}{P} \qquad (15)$$

To calculate the ferrous oxide activity of a certain gas mixture, the $P_{CO}^{i} / P_{H_2}^{i}$ of the ingoing gases was known and it was used in equation (11) to obtain a value of P as a function of $P_{H_2}^{i}$. Substituting both the value of $P_{CO_2}^{i}$ and P in terms of $P_{H_2}^{i}$ in equation (15) the value of the ferrous oxide activity was obtained.

The following table gives Δ G (the free energy change) and K for

reactions (1), (2), (3), (4) used to calculate the ferrous oxide activity of the gas mixture at the working temperatures of 1475°C and 1470°C[52].

Table (1)

Equation	ΔG at 1475°C 1748°K 'cal'	K at 1475°C 1748°K	ΔG at 1470°C 1743°K 'cal'	K at 1470°C 1743°K
1	+31280.36	1.223×10^{-4}	+31381.26	1.1601×10^{-4}
2	-35833	3.0250×10^{4}	-35902	3.1791×10^{4}
3	-36548	3.742×10^{4}	-36600.79	3.8887×10^{4}
4	-4543	3.698	-4519.72	3.688

The following table gives the calculated ferrous oxide activity from the various CO_2^i / H_2^i ratios at 1475°C and 1470°C.

Table (2)

$CO_2^i : H_2^i$	At 1475°C		At 1470°C	
	$P_{O_2}^{\frac{1}{2}} \times 10^{-4}$	σ_{FeO}	$P_{O_2}^{\frac{1}{2}} \times 10^{-4}$	σ_{FeO}
0.270	0.1091	0.408	0.1034	0.402
0.322	0.1350	0.505	0.1286	0.500
0.374	0.16307	0.610	0.1550	0.603
0.418	0.1884	0.705	0.1800	0.700
0.466	0.2155	0.806	0.2057	0.800
0.506	0.2417	0.904	0.2314	0.900

APPENDIX (2)

Calculation Of The Activities Of Components Other Than FeO By The Gibbs-Duhem Equation :

A. Calculation of the activity of silica in the $FeO-SiO_2$ binary system :

From the experimental data of the ferrous oxide activity in the $FeO-SiO_2$ binary system at $1475^{o}C$, the activity of silica was calculated using Gibbs-Duhem equation as follows :

$$\log \gamma_{SiO_2} = -\frac{N_{FeO}}{N_{SiO_2}} \int_{N_{SiO_2}=1}^{N_{SiO_2}=(saturation)} d \log \gamma_{FeO} - \frac{N_{FeO}}{N_{SiO_2}} \int_{N_{SiO_2}=(saturation)}^{N_{SiO_2}=N_{SiO_2}} d \log \gamma_{FeO}$$

From the $FeO-SiO_2$ phase diagram the solubility of SiO_2 at $1475^{o}C$ is 58% by weight and since the activity of SiO_2 is unity at saturation then

$$\gamma_{SiO_2(saturation)} = \frac{1}{N_{SiO_2}} = \frac{1}{0.562} = 1.779$$

but

$$-\frac{N_{FeO}}{N_{SiO_2}} \int_{N_{SiO_2}=1}^{N_{SiO_2}=(saturation)} d \log \gamma_{FeO} = \log \gamma_{SiO_2\,(saturation)}$$

and γ_{SiO_2} (saturation) = 1.779

$\log \gamma_{SiO_2}$ (saturation) = 0.25

Then the integration is given by the equation :-

$$\log \gamma_{SiO_2} = 0.25 - \frac{N_{FeO}}{N_{SiO_2}} \int_{N_{SiO}=\text{(saturation)}}^{N_{SiO_2}=N_{SiO_2}} d \log \gamma_{FeO}$$

2

By plotting $\frac{N_{FeO}}{N_{SiO_2}}$ against $- \log \gamma_{FeO}$ and by calculating the area under it the value of γ_{SiO_2} was determined and the integration is given by the equation:-

$$\log \gamma_{SiO_2} = 0.25 - \text{(area under the curve)}$$

The lower limit of integration is $\log \gamma_{FeO}$ at the N_{SiO_2} = (saturation) or at $N_{FeO} = 0.438$ at which the $a_{FeO} = 0.27$ and $\gamma_{FeO} = \frac{0.27}{0.438} = 0.616$ and $\log \gamma_{FeO} = 0.210$. The upper limit, of course, was the values of $\log \gamma_{FeO}$ corresponding to N_{SiO_2} at the desired composition. This integration gives the activity of silica relative to the pure solid silica as standard state. The following tables gives the calculated silica activities:-

Table (3)

a_{FeO}	0.904	0.806	0.705	0.610	0.505	0.408
N_{FeO}	0.853	0.776	0.724	0.665	0.629	0.583
a_{SiO_2}	0.098	0.164	0.238	0.341	0.464	0.646
N_{SiO_2}	0.147	0.224	0.276	0.335	0.371	0.417

B. Calculation of the activity of calcium oxide in the CaO-FeO binary system :

From the results of ferrous oxide activity in the FeO-CaO binary system at 1470°C the activity of CaO was calculated by Gibbs-Duhem equation :-

$$\log \gamma_{CaO} = - \frac{N_{FeO}}{N_{CaO}} \int_{N_{CaO}=1}^{N_{CaO}=(saturation)} d \log \gamma_{FeO} - \frac{N_{FeO}}{N_{CaO}} \int_{N_{CaO}=(saturation)}^{N_{CaO}=N_{CaO}} d \log \gamma_{FeO}$$

The first part of this integration

$$- \frac{N_{FeO}}{N_{CaO}} \int_{N_{CaO}=1}^{N_{CaO}=(saturation)} d \log \gamma_{FeO} = \log \gamma_{CaO} \text{ (saturation)}$$

From the FeO-CaO phase diagram the saturation with CaO is at $N_{CaO} = 0.459$ at which $\gamma_{CaO} = \frac{a_{CaO}}{N_{CaO}} = \frac{1}{0.459} = 2.177$, and $\log \gamma_{CaO}$ (saturation) $= 0.3379$.

Then the first part of the integration $= 0.3379$ and the integration is given by the equation :-

$$\log \gamma_{CaO} = 0.3379 - \frac{N_{FeO}}{N_{CaO}} \int_{N_{CaO}=(saturation)}^{N_{CaO}=N_{CaO}} d \log \gamma_{FeO}$$

The second part was calculated, as in the case of the $FeO-SiO_2$ system, from the area under the curve produced by plotting $\frac{N_{FeO}}{N_{CaO}}$ against $- \log \gamma_{FeO}$.

The value of γ_{CaO} is then given by the equation

$$\log \gamma_{CaO} = 0.3379 - \text{(area under the curve)}$$

The lower limit of integration was the value of γ_{FeO} at $N_{CaO} = 0.459$ at which $N_{FeO} = 0.541$, and from the activity-composition relation $a_{FeO} = 0.3$ at $N_{FeO} = 0.541$, then $\gamma_{FeO} = \frac{0.3}{0.541} = 0.555$, and $\log \gamma_{FeO} = - 0.255$.

The higher limit was $\log \gamma_{FeO}$ at the desired composition.

This integration gives the activity of CaO in this system relative to the pure solid CaO as standard state.

The calculated activities are given in table (4)

Table (4)

a_{FeO}	0.9	0.8	0.7	0.603	0.5	0.402
N_{FeO}	0.922	0.839	0.786	0.715	0.662	0.608
a_{CaO}	0.042	0.107	0.192	0.302	0.459	0.672
N_{CaO}	0.078	0.161	0.214	0.285	0.338	0.392

C. Calculation of the activity of titania in the $FeO-TiO_2-SiO_2$ ternary system :

In a ternary system of components 1, 2, 3 the Wagner[51] integration is used to determine the activity of components 1 and 3 if the activity of component (2) is known. This equation is in the following form :-

$$\log \gamma_1 = \left[\int_0^1 \frac{\log \gamma_2}{(1-N_2)^2} \, dN_2 \right]_{y=0} + \left[-y \int_1^{N_2} \frac{\partial}{\partial y} \frac{\log \gamma_2}{(1-N_2)^2} \, dN_2 \right]$$

$$- \frac{N_2 \log \gamma_2}{(1-N_2)} + \int_1^{N_2} \frac{\log \gamma_2}{(1-N_2)^2} \, dN_2 \Bigg]_y$$

where $y = \frac{n_3}{n_1 + n_3}$. $N_2 = \frac{n_2}{n_1 + n_2 + n_3}$

In the ternary system $FeO-TiO_2-SiO_2$ the activity of FeO was known and it was possible to calculate the activity of TiO_2 only, using the above integration. By replacing 1 by TiO_2 and 2 by FeO and 3 by SiO_2 the integration becomes :-

$$\log \gamma_{TiO_2} = \left[\int_0^1 \frac{\log \gamma_{FeO}}{(1-N_{FeO})^2} \, d N_{FeO} \right]_{y=0} + \left[-y \int_1^{N_{FeO}} \frac{\partial}{\partial y} \frac{\log \gamma_{FeO}}{(1-N_{FeO})^2} \, d N_{FeO} \right.$$

$$\left. - \frac{N_{FeO} \log \gamma_{FeO}}{(1-N_{FeO})} + \int_1^{N_{FeO}} \frac{\log \gamma_{FeO}}{(1-N_{FeO})^2} \, d N_{FeO} \right]_y$$

The same method as that used by Martin[38] was used to calculate the activity of titania in this ternary system.

The experimental results of ferrous oxide activity have been plotted as iso-activity coefficient curves as shown in Figure (1), and calculations of $\frac{\log \gamma_{FeO}}{(1-N_{FeO})^2}$ have been carried out at the points of intersection of the different y lines with the FeO iso-activity coefficient curves. These calculations are given in Table (5). It can be seen from this table that b is insensitive to composition along constant y lines. A plot of b average versus y gave a straight line of slope + 0.335 as shown in Figure (2). To calculate the γ_{TiO_2} using Wagner's integration, the first part = b for $FeO-TiO_2$ = -0.623. The second part was determined from the slope of the straight line produced by plotting b versus y. The third and the fourth parts were obtained from experimental results at the point of intersection

of the particular y line with the iso-activity coefficient curve chosen. To calculate the activity of TiO_2 at the point of intersection of y = 0.8 with the iso-activity coefficient curve of 0.969 the following method of calculation was followed :-

At the point of intersection $N_{FeO} = 0.765$,

$N_{TiO_2} = 0.048$

$\gamma_{FeO} = 0.969$, $\log \gamma_{FeO} = -0.0137$

(1) The first part b $FeO\text{-}TiO_2 = -0.623$

(2) The second part = $-y\ X\text{-}(1\text{-}N_{FeO})\ X\ b/y$

$= -0.8\ X\text{-}0.235\ X\ 0.335$

$= +0.06298$

(3) The third part $= \frac{N_{FeO}}{(1-N_{FeO})}\ X \log \gamma_{FeO}$

$= \frac{0.765}{0.235}\ X\ -0.137 = 0.0446$

(4) The fourth part = b average $X\ -(1-N_{FeO})$

$= -0.505\ X\ -0.235 = +0.1187$

Then $\log \gamma_{TiO_2}$ = the summation of the four parts = -0.4859

$\gamma_{TiO_2} = 0.3266$

$a_{TiO_2} = \gamma_{TiO_2}\ X\ N_{TiO_2}$

$= 0.3266\ X\ 0.048$

$= 0.0157$

It should be mentioned that Wagner's integration of Gibbs-Duhem equation gives the activity of TiO_2 relative to the pure liquid TiO_2 as standard state. The results of calculation of TiO_2 activity is given in Table (6). The calculation of SiO_2 activity has not been attempted in this system since the plot of $\log \gamma_{FeO}$ against $(1-N_{FeO})^2$ in the $FeO\text{-}SiO_2$ binary system did not give a straight line.

Appendix 2C

Table (5)

$y = 0.1$

γ_{FeO}	N_{FeO}	$(1-N_{FeO})$	$-\log \gamma_{FeO}$	$(1-N_{FeO})^2$	$\frac{-\log \gamma_{FeO}}{(1-N_{FeO})^2}$	b average
0.969	0.85	0.150	0.0137	0.0225	0.6089	
0.950	0.81	0.19	0.02228	0.0361	0.6171	
0.933	0.77	0.230	0.0301	0.0529	0.5699	0.633
0.900	0.73	0.27	0.0458	0.0729	0.628	
0.850	0.70	0.300	0.0706	0.09	0.7400	

$y = 0.2$

0.969	0.84	0.160	0.0137	0.0256	0.5352	
0.950	0.802	0.198	0.02228	0.392	0.5684	
0.933	0.775	0.225	0.0301	0.0506	0.5946	0.656
0.900	0.745	0.255	0.0458	0.650	0.7043	
0.850	0.725	0.75	0.0706	0.7562	0.88462	

$y = 0.3$

0.969	0.835	0.165	0.0137	0.272	0.503	
0.950	0.795	0.205	0.02228	0.4203	0.5300	
0.933	0.775	0.225	0.0301	0.0506	0.5946	0.6782
0.900	0.75	0.25	0.0458	0.0625	0.732	
0.850	0.732	0.268	0.0706	0.0718	0.9314	

$y = 0.4$

0.969	0.825	0.175	0.0137	0.306	0.4477	
0.950	0.79	0.21	0.2228	0.0441	0.505	
0.933	0.795	0.225	0.0301	0.0506	0.5945	0.662
0.900	0.755	0.245	0.0458	0.0600	0.7596	
0.850	0.735	0.265	0.0706	0.070	1.005	

$y = 0.5$

0.969	0.825	0.175	0.0137	0.342	0.400	
0.95	0.78	0.22	0.02228	0.0484	0.4603	
0.933	0.77	0.23	0.0301	0.0529	0.5689	0.64
0.9	0.75	0.25	0.0458	0.0625	0.7296	
0.85	0.74	0.26	0.0706	0.0696	1.044	

Appendix 2C Table (5) Contd.

γ_{FeO}	N_{FeO}	$(1-N_{FeO})$	$-\log\gamma_{FeO}$	$(1-N_{FeO})^2$	$\frac{-\log\gamma_{Feo}}{(1-N_{FeO})^2}$	b average
y = 0.6						
0.969	0.8	0.2	0.0137	0.04	0.343	
0.95	0.77	0.23	0.02228	0.0529	0.421	
0.933	0.76	0.24	0.0301	0.0576	0.523	0.591
0.9	0.745	0.255	0.0458	0.0650	0.7013	
0.85	0.73	0.27	0.0706	0.0729	0.968	
y = 0.7						
0.969	0.78	0.22	0.0137	0.0484	0.283	
0.95	0.76	0.24	0.0222	0.0576	0.3868	
0.933	0.75	0.25	0.0301	0.025	0.4816	0.545
0.9	0.74	0.26	0.0458	0.0676	0.6746	
0.85	0.72	0.28	0.0706	0.0784	0.9005	
y = 0.8						
0.969	0.76	0.24	0.0137	0.0576	0.2378	
0.95	0.75	0.25	0.0222	0.0625	0.3563	
0.933	0.735	0.265	0.0301	0.0702	0.4286	0.505
0.9	0.725	0.275	0.0458	0.0756	0.6030	
0.85	0.71	0.29	0.0706	0.0841	0.8989	
y = 0.9						
0.969	0.742	0.258	0.0137	0.0666	0.2058	
0.95	0.73	0.27	0.0222	0.0729	0.3056	
0.933	0.72	0.28	0.0301	0.0784	0.3839	0.426
0.9	0.705	0.295	0.0458	0.087	0.5239	
0.85	0.685	0.315	0.0706	0.0992	0.7115	

Appendix 2C

Table (6)

CALCULATED TITANIA ACTIVITIES

$y = 0.1$

N_{FeO}	0.85	0.805	0.77	0.73
a_{TiO_2}	0.0384	0.044	0.055	0.065

$y = 0.2$

N_{FeO}	0.845	0.805	0.775	0.745
a_{TiO_2}	0.0328	0.0414	0.0477	0.055

$y = 0.3$

N_{FeO}	0.835	0.795	0.775	0.755
a_{TiO_2}	0.0316	0.0394	0.0435	0.0455

$y = 0.4$

N_{FeO}	0.825	0.79	0.775	0.755
a_{TiO_2}	0.0297	0.0361	0.0383	0.0446

$y = 0.5$

N_{FeO}	0.815	0.78	0.77	0.75
a_{TiO_2}	0.026	0.0329	0.0333	0.0346

$y = 0.6$

N_{FeO}	0.8	0.77	0.76	0.745
a_{TiO_2}	0.0271	0.027	0.0281	0.0279

$y = 0.7$

N_{FeO}	0.785	0.76	0.75	0.74
a_{TiO_2}	0.0203	0.0224	0.0227	0.0227

Appendix 2C Table (6) Contd.

y = 0.8

N_{FeO}	0.765	0.75	0.735	0.725
a_{TiO_2}	0.015	0.0159	0.0167	0.0162

y = 0.9

N_{FeO}	0.745	0.73	0.72	0.685
a_{TiO_2}	0.0083	0.0094	0.0096	0.0075

D. Calculation Of The Activity Of Titania And Calcium Oxide In The $FeO-TiO_2-CaO$ Ternary System :

In this system b $FeO-TiO_2$ and b $FeO-CaO$ were known and it was possible to calculate the activty of both titania and calcium oxide. A method similar to that used in the $FeO-TiO_2-SiO_2$ system was employed in this system to determine both activities. Wagner's equations used were in the form :-

$$\log \gamma_{TiO_2} = \left[\int_0^1 \frac{\log \gamma_{FeO}}{(1-NFeO)} \, d N_{FeO} \right] + \left[-y \int_1^{N_{FeO}} \frac{\delta}{\delta y} \frac{\log \gamma_{FeO}}{(1-N_{FeO})^2} \, d N_{FeO} - \frac{N_{FeO} \log \gamma_{FeO}}{1-N_{FeO}} + \int_1^{N_{FeO}} \frac{\log \gamma_{FeO}}{(1-N_{FeO})^2} \, d N_{FeO} \right]_y$$

$$\log \gamma_{CaO} = \left[\int_0^1 \frac{\log \gamma_{FeO}}{(1-N_{FeO})} \, d N_{FeO} \right]_{y=0}$$

$$+ \left[(1-y) \int_1^{N_{FeO}} \frac{\partial}{\partial y} \frac{\log \gamma_{FeO}}{(1-N_{FeO})^2} \, d N_{FeO} - \right.$$

$$\left. \frac{N_{FeO} \log \gamma_{FeO}}{(1-N_{FeO})} + \int_1^{N_{FeO}} \frac{\log \gamma_{FeO}}{(1-N_{FeO})^2} \, d N_{FeO} \right]_y \quad (2)$$

The first part of each equation was the corresponding b function of the binary system. The second part was determined from the slope of the tangent to the curve produced by plotting b against y as in Figure (3). The third and fourth parts were determined from the point of intersection of the y line with the iso-activity coefficient chosen (see Figure 4).

To calculate the activity of CaO at the point of intersection of the line y = 0.9 with the iso-activity coefficient curve of 0.75 where :-

$\gamma_{FeO} = 0.75$ $\quad$ $\log \gamma_{FeO} = -0.1249$

$N_{FeO} = 0.615$ $\quad$ $N_{CaO} = 0.345$

The first part = b FeO-CaO = -1.473

The second part = $-0.1 \times -0.385 \times$ slope of the tangent

$= -0.1 \times -0.385 \times 2.75$

$= + 0.1059$

The third part = $\frac{0.615}{0.315} \times -0.1249$

$= -0.1995$

The fourth part = b (at the point of intersection)

$x - 0.385 = -0.8428$

$x - 0.385 = +0.3245$

Then $\log \gamma_{CaO}$ = The summation of the four parts = -1.2421

$\gamma_{CaO} = 0.0573$

$a_{CaO} = N_{CaO} \times \gamma_{CaO} = 0.0573 \times 0.345$

$= 0.0198$

Table (7) and Table (8) include the calculations used to determine the titania and calcium oxide activities.

APPENDIX 2D

Table (7)

γ_{FeO}	N_{FeO}	$(1-N_{FeO})$	$-\log \gamma_{FeO}$	$(1-N_{FeO})^2$	$\frac{\log \gamma_{FeO}}{(1-N_{FeO})^2}$
y = 0.1					
0.95	0.685	0.315	0.0223	0.0992	0.2247
0.9	0.65	0.35	0.0458	0.1225	0.3739
0.85	0.605	0.395	0.0706	0.156	0.4525
0.8	0.55	0.45	0.0969	0.2025	0.4785
0.75	0.525	0.475	0.1249	0.2256	0.5536
y = 0.2					
0.95	0.635	0.365	0.0223	0.1332	0.1674
0.9	0.6	0.4	0.0458	0.16	0.2863
0.85	0.56	0.44	0.076	0.1936	0.3647
0.8	0.52	0.48	0.0969	0.2304	0.4206
0.75	0.495	0.505	0.1249	0.255	0.4897
y = 0.3					
0.95	0.585	0.415	0.0223	0.1722	0.1295
0.9	0.555	0.445	0.0458	0.198	0.2313
0.85	0.525	0.475	0.0706	0.2256	0.3129
0.8	0.5	0.5	0.0969	0.25	0.3876
0.75	0.47	0.53	0.1249	0.2809	0.4446

Appendix 2D Table (7) Contd.

y = 0.4

γ_{FeO}	N_{FeO}	$(a-N_{FeO})$	$-\log \gamma_{FeO}$	$(1-N_{FeO})^2$	$\frac{\log \gamma_{FeO}}{(1-N_{FeO})^2}$
0.95	0.565	0.435	0.0223	0.1892	0.1178
0.9	0.54	0.46	0.0458	0.2116	0.2164
0.85	0.52	0.48	0.0706	0.2304	0.3065
0.8	0.505	0.495	0.0969	0.245	0.3955
0.75	0.475	0.525	0.1249	0.2756	0.4532

y = 0.5

γ_{FeO}	N_{FeO}	$1-N_{FeO}$	$-\log \gamma_{FeO}$	$(1-N_{FeO})$	$\frac{-\log \gamma_{FeO}}{(1-N_{FeO})^2}$
0.95	0.57	0.43	0.0223	0.1849	0.2106
0.9	0.54	0.46	0.0458	0.2116	0.2164
0.85	0.525	0.475	0.0706	0.2256	0.3129
0.8	0.51	0.49	0.0969	0.2401	0.4036
0.75	0.485	0.515	0.1249	0.2652	0.4709

y = 0.6

0.95	0.595	0.405	0.0223	0.1640	0.1360
0.9	0.57	0.43	0.0458	0.1849	0.2477
0.85	0.55	0.45	0.0706	0.2025	0.3486
0.8	0.53	0.47	0.0969	0.2209	0.4387
0.75	0.515	0.485	0.1249	0.2353	0.5310

y = 0.7

0.95	0.635	0.363	0.0223	0.1332	0.1674
0.9	0.605	0.395	0.0458	0.156	0.293
0.85	0.585	0.415	0.0706	0.1722	0.4099
0.8	0.565	0.435	0.0969	0.1892	0.5121
0.75	0.55	0.45	0.1249	0.2025	0.6168

Appendix 2D Table (7) Contd.

y = 0.8

γ_{FeO}	N_{FeO}	$1-N_{FeO}$	$-\log\gamma_{FeO}$	$(1-N_{FeO})^2$	$\frac{-\log\gamma_{FeO}}{(1-N_{FeO})^2}$
0.95	0.75	0.25	0.0223	0.0625	0.3568
0.9	0.66	0.34	0.0458	0.1156	0.3962
0.85	0.625	0.375	0.0706	0.1406	0.5020
0.8	0.605	0.395	0.0969	0.1560	0.6211
0.75	0.58	0.42	0.1249	0.1764	0.7080
y = 0.9					
0.95	0.81	0.19	0.0223	0.0361	0.6177
0.9	0.75	0.25	0.0458	0.0625	0.7328
0.85	0.67	0.33	0.0706	0.1089	0.6483
0.8	0.645	0.355	0.0969	0.1260	0.769
0.75	0.615	0.385	0.1249	0.1482	0.8428

Appendix 2D
Table (8)

A - CALCULATED TITANIA ACTIVITIES

y = 0.1					
N_{FeO}	0.69	0.65	0.605	0.55	0.525
a_{TiO_2}	0.075	0.091	0.107	0.132	0.139
y = 0.2					
N_{FeO}	0.64	0.6	0.56	0.525	0.495
a_{TiO_2}	0.079	0.093	0.108	0.125	0.141
y = 0.3					
N_{FeO}	0.585	0.555	0.525	0.5	0.47
a_{TiO_2}	0.078	0.089	0.1	0.113	0.124
y = 0.4					
N_{FeO}	0.565	0.535	0.515	0.5	0.47
a_{TiO_2}	0.065	0.074	0.082	0.09	0.102

Appendix 2D
Table (8)

B - CALCULATED CALCIUM OXIDE ACTIVITIES

y = 0.9					
N_{FeO}	0.815	0.75	0.67	0.645	0.615
a_{CaO}	0.0064	0.0098	0.0137	0.0169	0.0198

y = 0.8					
N_{FeO}	0.75	0.66	0.62	0.6	0.58
a_{CaO}	0.0082	0.0115	0.0149	0.0169	0.0179

y = 0.7					
N_{FeO}	0.635	0.605	0.585	0.565	0.545
a_{CaO}	0.0104	0.0125	0.014	0.0161	0.0184

y = 0.6					
N_{FeO}	0.595	0.57	0.55	0.53	0.515
a_{CaO}	0.0095	0.0126	0.117	0.0132	0.0179

APPENDIX (3)

Results :

The following tables give the final chemical analysis of the slags equilibrated with the different gas mixtures in every system investigated.

1. The Ternary System $FeO-TiO_2-SiO_2$ At 1475^oC.

Table (9) $a_{FeO} = 0.9$

	Mole %		
	FeO	TiO_2	SiO_2
A_1	84.93	-	15.07
A_2	85.58	-	14.42
B_1	88.69	1.05	10.26
B_2	88.56	0.6	10.82
C_1	91.21	2.5	6.29
C_2	90.04	2.49	7.47
D_1	90.38	2.85	6.76
D_2	91.46	2.95	5.59

Table (10) $a_{FeO} = 0.8$

	Mole %		
	FeO	TiO_2	SiO_2
A_1	77.35	-	22.65
A_2	77.86	-	22.14
B_1	79.0	1.39	19.6
B_2	77.96	1.65	20.39
C_1	79.03	3.4	17.57
C_2	80.03	2.94	17.05
D_1	79.58	4.24	6.17
D_2	80.69	4.3	5.01

Table (11) $a_{FeO} = 0.7$

	Mole %		
	FeO	TiO_2	SiO_2
A_1	72.5	-	27.09
A_2	71.82	-	28.18
B_1	72.86	3.47	23.76
B_2	73.5	3.47	23.0
C_1	75.73	7.04	17.23
C_2	74.92	6.95	18.14
D_1	75.98	10.41	13.61
D_2	75.47	10.50	14.3

Table (12) $a_{FeO} = 0.6$

	Mole %		
	FeO	TiO_2	SiO_2
A_1	66.43	-	33.57
A_2	66.53	-	33.47
B_1	69.01	3.36	27.63
B_2	69.03	3.45	27.53
C_1	68.62	5.02	26.36
C_2	68.37	4.93	26.96
D_1	71.22	7.79	20.98
D_2	71.35	6.90	21.7

Table (13) a_{FeO} = 0.5

	Mole %		
	FeO	TiO_2	SiO_2
A_1	63.45	-	36.55
A_2	62.40	-	37.6
B_1	65.88	2.91	31.21
B_2	66.35	3.08	30.56
C_1	67.44	7.12	25.43
C_2	67.95	6.95	25.09
D_1	68.73	11.01	20.26
D_2	68.65	10.64	20.71

Table (14) a_{FeO} = 0.4

	Mole %		
	FeO	TiO_2	SiO_2
A_1	58.21	-	41.79
A_2	58.32	-	41.68
B_1	63.07	3.24	33.69
B_2	62.59	3.50	33.92
C_1	66.57	7.11	26.32
C_2	66.59	6.94	26.48
D_1	67.5	9.89	22.61
D_2	67.32	10.07	22.61

2. The Ternary System FeO-TiO_2-CaO At 1470°C

Table (15) a_{FeO} = 0.9

	Mole %		
	FeO	TiO_2	CaO
A_1	91.69	-	8.31
A_2	92.68	-	7.32
B_1	88.62	1.94	9.44
B_2	88.93	2.12	8.95
C_1	87.02	4.70	8.27
C_2	88.23	4.62	7.15
D_1	89.95	5.83	4.22
D_2	89.90	5.37	4.73

Table (16) a_{FeO} = 0.8

	Mole %		
	FeO	TiO_2	CaO
A_1	84.15	-	15.85
A_2	83.67	-	16.33
B_1	82.90	3.24	13.86
B_2	83.02	3.46	13.52
C_1	80.62	8.42	10.96
C_2	79.80	8.40	10.79
D_1	76.81	12.48	10.71
D_2	76.67	12.32	11.0

Table (17) a_{FeO} = 0.7

	Mole %		
A_1	78.49	-	21.51
A_2	78.61	-	21.39
B_1	77.2	2.07	20.73
B_2	76.71	2.0	21.29
C_1	73.69	4.33	21.99
C_2	72.62	4.4	22.98
D_1	73.28	8.87	17.86
D_2	72.58	9.25	18.8
E_1	66.39	14.73	18.89
E_2	67.28	14.20	18.52
F_1	66.0	20.64	13.36
F_2	65.54	21.19	13.27

Table (18) a_{FeO} = 0.6

	Mole %		
A_1	70.94	-	29.06
A_2	72.07	-	27.93
B_1	67.58	1,87	30.55
B_2	68.73	1.98	29.29
C_1	67.73	4.73	27.53
C_2	66.6	4.73	28.67
D_1	64.72	8.46	26.82
D_2	64.88	8.64	26.48
E_1	65.0	11.67	23.32
E_2	64.19	11.56	24.25
F_1	61.31	14.82	23.87
F_2	60.36	15.52	24.12
G_1	60.48	21.03	18.49
G_2	59.8	21.24	18.96

Table (19) $a_{FeO} = 0.5$

	Mole %		
	FeO	TiO_2	CaO
A_1	65.61	-	34.39
A_2	66.71	-	33.29
B_1	64.77	2.32	32.91
B_2	63.73	2.47	33.80
C_1	63.30	5.62	31.08
C_2	62.93	5.66	31.40
D_1	60.0	9.42	30.58
D_2	59.99	8.58	31.43
E_1	57.03	13.14	29.83
E_2	58.0	13.08	28.91
F_1	55.59	16.98	27.43
F_2	56.56	16.38	27.06
G_1	55.38	20.85	23.77
G_2	55.05	21.04	23.92

Table (20) $a_{FeO} = 0.4$

	Mole %		
	FeO	TiO_2	CaO
A_1	60.8	-	39.2
A_2	60.82	-	39.18
B_1	58.19	3.05	38.76
B_2	58.99	3.23	37.78
C_1	58.36	6.35	35.29
C_2	57.64	6.51	35.85
D_1	56.01	9.67	34.31
D_2	55.95	9.84	34.21
E_1	53.78	17.5	28.72
E_2	53.44	17.38	29.17
F_1	51.74	26.84	21.42
F_2	51.74	26.84	21.42

3. The Quaternary System $FeO-TiO_2-SiO_2-MnO$ At 1475°C.

A. MnO average 8.11 - Mole %

Table (21) $a_{FeO} = 0.806$

	Mole %			
	FeO	MnO	TiO_2	SiO_2
A_1	78.11	8.96	1.77	11.17
A_2	77.82	9.17	1.86	11.16
B_1	80.95	8.74	4.53	8.78
B_2	79.87	8.69	4.81	6.83
C_1	81.06	8.7	6.75	3.5
C_2	81.19	8.69	6.5	3.61

Table (22) $a_{FeO} = 0.7$

	Mole %			
	FeO	MnO	TiO_2	SiO_2
A_1	68.32	9.66	2.31	19.71
A_2	69.34	9.53	2.05	19.08
B_1	69.84	9.44	5.12	15.59
B_2	71.09	9.49	4.94	14.48
C_1	70.83	9.42	6.28	13.47
C_2	71.92	9.33	6.20	12.55
D_1	72.59	8.8	9.43	9.17
D_2	73.25	8.65	9.27	8.82

Table (23) $a_{FeO} = 0.6$

	Mole %			
	FeO	MnO	TiO_2	SiO_2
A_1	64.32	8.04	2.33	25.03
A_2	63.26	7.84	2.48	26.04
B_1	65.6	7.62	4.52	22.26
B_2	65.79	7.68	4.32	22.21
C_1	66.69	7.47	6.14	19.7
C_2	67.28	7.44	6.33	18.95
D_1	67.67	6.33	7.11	18.69
D_2	67.53	6.34	7.39	18.73

Table (24) $a_{FeO} = 0.5$

	Mole %			
	FeO	MnO	TiO_2	SiO_2
A_1	60.45	7.97	1.71	29.87
A_2	60.95	7.56	1.8	29.69
B_1	62.24	8.3	4.68	24.78
B_2	62.35	7.31	4.67	25.67
C_1	63.39	7.92	6.29	22.39
C_2	64.13	7.87	5.93	22.06
D_1	65.42	7.02	8.17	19.39
D_2	65.33	7.02	8.25	19.39

Table (25) $a_{FeO} = 0.4$

	Mole %			
	FeO	MnO	TiO_2	SiO_2
A_1	55.48	8.53	1.44	34.55
A_2	55.05	8.98	1.65	34.72
B_1	57.55	7.8	4.19	30.47
B_2	58.21	7.68	4.06	30.03
C_1	61.01	7.21	6.29	26.49
C_2	60.98	7.66	5.74	25.62
D_1	63.14	6.98	7.69	22.19
D_2	63.26	6.93	7.24	22.57

B. MnO average 16.06 Mole %

Table (26) $a_{FeO} = 0.806$

	Mole %			
	FeO	MnO	TiO_2	SiO_2
A_1	75.59	16.05	-	8.36
A_2	74.64	16.76	-	8.60
B_1	76.85	14.91	0.26	7.80
B_2	77.05	14.76	0.23	7.96
C_1	79.56	13.93	0.66	5.85
C_2	79.52	13.82	0.64	6.01
D_1	80.03	13.37	1.96	4.64
D_2	79.58	13.47	1.94	5.0

Table (27) $a_{FeO} = 0.705$

	Mole %			
	FeO	MnO	TiO_2	SiO_2
A_1	65.58	19.43	2.11	22.88
A_2	65.84	18.5	1.76	13.9
B_1	67.57	16.97	4.52	10.85
B_2	68.25	17.03	4.70	10.2
C_1	69.88	17.09	7.93	5.1
C_2	70.43	17.2	7.28	5.1
D_1	71.94	17.02	9.59	1.44
D_2	72.0	16.38	9.21	2.4

Table (28) $a_{FeO} = 0.610$

	Mole %			
	FeO	MnO	TiO_2	SiO_2
A_1	57.57	16.7	1.47	24.26
A_2	57.76	16.74	1.81	23.68
B_1	59.9	17.14	4.46	18.5
B_2	60.79	16.65	4.29	18.27
C_1	59.67	16.92	6.24	17.17
C_2	60.59	16.21	5.8	17.51
D_1	62.78	14.95	8.14	14.13
D_2	62.02	15.76	8.32	13.9

Table (29) $a_{FeO} = 0.505$

	Mole %			
	FeO	MnO	TiO_2	SiO_2
A_1	52.71	16.9	1.66	29.44
A_2	53.74	16.22	1.53	28.5
B_1	54.15	17.01	2.22	26.62
B_2	55.21	16.79	2.37	25.63
C_1	56.16	16.8	5.95	21.8
C_2	57.0	16.52	5.95	20.43
D_1	60.48	15.99	7.90	15.66
D_2	60.28	16.43	8.58	14.7

Table (30) $a_{FeO} = 0.408$

	Mole %			
	FeO	MnO	TiO_2	SiO_2
A_1	50.17	15.63	1.7	32.5
A_2	49.13	15.88	1.53	33.46
B_1	52.7	15.79	3.66	27.83
B_2	53.76	15.63	3.59	26.82
C_1	58.34	14.23	8.17	19.26
C_2	58.73	13.52	7.71	20.4

C. MnO average 24.08 Mole %

Table (31) $a_{FeO} = 0.705$

	Mole %			
	FeO	MnO	TiO_2	SiO_2
A_1	66.76	25.59	0.8	6.86
A_2	65.81	25.67	0.85	7.67
B_1	66.84	24.43	1.32	7.41
B_2	67.63	24.00	1.22	7.15
C_1	69.01	22.05	2.5	6.44
C_2	68.28	22.38	2.4	6.94

Table (32) $a_{FeO} = 0.61$

	Mole %			
	FeO	MnO	TiO_2	SiO_2
A_1	53.56	25.19	3.67	17.57
A_2	52.73	25.90	3.35	18.01
B_1	55.13	25.71	7.79	11.37
B_2	55.28	26.45	7.47	10.79
C_1	56.02	23.86	9.35	10.76
C_2	56.21	23.86	9.82	10.12

Table (33) $a_{FeO} = 0.505$

	Mole %			
	FeO	MnO	TiO_2	SiO_2
A_1	48.2	23.51	1.56	26.72
A_2	47.45	24.02	1.49	27.04
B_1	49.93	24.43	4.61	21.02
B_2	50.43	23.71	4.03	21.83
C_1	52.2	23.8	7.21	16.79
C_2	52.43	23.55	6.94	17.8
D_1	52.95	23.79	9.75	13.5
D_2	52.99	23.74	9.48	13.79

Table (34) $a_{FeO} = 0.408$

	Mole %			
	FeO	MnO	TiO_2	SiO_2
A_1	43.12	24.89	1.36	30.62
A_2	42.40	24.88	1.63	31.10
B_1	48.74	24.79	4.24	22.24
B_2	48.74	24.38	4.46	22.42
C_1	50.71	20.25	7.84	21.2
C_2	50.33	21.20	7.98	20.5

4. The Quaternary System FeO-TiO_2-SiO_2-CaO At 1470°C

A. CaO average 5.75 Mole %

Table (35) $a_{FeO} = 0.9$

	Mole %			
	FeO	TiO_2	CaO	SiO_2
A_1	76.77	-	5.96	17.26
A_2	76.77	-	5.87	17.36
B_1	82.89	2.37	5.93	8.91
B_2	83.89	1.84	5.71	8.57

Table (36) $a_{FeO} = 0.8$

	Mole %			
	FeO	TiO_2	CaO	SiO_2
A_1	69.93	-	5.44	24.62
A_2	70.89	-	5.67	23.43
B_1	74.37	5.41	5.4	14.83
B_2	73.32	5.66	5.8	15.2
C_1	76.37	9.92	5.55	8.14
C_2	76.38	9.93	5.55	8.14

Table (37) $a_{FeO} = 0.7$

	Mole %			
	FeO	TiO_2	CaO	SiO_2
A_1	66.06	-	5.61	28.33
A_2	65.36	-	5.61	29.03
B_1	67.32	3.33	5.96	23.37
B_2	68.32	2.99	5.97	22.71
C_1	70.52	9.19	5.22	15.05
C_2	70.29	9.64	5.95	14.11
D_1	70.37	15.6	5.8	8.23
D_2	70.01	16.52	5.94	7.53

Table (38) $a_{FeO} = 0.6$

	Mole %			
	FeO	TiO_2	CaO	SiO_2
A_1	60.38	-	5.68	33.94
A_2	60.39	-	5.57	33.83
B_1	62.88	6.08	5.56	25.47
B_2	63.42	6.09	5.51	24.97
C_1	63.94	11.33	5.82	18.91
C_2	65.03	11.34	5.83	17.79
D_1	64.14	17.75	5.98	12.12
D_2	65.17	17.32	5.7	11.81

Table (39) $a_{FeO} = 0.5$

	Mole %			
	FeO	TiO_2	CaO	SiO_2
A_1	56.79	-	4.75	38.45
A_2	57.51	-	4.7	37.79
B_1	58.69	6.39	5.54	29 38
B_2	58.69	6.39	5.54	29.38
C_1	59.81	12.23	5.63	22.33
C_2	59.85	12.32	5.24	22.59
D_1	60.13	19.59	5.26	15.05
D_2	60.15	19.59	5.52	14.74

Table (40) $a_{FeO} = 0.4$

	Mole %			
	FeO	TiO_2	CaO	SiO_2
A_1	52.88	-	5.26	41.85
A_2	53.1	-	5.02	41.88
B_1	54.93	5.8	5.46	33.8
B_2	54.88	5.52	5.45	34.15
C_1	56.46	12.02	5.55	25.95
C_2	55.55	12.25	5.68	26.92
D_1	57.0	19.85	5.6	17.54
D_2	57.88	19.88	5.46	16.98

B. CaO average 11.2 Mole %

Table (41) $a_{FeO} = 0.8$

	Mole %			
	FeO	TiO_2	CaO	SiO_2
A_1	66.28	-	11.49	22.22
A_2	65.58	-	11.81	22.61
B_1	66.98	1.27	10.53	21.22
B_2	66.25	1.36	10.52	21.87
C_1	68.84	3.42	10.99	16.64
C_2	68.87	3.51	10.63	16.98
D_1	73.12	9.2	11.38	6.30
D_2	72.96	9.29	11.38	6.37
E_1	75.74	10.7	10.85	2.71
E_2	76.30	10.71	10.86	2.12

Table (42) $a_{FeO} = 0.7$

	Mole %			
	FeO	TiO_2	CaO	SiO_2
A_1	59.1	-	11.56	29.33
A_2	59.27	-	11.33	29.4
B_1	58.48	4.04	11.77	25.71
B_2	58.44	4.13	11.89	25.54
C_1	60.26	10.23	11.66	17.85
C_2	59.17	10.21	12.0	16.81
D_1	61.91	14.41	12.2	11.48
D_2	66.86	14.58	12.19	12.37
E_1	65.13	17.72	11.13	6.02
E_2	65.21	18.66	11.28	4.85

Table (43) $a_{FeO} = 0.6$

	Mole %			
	FeO	TiO_2	CaO	SiO_2
A_1	56.33	-	11.37	32.3
A_2	56.22	-	11.46	32.32
B_1	53.26	3.81	10.48	32.45
B_2	54.32	3.40	10.48	31.8
C_1	55.05	9.36	10.93	24.66
C_2	54.63	9.9	10.94	24.53
D_1	55.91	15.36	10.85	17.89
D_2	55.92	15.45	10.85	17.78
E_1	58.19	19.08	10.88	11.85
E_2	58.21	20.0	11.07	10.71

Table (44) $a_{FeO} = 0.5$

	Mole %			
	FeO	TiO_2	CaO	SiO_2
A_1	52.08	-	10.7	37.22
A_2	51.42	-	10.94	37.63
B_1	48.38	3.94	11.34	36.33
B_2	48.97	4.02	11.13	35.88
C_1	49.71	7.97	11.43	30.89
C_2	49.13	8.05	11.38	31.44
D_1	50.79	15.91	11.86	21.44
D_2	50.9	15.92	11.85	21.44
E_1	52.1	24.75	11.91	11.24
E_2	53.03	23.84	11.84	11.28

Table (45) $a_{FeO} = 0.4$

	Mole %			
	FeO	TiO_2	CaO	SiO_2
A_1	47.17	-	10.84	41.98
A_2	47.18	-	10.64	42.18
B_1	46.41	8.10	11.02	34.47
B_2	46.34	8.22	10.7	34.75
C_1	46.45	16.53	11.0	26.03
C_2	46.63	16.48	11.01	25.87
D_1	47.26	20.82	11.41	20.5
D_2	46.97	21.01	11.41	20.59

C. CaO average 16.1 Mole % -

Table (46) $a_{FeO} = 0.7$

	Mole %			
	FeO	TiO_2	CaO	SiO_2
A_1	58.2	-	15.78	26.03
A_2	59.13	-	15.74	25.13
B_1	54.86	4.16	16.02	24.96
B_2	54.76	4.16	16.02	25.06
C_1	56.22	8.47	15.97	19.35
C_2	56.15	8.45	16.07	19.32
D_1	57.47	12.87	16.46	13.2
D_2	57.47	12.87	16.48	13.7

Table (47) $a_{FeO} = 0.6$

	Mole %			
	FeO	TiO_2	CaO	SiO_2
A_1	55.04	-	15.53	29.4
A_2	55.19	-	16.06	28.75
B_1	50.28	4.26	16.24	29.22
B_2	50.27	4.21	16.25	29.27
C_1	51.36	8.38	16.56	23.69
C_2	51.26	8.38	16.53	23.73
D_1	53.04	17.71	16.16	13.09
D_2	54.3	17.37	16.48	12.12

Table (48) $a_{FeO} = 0.5$

	Mole %			
	FeO	TiO_2	CaO	SiO_2
A_1	51.59	-	15.96	32.65
A_2	51.59	-	15.96	32.65
B_1	45.58	6.19	15.49	32.75
B_2	45.58	6.19	15.68	32.56
C_1	45.92	11.31	15.98	26.78
C_2	46.11	11.31	16.33	26.24
D_1	47.74	18.81	16.6	16.85
D_2	47.85	18.86	16.62	16.67

Table (49) $a_{FeO} = 0.4$

	Mole %			
	FeO	TiO_2	CaO	SiO_2
A_1	48.11	-	15.32	36.57
A_2	48.21	-	15.43	36.56
B_1	41.46	7.32	15.6	35.63
B_2	41.46	6.56	15.56	36.43
C_1	42.88	14.21	16.19	26.73
C_2	42.5	14.37	15.95	27.17
D_1	44.17	21.5	16.94	17.39
D_2	43.67	21.45	16.07	18.81

D. CaO average 21.89 Mole %

Table (50) $a_{FeO} = 0.7$

	Mole %			
	FeO	TiO_2	CaO	SiO_2
A_1	59.93	-	21.66	18.4
A_2	60.98	-	21.23	17.79
B_1	47.74	1.57	22.55	28.14
B_2	47.8	1.31	22.53	28.36
C_1	50.66	6.49	22.76	20.09
C_2	51.26	6.5	22.55	19.69
D_1	54.84	12.5	22.37	10.28
D_2	53.86	12.48	22.82	10.85
E_1	64.98	13.95	19.91	1.16
E_2	65.0	13.5	19.76	1.74

Table (51) $a_{FeO} = 0.6$

	Mole %			
	FeO	TiO_2	CaO	SiO_2
A_1	54.83	-	21.22	23.94
A_2	55.89	-	20.10	24.01
B_1	45.13	1.1	21.52	32.24
B_2	44.16	1.2	21.5	33.15
C_1	45.62	4.92	21.07	28.38
C_2	44.73	5.75	21.67	37.85
D_1	45.25	13.23	20.75	20.76
D_2	45.89	12.51	19.78	21.82
E_1	48.3	22.14	21.59	7.97
E_2	49.26	21.4	21.02	8.31

Table (52) $a_{FeO} = 0.5$

	Mole %			
	FeO	TiO_2	CaO	SiO_2
A_1	51.31	-	21.24	27.45
A_2	51.31	-	21.24	27.45
B_1	41.6	2.02	19.99	36.39
B_2	40.96	2.18	20.58	36.28
C_1	41.67	9.69	21.27	27.37
C_2	41.83	9.7	21.28	27.2
D_1	42.6	21.18	22.73	13.49
D_2	42.51	20.63	22.86	14.0
E_1	44.23	28.44	24.84	2.49
E_2	44.52	28.45	24.74	2.28

Table (53) $a_{FeO} = 0.4$

	Mole %			
	FeO	TiO_2	CaO	SiO_2
A_1	47.32	-	21.51	31.16
A_2	47.74	-	20.96	31.31
B_1	37.57	2.98	20.21	39.24
B_2	37.21	2.85	21.32	38.62
C_1	37.7	10.54	20.77	30.98
C_2	36.66	11.02	21.90	30.42
D_1	39.9	24.01	23.0	13.9
D_2	38.17	24.89	23.14	13.8
E_1	39.7	33.58	24.02	2.7
E_2	40.37	33.94	23.65	2.04

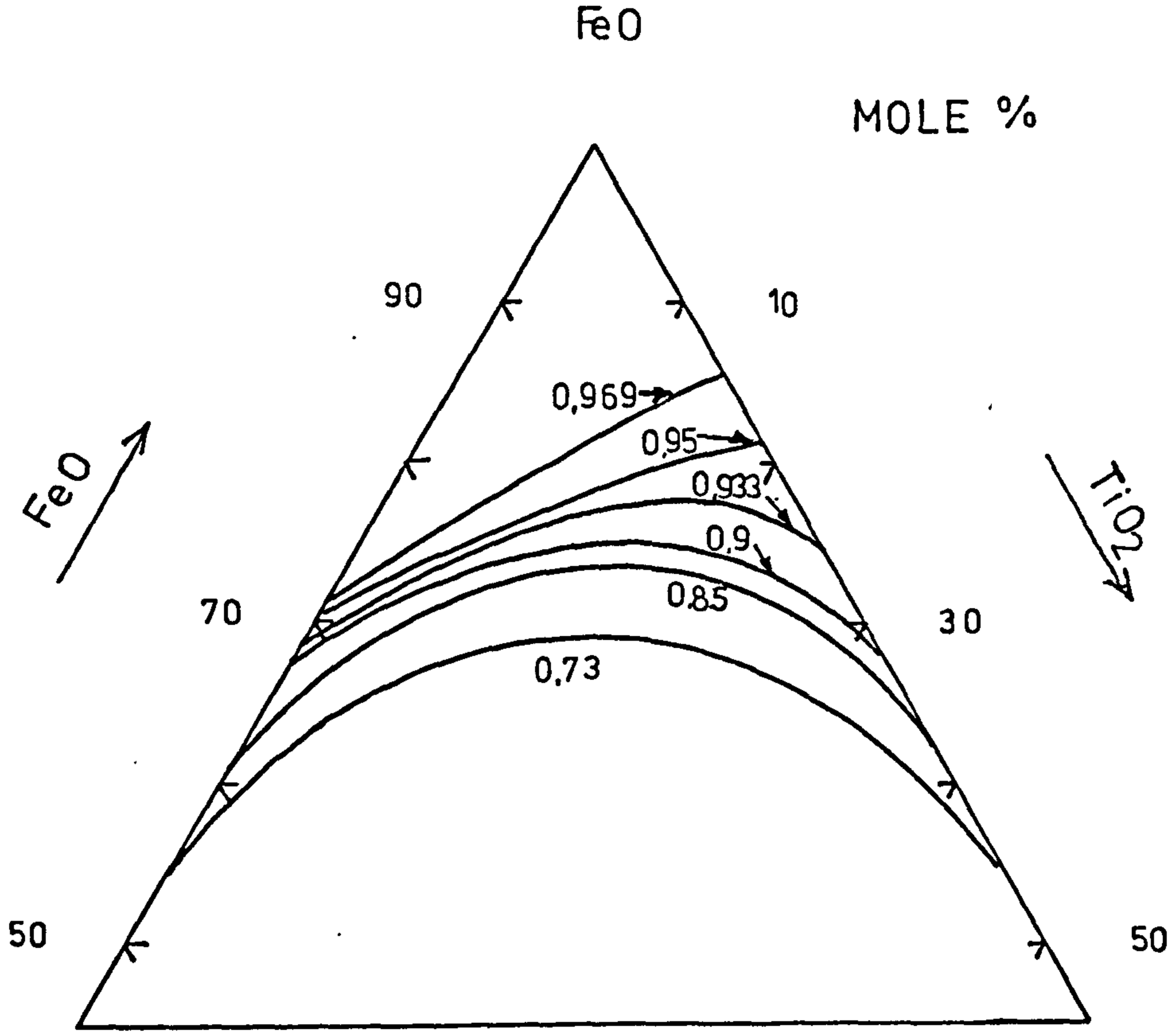

Fig. (1) FeO Iso-Activity Coefficient Curves In The System FeO-TiO_2-SiO_2 At 1475°C.

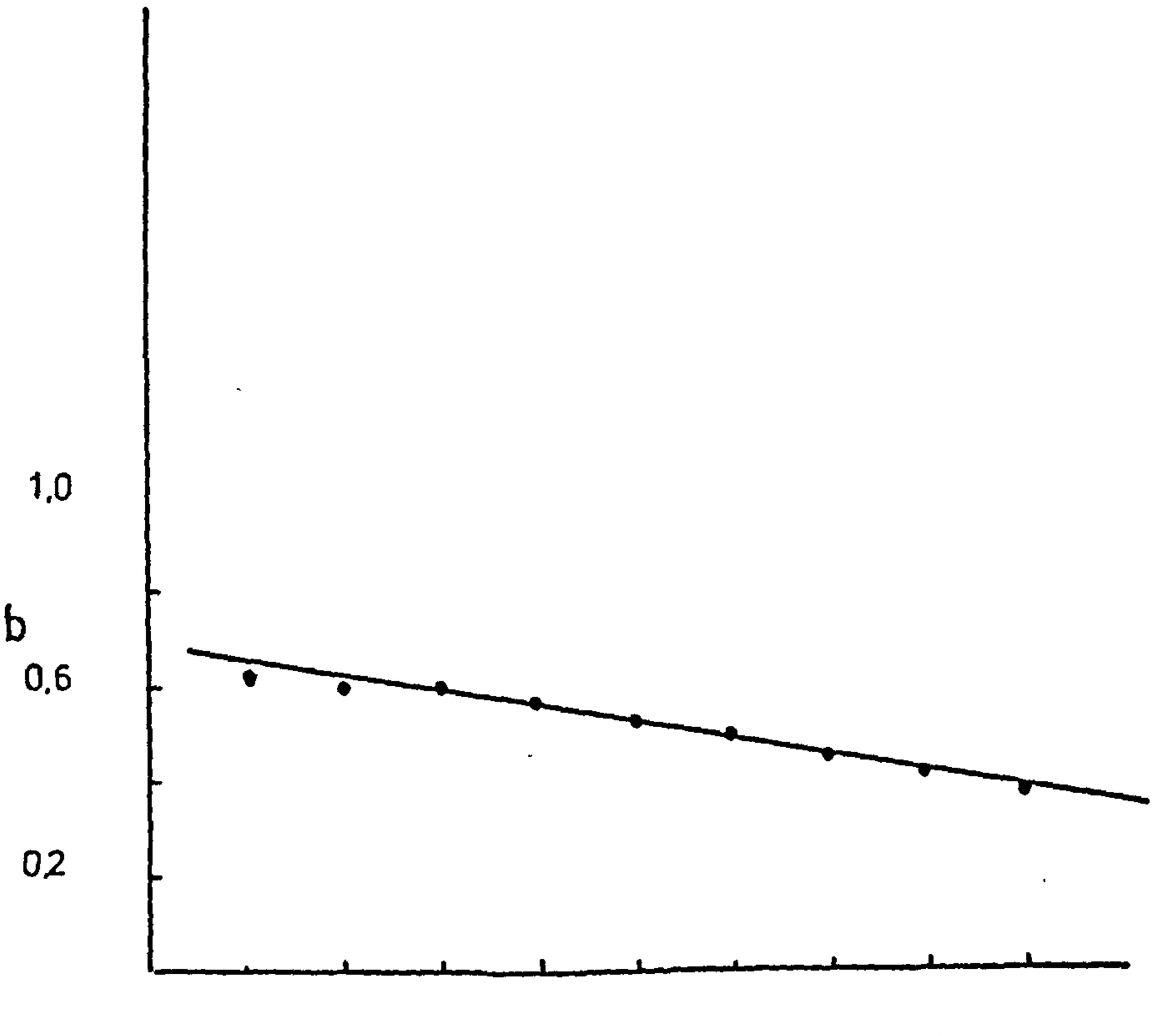

Fig. (2) The Plot Of b Versus y In The System $FeO-TiO_2-SiO_2$ At 1475°C.

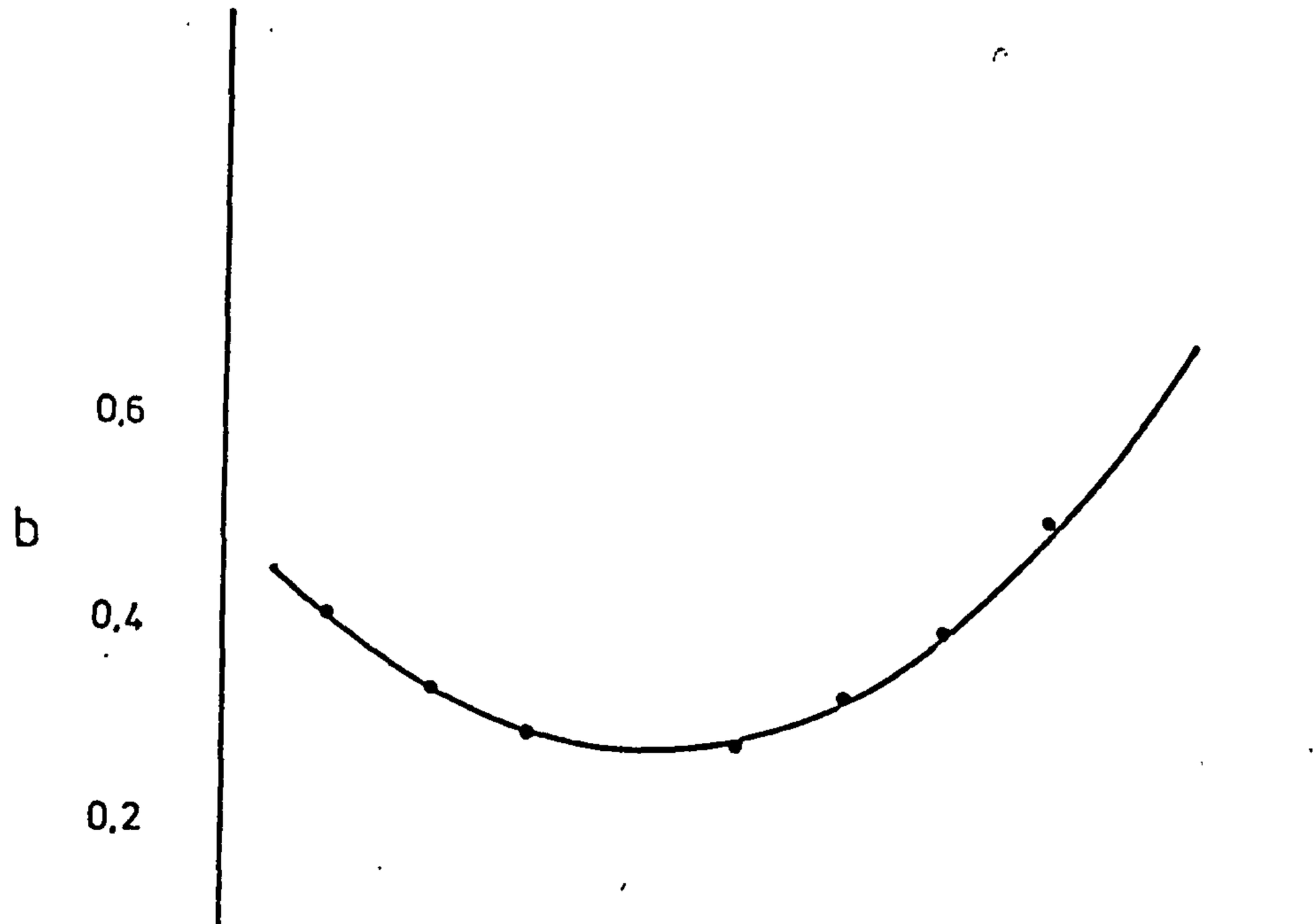

Fig. (3) The Plot Of b Versus y In The System $FeO-TiO_2-CaO$ At $1470^{o}C$.

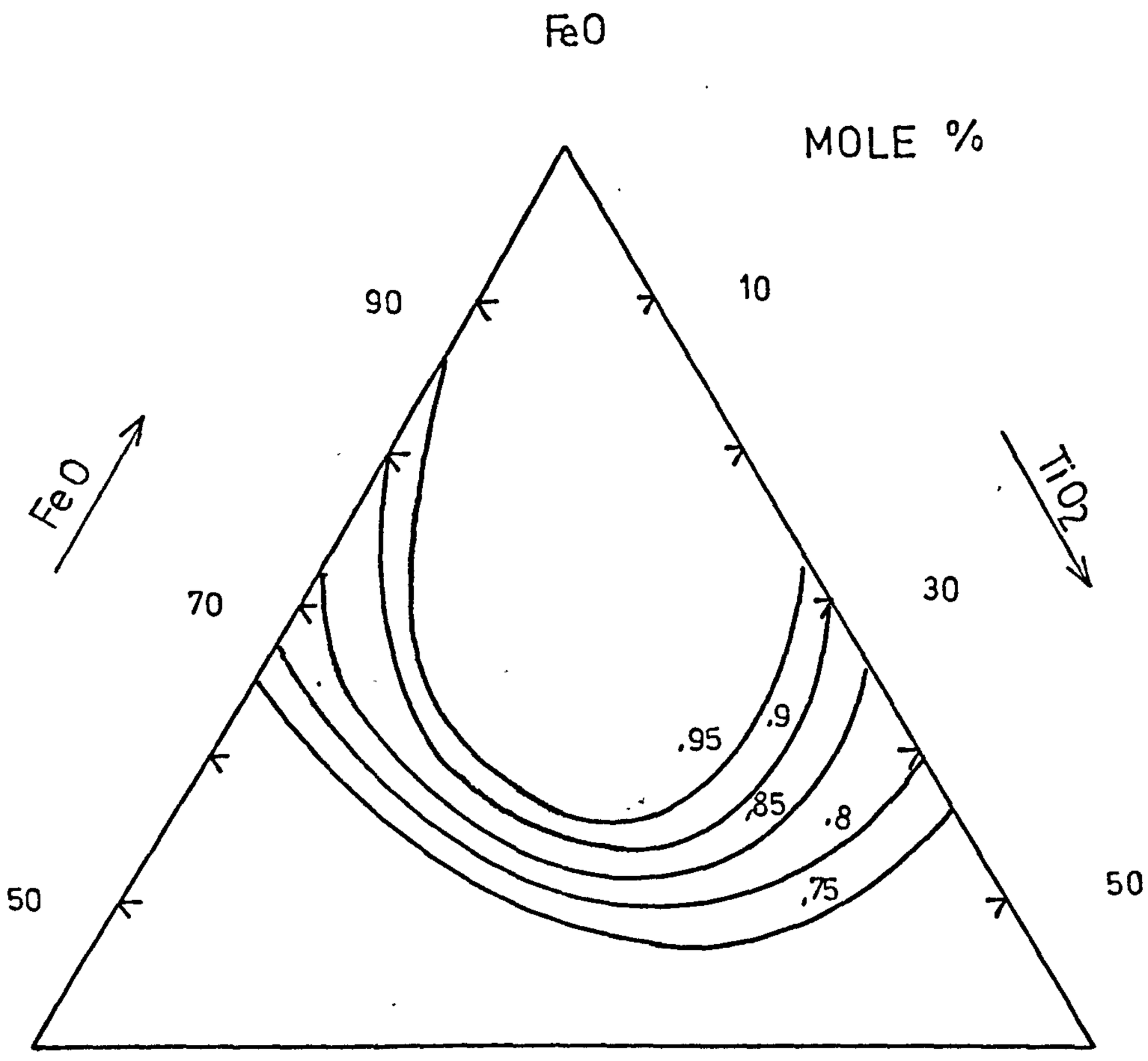

Fig. (4) FeO Iso-Activity Coefficient Curves In The System FeO-TiO_2-CaO At 1470°C.

REFERENCES

1. L.S. Darken, R.W. Gurry, Journal of The American Chemical Society, 1945, Vol.67, p.1398.

2. L.S. Darken, R.W. Gurry, Journal of The American Chemical Society, 1946, Vol. 68, p.799.

3. C.R. Taylor, J. Chipman, Transactions of AIME, 1943, Vol. 154, p.228.

4. K.L. Fetters, J. Chipman, Transactions of AIME, 1941, Vol. 145, p.95

5. J.E. Elliot, Transactions of AIME, 1955, Vol. 203, p.485.

6. T.B. Winkler, J. Chipman, Transactions of AIME, 1946, Vol. 167, p.111

7. H.B. Bell, A.B. Murad, P.T. Carter, Transactions of AIME, 1952, Vol. 194, p.718.

8. H.L. Bishop, N.J. Grant, J. Chipman, Transactions of AIME, 1958, Vol. 212, p.187.

9. H.L. Bishop, H.N. Lander, N.J. Grant, J. Chipman, Transactions of AIME, 1956, Vol. 206, p. 862.

10. H.L. Bishop, N.G. Grant, J. Chipman, Transactions of AIME, 1958, Vol. 212, p.890.

11. H.B. Bell, Journal of The Iron and Steel Institute, 1963, Vol. 201,p.116.

12. R. Schulmann, P.J. Ensio, Transactions of AIME 1951, Vol. 191, p. 401.

13. E.J. Michal, R. Schuhmann, Transactions of AIME 1952, Vol. 194, p. 723.

14. C. Bodsworth, Journal of The Iron and Steel Institute, 1959, Vol. 193, p.13.

15. I.M. Davidson, C. Bodsworth, Journal of The Iron and Steel Institute, 1960, Vol. 195, p.164.

16. I.C. Smith, H.B. Bell, Transactions of The Institute of Mining and Metallurgy, 1970, Vol.79, C253.

17. I.C. Smith, H.B. Bell, Transactions of The Institute of Mining and Metallurgy, 1971, Vol.80, C55.

18. H. Larson, J. Chipman, Transactions of AIME, 1953, Vol. 197, p.1089.

19. H. Larson, J. Chipman, Transactions of AIME, 1954, Vol.200, p.759.

20. T.Turkdogan, P.M. Bills, Journal of The Iron and Steel Institute, 1958, Vol. 186, p. 329.

21. T. Turkdogan, P.M. Bills, Journal of The Iron and Steel Institute, 1958, Vol. 188, p.143.

22. C. Bodsworth, "Physical Chemistry of Iron and Steel Manufacture", Longmans, London 1963.

23. M. Timucin, A.E., Morris, Metallurgical Transactions, 1970, Vol. 1, p.3193.

24. Y. Wanibe, Y. Yamachi, K. Kawai, H. Sakoa, Transactions of The Iron and Steel Institute of Japan, 1972, Vol.12 (6) p.472.

25. E.T. Turkdogan, J. Pearson, Journal of The Iron and Steel Institute, 1953, Vol. 173, p.214.

26. E.T. Turkdogan, Transactions of AIME, 1961, Vol.221, p.1090.

27. J. O'M. Bockris, J.A. Kitchener, S. Ignatowiz, J.W. Tomlinson, Transactions of Faraday Society 1952, Vol. 48, p.75.

28. J. O'M. Bockris, J.D. MacKenzie, J.A. Kitchener, Transactions of Faraday Society, 1955, Vol. 51, p.1734.

29. J.O'M. Bockris, J.W. Tomlinson, J.L. White, Transactions of Faraday Society, 1956, Vol. 52, p.299.

30. C.R. Masson, Journal of The Iron and Steel Institute, 1972, Vol. 210, p.89.

31. C.R. Masson, Proceedings of Royal Society of London, 1965, Vol.287A, p.201.

32. C.R. Masson, Journal of The American Ceram. Society, 1968, Vol. 51, p.143.

33. M. Temkin, Acta Physicochemica URSS, 1945, vol. 20, p.411

34. A. Samaritan, M. Temkin, L. Shwartzmann, Acta Physicochemica, 1945, Vol. 20, p.421.

35. C.R. Masson, I.B. Smith, S.G. Whiteway, Canadian Journal of Chemistry, 1970, Vol. 48, p.1456.

36. I.B. Smith, C.R. Masson, Canadian Journal of Chemistry, 1971, Vol. 49, p.683.

37. J. Lumsden,"Physical Chemistry of Process Metallurgy," Interscience, New York etc., 1961, p.165-205.

38. E. Martin, Ph.D. Thesis, Strathclyde University, October 1974.

39. M.G. Fronberg, R. Weber, Arch. Eisenhuttenwesen, Vol. 7, 1965, p.447.

40. G. Handfield, G.G. Charette, Canadian Metallurgical Quarterly, Vol. 10, 1971,p235.

41. K. Mori, Tetsu to Hagane, Vol. 42, 1956, p.1024.

42. V.A. Reznichenko, Izv. A Kad, Nauk S.S.S.R. Metallurgy, Vol.5, 1967, p.43.

43. S.I. Denisov, V.A. Degtyarev, Izv. A Kad.Nauk, S.S.S.R. Metally., Vol. 1, 1970, p.80.

44. K. Mori, Tetsu to Hagane, Vol. 46, 1960, p.134.

45. H.B. Bell, private communications.

46. A. Harrison, Ph.D. Thesis, University of Strathclyde, June 1973.

47. Perkin-Elmer 103, Instruction Manual for Atomic Absorption Spectrometer, March 1971.

48. A.I. Vogel, "Quantitative Inorganic Analysis", Green and Co., London, New York, Toronto, 1945, p.368.

49. R.S. Young, "Chemical Analysis in Extractive Metallurgy", Griffin & Co. Ltd., London, 1971, p. 173.

50. C. Bodsworth, I.M. Davidson, "Physical Chemistry of Process Metallurgy", Interscience, New York, etc., 1961, p.233.

51. C. Wagner, "Thermodynamics of Alloys", Addison-Wesely Press, 1952, p.19-22

52. J. Elliot, M. Gleiser, "Thermochemistry of Steel Making", Vol. 2.

ACKNOWLEDGEMENT

Thanks are due to Dr. I.D. Sommerville for his supervision and help.

The author is greatly indebted to Professor H.B. Bell for his encouragement, stimulating discussions and his invaluable assistance in the preparation of many parts of this thesis.

Thanks are also due to Professor Grieveson for the research facilities, Unesco for the Fellowship and the Suez Canal University for the study leave.